HWR No. 00-030

SIMULATION OF GROUNDWATER CONDITIONS IN THE UPPER SAN PEDRO BASIN FOR THE EVALUATION OF ALTERNATIVE FUTURES

by

Tomas Charles Goode
and
Thomas Maddock III

Department of Hydrology and Water Resources, and
University of Arizona Research Laboratory for Riparian Studies
University of Arizona
Tucson, Arizona 85721

ACKNOWLEDGEMENTS

This study is a part of The Alternative Futures Project that was conducted in collaboration with team of investigators from Harvard University Graduate School of Design, the Desert Research Institute, Instituto del Medio Ambiente y el Desarrollo Sustenable del Estado de Sonora (I.M.A.D.E.S.), the United States Army Training and Doctrine Command, and the United States Army Engineer Research and Development Laboratory, with the cooperation of the regional planning agencies of the area, the Semi-Arid Land-Surface-Atmosphere Program (SALSA) and Fort Huachuca. The research was funded by a grant obtained by the U.S. Army Training and Doctrine Command's Environmental Division from the Department of Defense Legacy Resources Management Program. The publication of this report was also funded in part by the NSF Science and Technology Center for Sustainability of semi-Arid Hydrology and Riparian Areas.

We would like to express our gratitude for the many individuals that assisted us in the creation of this study. First, for their information and technical assistance with the geology and the hydrologic modeling, we would like to thank Don Pool and Stan Leake of the USGS, Dale Mason of ADWR, Dave Goodrich of ARS-USDA, and Hector Arias of IMADES. We would like to thank the Harvard Graduate School of Design, specifically Carl Steinitz and Richard Peiser for their insights into geography and development; Scott Bassett, Alan Shearer and Mike Flaxman for their assistance with GIS modeling methods and their patience through numerous computer difficulties. To Dave Mouat and Mary Cablk of the Desert Research Center, our thanks for input on evapotranspiration and an education in fine wines. To the Army crew, Bob Anderson, Bob Lozar and Winifred Rose, our thanks for their support, both financial and belief in the project. Finally our office mates, Kate Baird, Martha Whitaker, Chris Adams, and Jim Leenhouts, who were a huge help as they thought about and responded to innumerable "what if" questions.

TABLE OF CONTENTS

LIST OF FIGURES

LIST OF TABLES

LIST OF PLATES

ABSTRACT

The creation of the groundwater model of the Upper San Pedro Basin included two developmental phases: the creation of a conceptual and numerical model. The creation of the conceptual model was accomplished through the utilization of Geographic Information System (GIS) software, namely ArcView, used primarily to view and create point, line, and polygonal shapes. The creation of a numerical model was accomplished by the infusion of the conceptual model into a 3D finite difference grid used in MODFLOW groundwater software from the U.S. Geological Survey. MODFLOW computes the hydraulic head (water level) for each cell within the grid. The infusion of the two models (conceptual and numerical) was allowed through the use of Department of Defense Groundwater Modeling System (GMS) software.

The time period for groundwater modeling began with predevelopment conditions, or "steady state." Steady state conditions were assumed to exist in 1940. The steady state was used as the initial condition for the subsequent transient analysis. The transient simulation applied historical and current information of pumping stresses to the system from 1940 to 1997. After modeling current conditions, Alternative Futures' scenarios were simulated by modifying current stresses and by adding new ones. The possible future impacts of to the hydrologic system were then evaluated.

CHAPTER 1
OVERVIEW

1.1 INTRODUCTION

The San Pedro Basin in southeastern Arizona has had its share of controversial events throughout history. Apache wars, Mexican-American war, and the Earps vs. the Clantons and McLaurys in the shoot out at the O.K. corral, conjure up images of the wild days of the "old west." Over a hundred years after those wild days, one still find controversy. Although issues surrounding the use of water have always found a place in the arid regions of the west, lawsuits and courtrooms have taken over as means and venues for "shoot outs." In the new west, population growth, Federal reserved rights, endangered species protection, and agriculture are some of the many interests finding themselves at odds concerning the best uses of the limited water resources in the area.

Around the year 1940, the completion of rural electrification and the advent of electric high-powered hydraulic lift pumps provided means for larger volumes of water to be extracted from wells. Until this time, water users in the San Pedro Basin had been using spring discharge, stream flow, artesian wells or shallow wells for their water needs. These needs exhibited little disruption to the equilibrium of the hydrologic cycle. With the high-powered pumps allowing large volumes of water to be taken from beneath the ground, the equilibrium in hydrologic cycle was disrupted.

The disruptions have caused several new issues to arise in the area. Because of surface water diversions and depletions of surface water due to groundwater pumping, the once perennial stream flow of the San Pedro River has now become intermittent in some areas. Groundwater withdrawals threaten to lower water table conditions in riparian areas near the river, which could eliminate the currently available shallow water and the plant life reliant upon it, subsequently effecting valuable wildlife habitat. The lowering of the water table by groundwater pumping may create areas prone to aquifer compaction, and produce subsidence problems like those seen in the larger urban area of nearby Tucson, Arizona. Irrigation interests along the floodplain of the river, that once used readily available flow of the San Pedro River, are now forced to rely more heavily on groundwater withdrawals, thus compounding water problems near the river. Residing within the above issues is one created by the growth of population centers. Within the basin, there is a growing demand for public water supply, and groundwater is the only source that can satisfy that demand at the present time. How will past and present uses of groundwater impact the future of the San Pedro Basin?

The current study works to improve the knowledge of how the ground and surface water systems respond to past water demands by applying the most current information on geology, hydraulic properties, well locations and attributes, groundwater recharge and its distribution, streamflows and diversions, and riparian use. What results from this improved knowledge of the past is a hydrologic model that simulates the impacts on the ground and surface waters systems due to past development, and predicts these impacts for the present and future development. The hope is that through the use of this model

that water managers will better understand alternative futures, thereby making better water-development choices today.

1.2 ALTERNATIVE FUTURES STUDY

The current study is a component of the Alternative Futures study conducted by the Department of Defense, Desert Research Institute, and the Harvard Graduate School of Design. The Alternative Futures study explores how urban growth and change in the rapidly developing Upper San Pedro Basin might influence the hydrology and the ecological biodiversity of the area. The study evaluates individual scenarios from the present time (1997-2000) to 20 years in the future (2020). It is hoped the study will provide valuable information to stakeholders in the area regarding issues and planning choices, and their possible consequences to the built and natural environment.

As a component of the larger Alternative Futures study, the hydrological model presented in this report interacts with the other non-hydrologic components, which in turn impact many facets of the natural, and anthropogenic environment of the Upper San Pedro Basin. However, the hydrological model is presented here as a stand-alone document. Impacts to the hydrologic system may be evaluated in their own context.

1.3 PURPOSE AND GOALS OF MODEL

Improvements to methodology were of primary concern in creating a new model of this already highly investigated area. An extensive graphic information system (GIS) was developed for land surface, geology, hydraulic properties, mountain front recharge,

riparian evapotranspiration, irrigated agriculture, well location, and steam network. This GIS enabled the follow primary changes in methods and information.

- Estimated pumping rates were distributed to known well locations, corresponding to records held by the State of Arizona.
- Mountain front recharge was given a weighted distribution based on elevation and average precipitation of contributing basins.
- Results from recent studies of evapotranspiration were applied in riparian areas.
- Model boundaries were extended outward towards mountain front areas and included the entire Mexican portion of the Upper San Pedro Basin as well as the headwaters of the Babocomari River watershed.

The above changes provide a more comprehensive framework for the evaluation of alternative futures within the Upper San Pedro Basin than previous investigations. The model covers the entire Upper San Pedro Basin, and integrates the newer hydrologic information developed for the basin by the USGS and other entities such as Semi Arid Land Surface and Atmospheric (SALSA) group. The model also includes Mexico as a key component to the analysis of the Upper San Pedro Basin, which was not done previously.

1.4 PREVIOUS INVESTIGATIONS/MODELS

Several individuals and organizations have conducted groundwater models to simulate a portion or all of the groundwater flow in the San Pedro River Valley. The most recent studies were relied on heavily for information regarding conditions and

stresses in the Upper San Pedro Basin. Freethey (1982) modeled the Upper San Pedro Basin from just within Mexico to Fairbank, Arizona. Putman *et al* (1988), using updated pumping data, ran Freethey's model on MODFLOW using the standard river package. Vionnet and Maddock (1992) modified Freethey's Upper San Pedro model by using MODFLOW with the Stream-Aquifer package (1989). This provided a more realistic analysis of stream/groundwater interactions. Rovey (1989) modeled both the Upper and Lower San Pedro Basins from the Mexico border to the confluent of the Gila River at Wilkelman. Jahnke (1994) modeled the Benson Subbasin from Fairbanks to Redington, providing a detailed analysis of hydrologic conditions from 1940-1990. The Arizona Department of Water Resources (Corell et al., 1996) created an expanded model of the Upper San Pedro Basin, including a larger area of the Mexican portion of the watershed, expansion of model boundaries towards the mountain fronts, and updated pumping information. Figure 1-1 shows the relationship of some of the above-mentioned models with each other and with the boundaries of the current study (referred to as Active Model Boundary). For a more comprehensive examination of previous studies, the reader is referred to Jahnke (1994) and Vionnet (1992) or Corell et al. (1996).

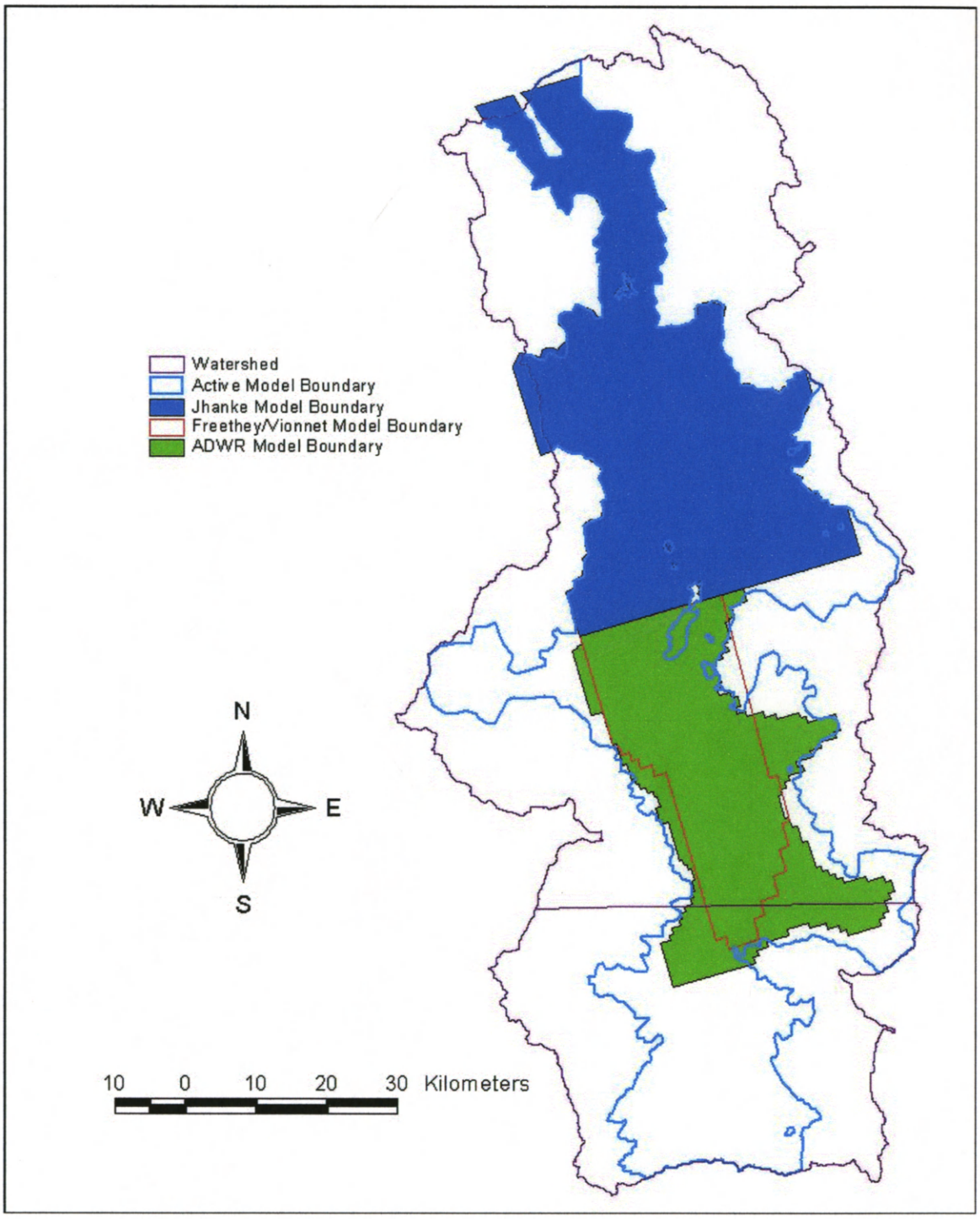

Figure 1-1 Location of previous models within the Upper San Pedro Basin

CHAPTER 2
DESCRIPTION OF STUDY AREA

2.1 LOCATION AND PHYSIOGRAPHY

The San Pedro Basin is located in the northern portion of Sonora, Mexico and southeastern Arizona. The basin is traditionally divided into two sections, the Upper and Lower San Pedro Basins, which are separated by the geologic formation known as "The Narrows." This study includes the Upper San Pedro Basin and a portion of the Lower San Pedro Basin. The Upper San Pedro Basin is that portion of the watershed elevated above "The Narrows" extending southward into Mexico. The portion of the Lower San Pedro Basin included in the study extends north from "The Narrows" to the Redington stream gauge, also known as the Redington sub-basin. For convenience, all references to the Upper San Pedro Basin in this text include this upstream portion of the Lower San Pedro Basin, unless otherwise noted.

The Upper San Pedro Basin is bounded by generally north-northwest trending mountains, which range in height from 5000 to nearly 10000 feet. The primary mountains being Huachuca, Mustang, Whetstone, and Rincon mountains along the west, the Mule, Dragoon, Little Dragoon and Winchester Mountains to the east, and San Jose, Los Ajos, Mariquita, and Elenita mountains in the south. The drainage of these mountains is focused into the San Pedro River (Putman, 1988; Huckleberry, 1996).

The San Pedro Basin is defined by its drainage into the San Pedro River, beginning with its headwaters in northern Sonora, Mexico, near the city of Cananea. The

San Pedro River flows northwards from Mexico into the southeastern portion of Arizona, to its confluence with the Gila River. The river is perennial in many places and intermittent in others. A major tributary, the Babocomari River, is also perennial in places. A few small intermittent streams also contribute to the San Pedro River, but the majority of contributing drainages are ephemeral (Putman, 1988).

2.2 CLIMATE

The climate in the San Pedro Basin is generally semi-arid, having temperatures ranging from a maximum above 100 degrees in the summers, to lows below freezing. Generally the upper elevations remain much cooler and are moister. Precipitation in the basin is typically within the range of nine to twenty five inches per year. The amount of rainfall increases and the temperature decreases when moving higher in altitude (ADWR, 1991; Bahre 1991).

The rainfall patterns within the basin are bimodal, having summer and winter precipitation interrupted by spring and fall dry seasons. Summer precipitation, providing the bulk of the rainfall in the area during July, August and September, can be as much as 70 percent of the annual total. Winter precipitation peaks during the months of December and January. The winter precipitation, largely originating in storm centers to the west, provides regionally extensive, steady rainfall events. This contrasts with the high intensity, short duration storms occurring during the summer "monsoon" season (Bahre 1991).

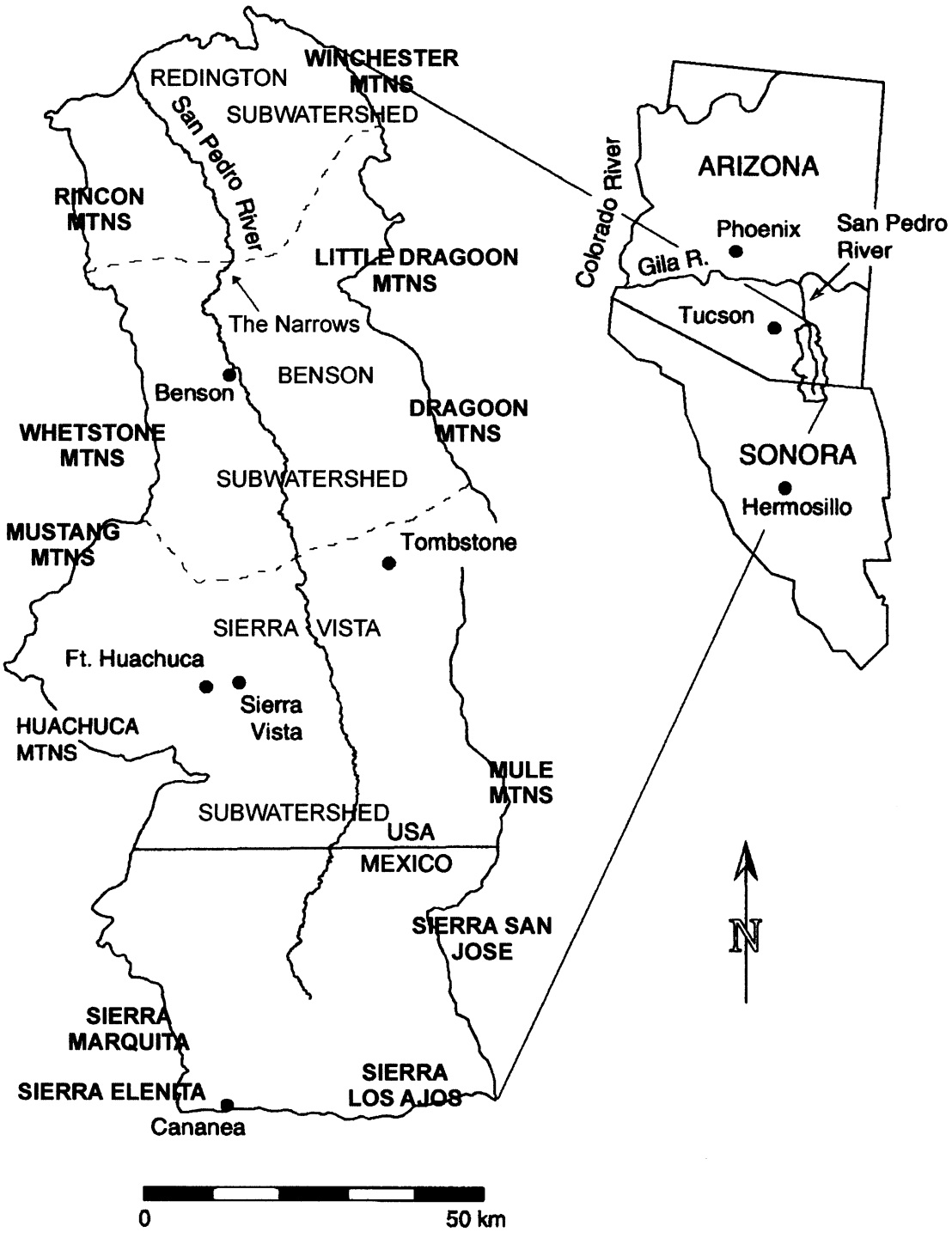

Figure 2-1 Location of study area (adapted from MacNish et al, 2000)

2.3 VEGETATION AND WILDLIFE

The San Pedro Basin is extremely diverse in both vegetation and wildlife. Historical descriptions have reinforced this image of abundance in vegetation and wildlife. American trappers once referred to the San Pedro River as "Beaver River." One group of trappers collected 1,200 skins between March 3 and 10, 1833. Members of the Mormon Battalion caught "salmon trout" up to eighteen inches long near the Babacomari River. James Tevis noted that the grass in the San Pedro Valley was so tall he could not see the heads of antelope in numerous herds (Huckleberry, 1996).

Currently the basin supports a mature riparian forest gallery of cottonwood, willow, mesquite trees and numerous grasses along the valley floor. The upland areas of the basin find desert scrub, oak savannah and ponderosa pine forests. An estimated 390 species of birds, 83 species of mammals and 47 species of amphibians and reptiles can also be found in the basin. Several million migrating songbirds have been found to use the riparian habitat along the San Pedro River. The Upper San Pedro is also home to at least three endangered species; the southwestern willow flycatcher, the Huachuca water-umbel, and the jaguar.

2.4 HISTORY AND LAND USE

The earliest people known to occupy the San Pedro Basin were hunters and gatherers. Transition from hunting and gathering to an economy that relied, in part, on agriculture began the first century AD. The Hohokam brought advanced agricultural techniques and irrigation from Mexico. Settlements increased in size and trade took place

with groups as distant as central Mexico. Between 1250 and the arrival of the Spaniards in the 1500s, however, human activity in the region declined dramatically.

Spanish explorers wrote the first descriptions of the San Pedro River Basin. Journals of Fray Marcos de Niza's 1539 expedition and those describing Francisco Vásquez de Coronado's expedition two years later concur that many small villages with irrigated farms dotted the "Nexpa River," a river assumed to be the San Pedro River. By the mid-1600s, Athabascan-speaking Apaches established strongholds in the mountains nearby. In 1686, the first mining operations began at "La Cananea" (Agüero, 1999 and Hadley, 1999).

During the late 1690s, Jesuit missionary Father Eusebio Kino made several trips down the river he called the Río de San Joseph de Terrenate or the Río de Quiburi, where approximately 2,000 Sobaipuri Pimas were living in twelve to fifteen villages. They practiced irrigated agriculture, lived in reed houses, and raised corn, beans, cotton, and squash. Kino established missions and visiting stations at Quiburi, Gaybanipitea, and Cuachuca. Along with the Catholic faith, Kino introduced European crops, livestock, and tools (Hadley, 1999).

The missions were abandoned and the agrarian Pimas were relocated during the early 1700s because of Apache raids along the river corridor and outbreaks of malaria. In the 1770s, Spaniards made another attempt to reoccupy the San Pedro River valley. They established a garrisoned fort, near the abandoned mission at Quiburi, but the presidio remained only a few years withstanding several attacks by Apaches. In 1780 the presidio was moved south to Las Nutrias near the headwaters of the San Pedro River (Hadley, 1999).

Land grants, in the San Pedro Basin and the surrounding area, were given by the early Mexican government, permitting the introduction of large cattle ranches. By the 1830s, however, frequent Apache attacks forced the owners to abandon their ranches leaving herds of cattle to become wild. Strangely, the wild cattle in the area later served as combatants in the Mexican-American war (1846-1848). The wild bulls stampeded a line of American troops known as the Mormon Battalion, en route to southern California. Ten to fifteen animals were killed, and three soldiers were wounded. The "battle" lasted only a few minutes but has been immortalized as the Battle of the Bulls (Church History, 1989).

In 1854, the Gadsden Purchase transferred approximately 1,700 square miles (4,403 square kilometers) of the Upper San Pedro River watershed to the United States. In 1858 a protective garrison was completed near the mining operations in Cananea, allowing increased production. In 1877, mineral discoveries at Tombstone and Bisbee launched the area's mining production, along with associated activities, including ore milling, fuelwood cutting, and lumbering.

In 1877, the Church of Jesus Christ of Latter-Day Saints (Mormons) authorized settlement along the San Pedro River, and Mormon farmers began constructing irrigation canals, draining beaver dams, and digging wells. In 1881, the Southern Pacific Railroad was completed across southern Arizona, allowing increased mining development and fast importation of livestock. Within four years, the watershed's grazing ranges were stocked to capacity (Hadley, 1999).

Mining and ranching have remained a large part of the land use of the Upper San Pedro Basin, especially in Mexico. Currently the mine in Cananea is the only large

active mine remaining in the Upper San Pedro Basin. In 1959, many of the large tracts of land in Mexico, once used for large scale ranching, were broken into smaller parcels of public land in the form of ejidos, converting over 253,000 hectares to 853 ejidatarios in seven new population centers (Agüero, 1999).

In the United States since the end of World War II, a population boom has occurred in the Upper San Pedro Basin. Since that time there has been an increase and recently a small decrease in agriculture, where recently land has been removed as part of conservation efforts. Grasslands and desert scrub once used for grazing are being converted into subdivisions to support the increasing populous. The driving forces behind the population growth in the area include its appeal as a retirement destination, military and border patrol staffing, as well as its self-sustaining service industries.

CHAPTER 3
HYDROGEOLOGY

3.1 HYDROGEOLOGIC UNITS

The basement complex of the San Pedro Basin consists of crystalline and consolidated sedimentary rocks. These granitic, metamorphic, volcanic and consolidated sedimentary rocks comprise the mountain ranges encompassing the basin. Because of their low permeability and porosity, these rocks are not generally utilized for their water bearing capacity, except in a few locations. For the purposes of this study, these rocks are considered impermeable. This bedrock lies unconformably beneath the hydrogeologic units discussed below.

3.1.1 Pantano Formation

The Pantano Formation is potentially an important water-bearing unit locally and yields water through fractures to many wells in the Sierra Vista area. The unit is described as semi-consolidated brownish red to brownish gray conglomerate (Pool and Coes, 1999). Halverson (1984) indicated that the formation ranges in thickness to over 2500 meters in the central portion of the Upper San Pedro Basin. It is considered in this study first, as it is the lowest significant hydrogeologic unit. Because the Pantano Formation consists of consolidated pre-Basin and Range sediments, it has not been traditionally considered as part of the regional aquifer system.

3.1.2 Regional Aquifer

The primary regional aquifer consists of the weathered material from the surrounding mountains and deposited in the structural depression between mountain ranges (see Figure 3-1). Within the San Pedro Basin, the composition of the material making up the basin fill varies with depth, distance from source, and from region to region. The variance is due in part to sediment composition, transport and depositional processes occurring in the basin region (ADWR, 1991). The basin fill of the regional aquifer is typically divided into two parts: the upper basin fill and the lower basin fill.

Where saturated, the lower and upper alluvial units of the basin fill are in direct hydraulic connection with each other. Because of their vertical and horizontal changes in composition, the upper and lower basin fill units behave as one hydrologic unit (Freethey, 1982). Silt and clay layers within the upper and lower units of basin fill split the groundwater flow into deep and shallow flow systems (Pool and Coe, 1999). A large clay unit exists near the St. David and Benson area. This large clay unit is referred to as the St David Formation (Gray 1965).

3.1.2.1 The Lower Basin Fill

The lower basin fill is an important water-bearing unit throughout most of the basin. This unit overlies the Pantano Formation and consists of poorly sorted interbedded gravel and sandstone of variable cementation. The thickness of the lower basin fill ranges from a few meters along the edges of the valley to possibly more than 300 meters in the center of the basin.

3.1.2.2 The Upper Basin Fill

The upper basin fill overlies the lower basin fill and has a depth of greater than 200 meters in some portions of the Upper San Pedro Basin. The upper unit consists of poorly cemented, to unconsolidated sediments consisting of compacted silty and clayey gravel beds along the mountain fronts to well bedded silt and sandy silt in the central portion of the basin (ADWR, 1991).

3.1.2.3 Confining Zones

The St David Formation consists of nearly 300 meters of clays, silts and in some places freshwater limestones. The thickness of the clays may be up to nearly 100 meters thick near the center of the Benson sub-watershed. The clay layers form an aquitard between the coarse grained sediments of the overlying floodplain aquifer and the regional aquifer below (Jahnke, 1994). These clay layers are observed to confine the water bearing units below, thus creating artesian conditions in wells penetrating the confined sediments. In some areas, artesian conditions exhibit flow above the ground surface, creating flowing artesian wells. However, Vionnet (1992) and the ADWR (1991) indicate a reduction in the water level of artesian wells due in part to pumping from the confined aquifer and the release of water pressure by uncapped flowing artesian wells

In 1887 a major earthquake struck the San Pedro Basin. This earthquake is believed to have caused swamps and cienega (cienaga is Spanish for "swamp") areas in the St David area to be eliminated as well as causing some springs to dry while others emerged. The quake also caused artesian pools to appear and many existing wells and

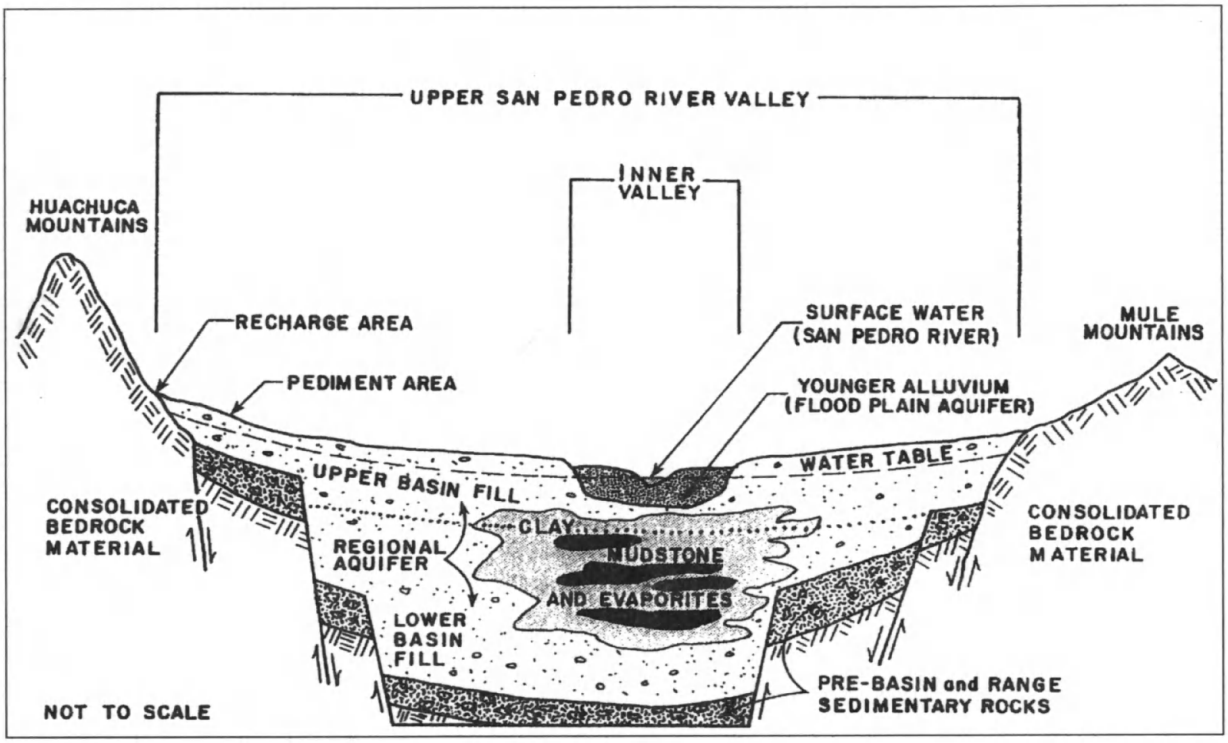

Figure 3-1 Conceptual cross-section of the Upper San Pedro Basin (adapted from ADWR, 1991)

wells drilled after the earthquake began to flow under artesian conditions (Hadley, 1999 and ADWR, 1991).

Other areas where artesian conditions exist in the Upper San Pedro Basin include the Palominas-Hereford and Redington areas, where the regional aquifer is locally confined. The St. David clays are not a significant water-bearing unit, and are not generally considered as part of the aquifer systems in the basin. However, the clays have significant effects on flow in the more permeable sediments, and are thus important to recognize within the regional aquifer system.

3.1.3 Floodplain Aquifer

The floodplain alluvium consists of unconsolidated gravel, sand, and silt laid down by recent stream action along the San Pedro River and its tributaries. The alluvium

forms a long, narrow and relatively shallow aquifer beneath and on both sides of the San Pedro River. The floodplain generally overlies the regional aquifer and confining clays mentioned above. The floodplain ranges in thickness from over 50 meters in central portions of the basin, to very shallow (virtually non-existent) as stream flow runs over exposed bedrock.

3.2 STREAMFLOW

The San Pedro River has a variably entrenched channel that meanders through its floodplain and riparian forest area. The depth of entrenchment generally increases downstream along the reach from the Mexican border to Fairbank. Most of the sediment in the channel is coarser than that exposed in the arroyo walls, especially near the mouths of tributaries (Huckleberry, 1996).

Stream flow in the river is variable spatially and temporally. The reaches from Hereford to Cahrleston are generally gaining and are perennial. The shallow and exposed bedrock found near Charleston and the Lewis Springs areas governs the gains in this portion of the stream. This geologic restriction near Charleston forces the water traveling in the regional aquifer upward into the floodplain and into the stream contributing baseflow to the river. The San Pedro River from Fairbank to "The Narrows" flow is intermittent, however a similar geologic constriction to the one mentioned previously, exists at "The Narrows", which forces regional groundwater upward into the floodplain. Below "The Narrows" to Redington, stream flow is generally intermittent except for short perennial segments where bedrock is at or near the surface, such as the case above the Redington streamgage (Huckleberry, 1996).

CHAPTER 4
CONCEPTUAL MODEL

4.1 MODELING METHOD

The creation of a conceptual model was accomplished through the use of a Geographic Information System (GIS) software, namely ArcView. ArcView is produced by Environmental Systems Research Institute, Inc. (ESRI) and used primarily to view point, line, and polygonal shapes (or coverages) in a spatial context. These shapes are linked to attribute information contained in a database format (topology). Points, arc, and polygons represent map features within a coverage. All shapes used in the conceptual model conform to the Universal Transverse Mercator (UTM) coordinate system using North American Datum (NAD) 1927.

4.2 GEOLOGIC BOUNDARIES

Geologic boundary conditions in the San Pedro Basin were determined visually using geologic coverages and Digital Elevation Models (DEM's) obtained from the USGS, The Environmental Protection Agency, and IMADES. These coverages are working documents, and therefore have no associated guarantee as to the accuracy of the content. The geologic coverage designates differing rock types. From the geology, the areal extent of the active model domain was determined. The model contains only those. areas designated as alluvial. Within this area, however, there are bedrock outcrops. These outcrops were removed from the model domain. Figure 4-1 is an image adapted from the geologic coverages of the Upper San Pedro Basin.

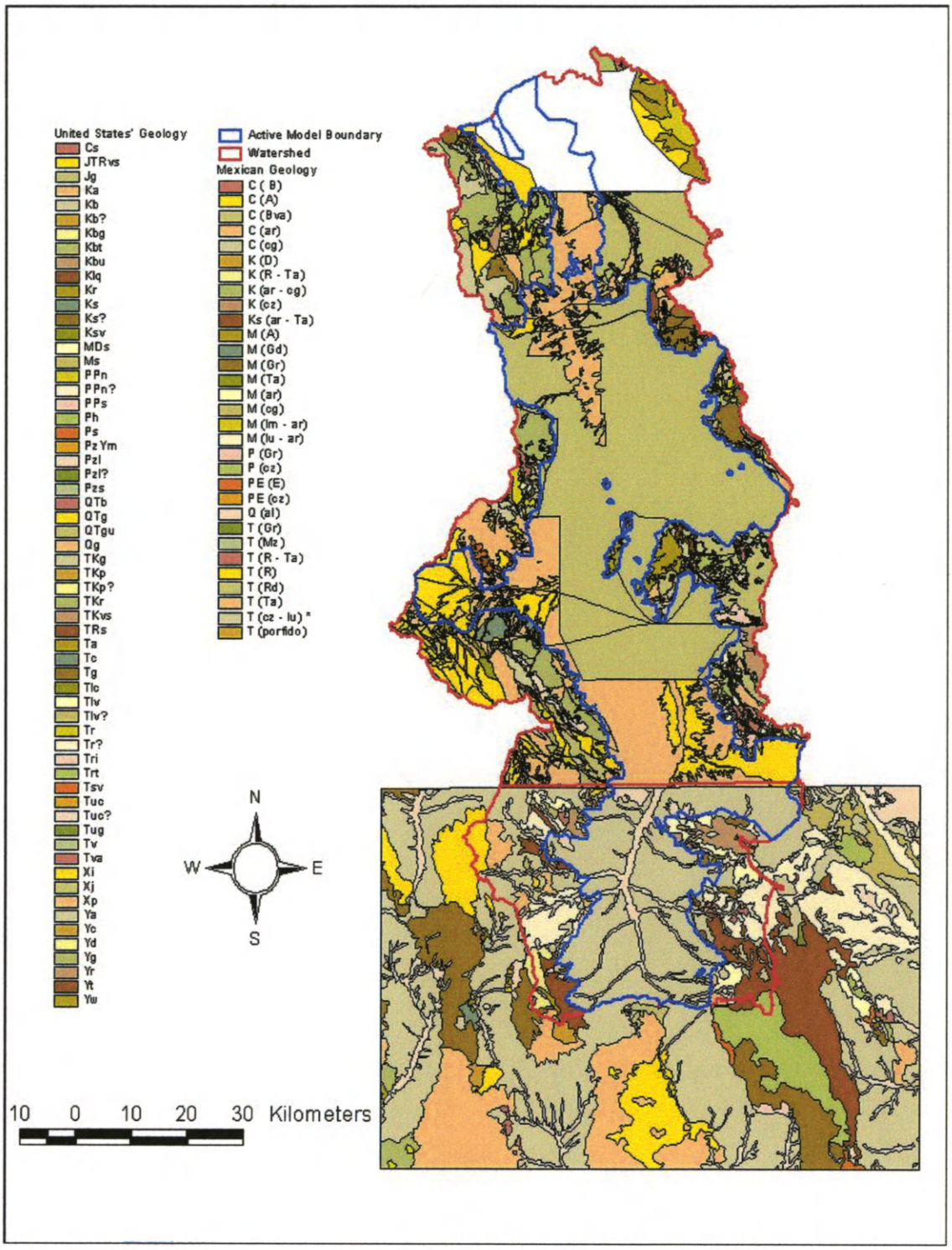

Figure 4-1 Geology of the Upper San Pedro Basin (USGS, 1999; Arias, 1999)

4.3 LAYER 1

Many areas along the mountain front have steep hydraulic gradients and perched conditions due to shallow bedrock. In order to simulate these observed conditions, and retain water in the steeper portions of the San Pedro model domain, a layer was created in the areas having greater than 3.0-degree slope. This layer provides a different modeling strategy than has been used in previous modeling exercises in the San Pedro Basin. In order to determine the areas having the greater slope, a slope analysis was performed using the DEM's of the San Pedro Basin. The slope analysis indicated that there are four major areas which have a steeper than 3.0 degree slope. These areas are along the Babocomari river, northeast of Tombstone, and the areas on the east and west sides of the floodplain extending from "The Narrows" to Reddington. Figure 4-2 delineates the portions of the active model area with the steeper slopes.

The hydraulic properties of Layer 1 are those of the regional aquifer system. Estimates for hydraulic conductivity within the regional aquifer, taken from previous studies of the basin, range from 0.03 to nearly 4.0 m/day. Hydraulic conductivity zones were created to roughly correspond to those of Jahnke (1994) and Corell et al. (1996). These areas were given very low vertical conductances representative of clay lenses and shallow bedrock, which restrict the vertical flow of water in these areas.

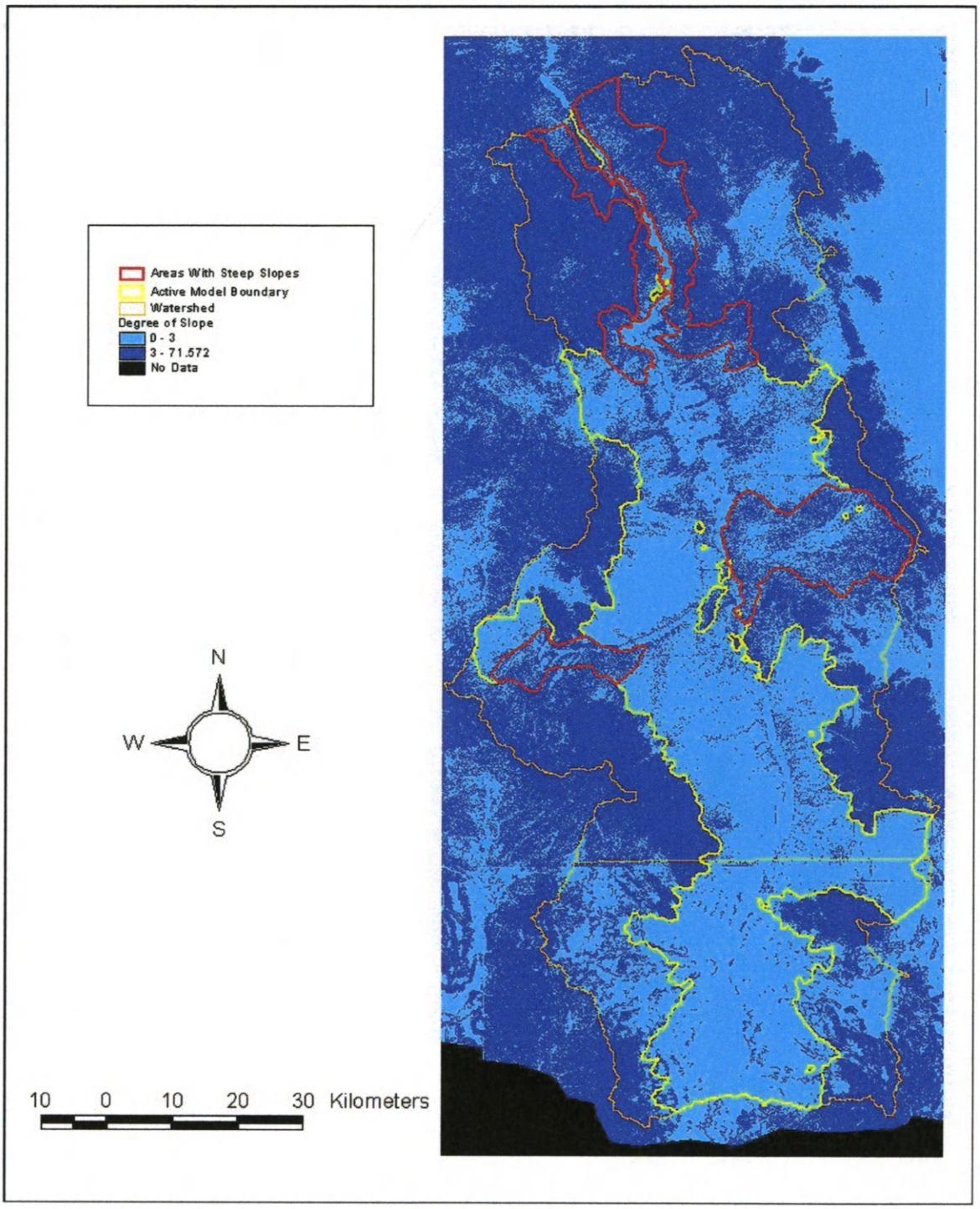

Figure 4-2 Steep sloping areas of the Upper San Pedro Basin

4.4 LAYER 2

Just as in layer 1, layer 2 does not conform to the way that the San Pedro Basin has traditionally been modeled. Layer 2 includes both the Upper Basin fill of the regional aquifer, and the floodplain aquifer. This modeling technique was necessary to provide for a layer beneath layer 1. The layer below layer 1 was necessary in order to allow water to be transmitted from layer 1 to layer 2. In other words, model layers need to be ordered vertically, and consecutively. Layer 1 must overly layer 2, and layer 2 must overly layer 3 (the numerical model does not allow water to transmit from layer 1 directly to layer 3). The top elevations of layer two are the surface elevation, except where layer 2 is overlain by layer 1.

The floodplain portion of layer 2 was given the constant hydraulic conductivity value of 50 m/day, and a constant depth of 35 m. The lateral extent of the floodplain was determined using the hillshade of the DEM (which provides a three dimensional appearance) and geologic map provided by the USGS, see Figure 4-1. Specific yield of the floodplain and upper basin fill were given the constant values of 0.15 and 0.08 respectively. Layer 2 was given the constant storage coefficient of 0.0001. The values for specific yield and storage coefficient are consistent with the study by Corell et al (1996). Hydraulic conductivities of the upper basin fill portion of layer 2 range from 0.1 to over 10 m/day.

4.5 LAYER 3

Layer 3 loosely corresponds to the lower basin fill of the regional aquifer system. The lateral extent of layer 3 has been constricted in many areas from that of layer 2. The

reduction in lateral extent is representative of the bowl-like nature of the underlying crystalline bedrock of the geologic basin.

The hydraulic properties of layer 3 are similar to the regional aquifer properties of layer 2. Namely, hydraulic conductivities fall within the same range, and specific storage and specific yield are given the constant values of 0.0001 and 0.08 respectively.

4.6 LAYER 4

Layer 4 represents the consolidated sediments 305 meters (~1000 feet) below the ground surface. Halverson (1984) conducted a gravity study in the Upper San Pedro Basin that was used to determine the lateral extent and depth to bedrock measurements utilized in this study. The sediments below 305 m (which are above crystalline "bedrock") are representative of the Pantano Formation.

The conductive property of the layer 4 differs from the other layers in that it is addressed as transmissivity. The thickness of the layer is known, and an average hydraulic conductivity was assumed over the thickness. Relatively little is known about the hydraulic properties of this layer at depth. However zones of transmissivity were easily established using layer thickness. Hydraulic conductivities of the sediments were given a constant value of 0.1524 m/day. This hydraulic conductivity value translates into values of transmissivity ranging between 46.45 to 418.06 m^2/day depending on thickness. The thickness of layer 4 ranges between 305 meters along the edges to nearly 2500 meters in the center of the basin near the Mexican border. Figure 4-3 shows the relationship of all 4 layers contained in the model.

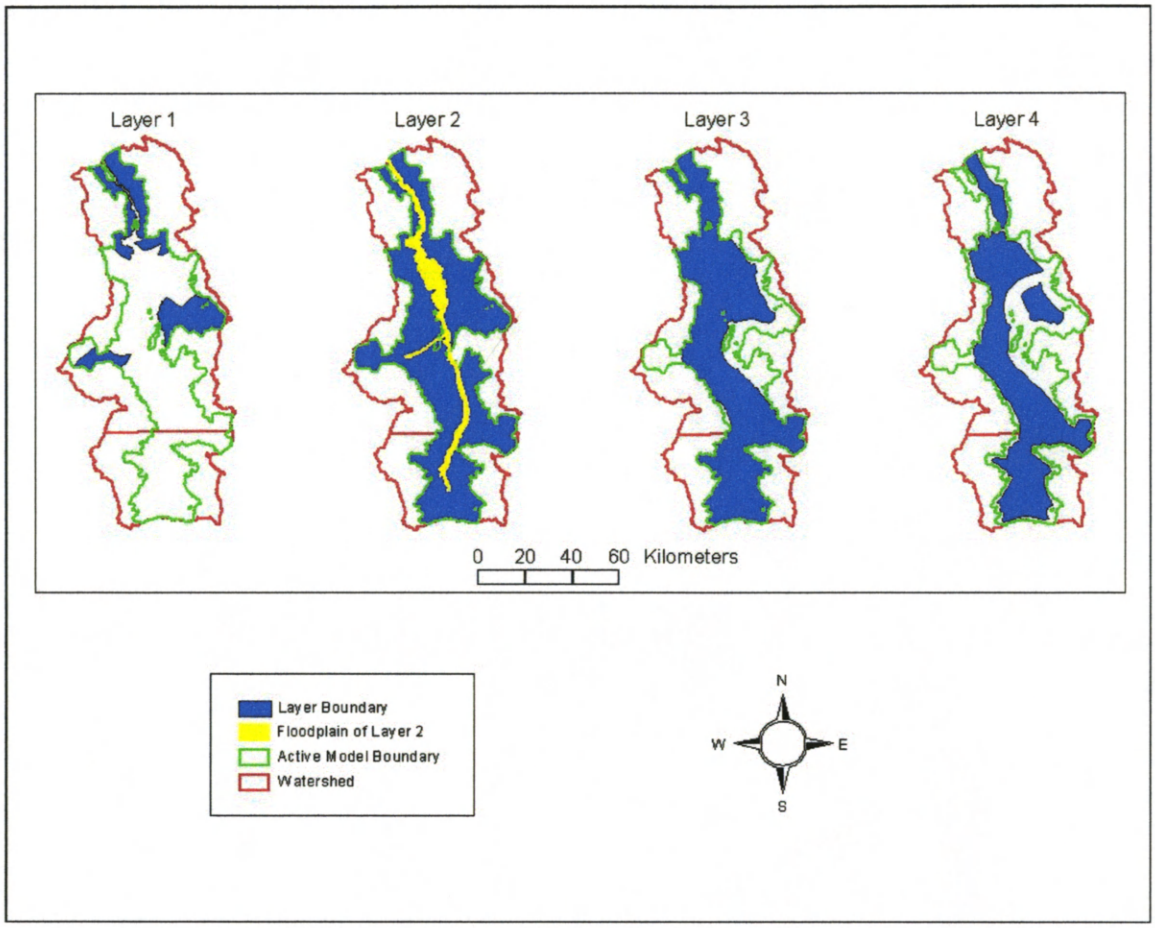

Figure 4-3 Conceptual model layers of the Upper San Pedro Basin

4.7 AREAL RECHARGE AREAS

The primary sources of areal recharge into the San Pedro Basin are from mountain front recharge and infiltration of irrigation waters.

4.7.1 Mountain Front Recharge

The primary source of groundwater recharge into the San Pedro Basin occurs along the mountain front. Mountain front recharge is the water that infiltrates into the zone of coarse alluvium that extends from the base of the mountain into the basin. Water flows downward through the unsaturated zone in a broad band paralleling the mountain

front. The width of the recharge zone is dependent on the nature and magnitude of the runoff from the consolidated rock areas. Infiltration takes place in the coarse grained unconsolidated sediments. Subsequent movement of water through the unsaturated zone is controlled by the unsaturated hydraulic conductivity, which varies with the physical nature and the moisture content of the sediments. Some perched water may occur on hardrock pediments near the mountains or overlying low permeability fine-grained sediments in the recharge zone (Anderson, 1992).

The quantity of water potentially available for recharge is assumed to be equal to the precipitation minus evapotranspiration on the watershed. Part of the precipitation accounts for changes in soil moisture, which are assumed to be small over a long period. The equation developed by Anderson and others, Equation (1), is used to determine regional mountain front recharge amounts.

$$\text{Log } Q_{rech} = -1.40 + 0.98 \text{ Log } P \qquad (1)$$

The Q_{rech} is the recharge rate, in inches per year, and P represents the average amount of basin-wide precipitation in excess of 8 inches per year (Anderson, 1992). The average precipitation for the Upper San Pedro Basin is 0.418 m/yr, which equates to 16.47 in/yr. Precipitation (P) for the Anderson equation is 8.47 inches. Solving for Q, the resulting recharge rate equals 0.0082 m/day. Multiply the recharge rate by the area of the basin, 7.56×10^9 m^2, the resulting volume of mountain front recharge to the basin is 1.7×10^5 m^3/day (50,306 Acre-ft/yr). Figure 4-4 shows the average precipitation within each mountainous catchment contributing to the Upper San Pedro Basin.

Estimates from the ADWR (1991) assume approximately 10138 m^3/day (3000 acft/yr) of mountain front recharge occurs in Mexico, which in turn flows into the United

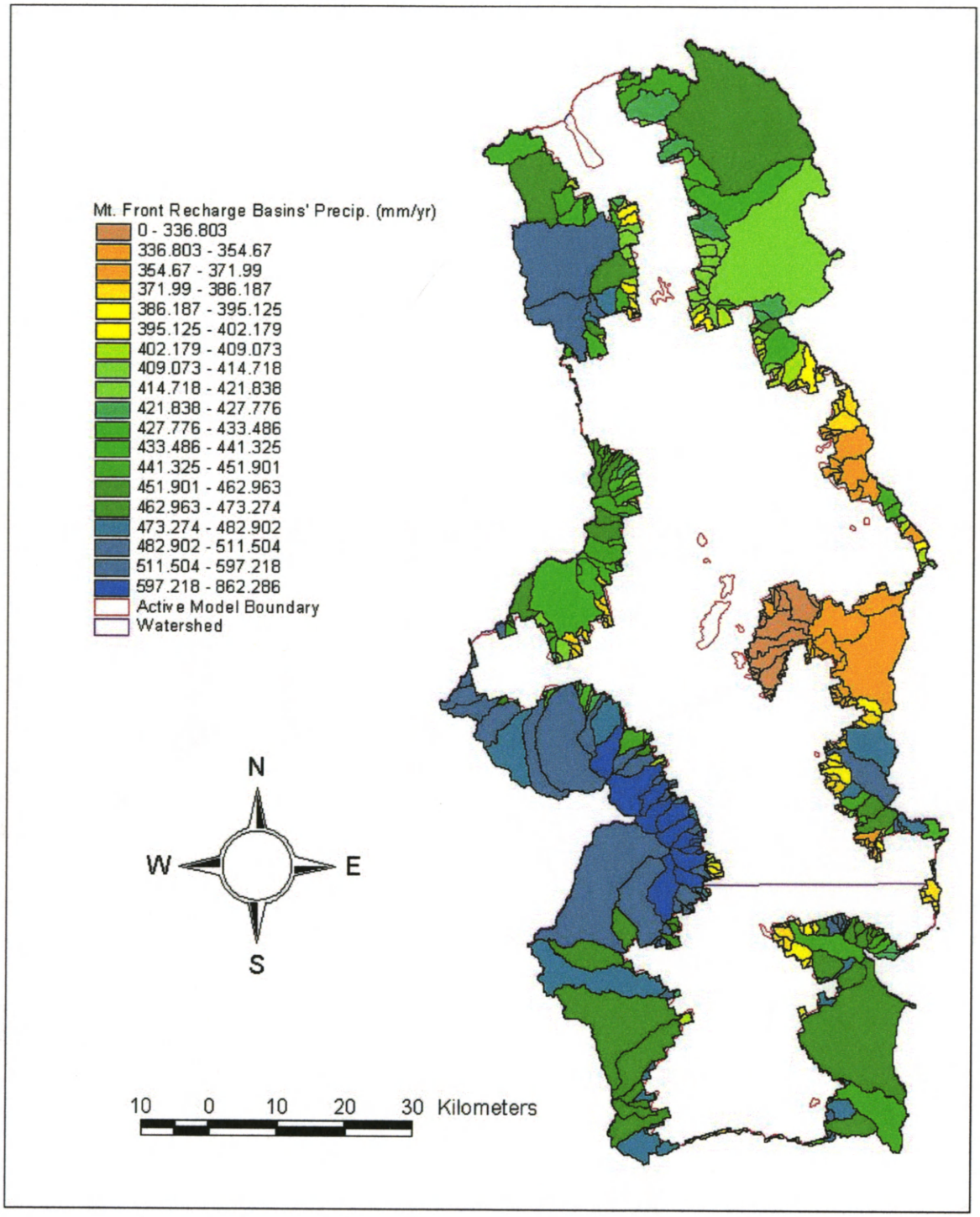

Figure 4-4 Mountain front recharge basins

States at the international border. The Sierra Vista sub-watershed adds an estimated 54070 m^3/day (16000 acft/yr). The Benson sub-watershed adds another 39742 m^3/day (11760 acft/yr). Assuming half of the recharge of the Redington sub-watershed occurs between "The Narrows" and the city of Redington, recharge to this portion of the study area is approximately 34385 m^3/day (10175 acft/yr). The mountain front recharge estimates of the ADWR add up to 138336 m^3/day (40935 acft/yr) throughout the Upper San Pedro Basin (ADWR, 1991 and Corell et al, 1996).

It was assumed that given the two estimates of regional mountain front recharge above, a reasonable value for recharge would fall within the range of 138336 m^3/day (40935 acft/yr) and $1.7x10^5$ m^3/day (50,306 Acre-ft/yr). The initial mountain front recharge estimate used within this study is 154170 m^3/day (45621 acft/yr) for the Upper San Pedro Basin. The distribution of mountain front recharge into the numerical model is discussed in Chapter 6.

4.7.2 Agricultural Recharge

Agriculture is a major water user in the basin, especially along the floodplain where water is used mostly for irrigation. The water used for irrigation may be applied in a number of ways including flood, furrow, and sprinkler methods. Each of these methods provides water for plant use as well as water evaporation. The water not consumed by plants and evaporation percolates through the soil and recharges the aquifer beneath. The ratio for consumed water to recharged water is 70:30, where 70% of irrigation water is consumed and 30% of the water is recharged into the underlying aquifer. This general percentage distribution is deemed reasonable by Slack (2000), and is consistent with agricultural recharge percentages presented by Freethey (1982).

Agricultural lands where recharge occurs were determined by 1997 satellite coverage information concerning land use. Agricultural lands are seen as polygons. These polygons include both currently active agricultural lands as well as those lying fallow. Agricultural polygons within 120 meters of each other were grouped together as the same polygon. The polygon needed to be at least 10000 m^2 (1 ha) in size to be considered significant in the model.

A recharge rate for each polygon was computed using the pumping rate for all irrigation wells within 300 meters of a polygon. The pumping rate for all of these wells were added together and then divided by the area of their associated polygon. This irrigation rate was then reduced by 70%, leaving 30% of the total irrigation rate to be applied to the polygon as recharge. See Figure 4-5 showing agricultural and riparian areas together.

As irrigation areas and wells were removed from the model over time, such as the case with the creation of a conservation area, the recharge polygon was removed in addition to its associated wells. This process removed not only the recharge process but the local pumping stress as well. If irrigation wells were not associated with an agricultural polygon, or one large enough to meet the size criteria, none of their pumping was attributed to recharge.

A total of 592 wells were associated with recharge polygons for the entire basin. An additional 33 wells were not associated with an agricultural recharge polygon, 2 of which were associated with agricultural polygons smaller than 10000 m^2. For further discussion of wells see Chapter 5.

4.8 EVAPOTRANSIRATION AREAS

Riparian areas exist along the floodplain of the San Pedro River. The areal extent of the riparian area was determined from satellite coverages of the San Pedro Basin from 1997 (the extent of the riparian area in 1940 is assumed to be the same as 1997). It is generally accepted that phreatophytes, groundwater-using plants, only exist along the floodplain due to the relatively shallow water table conditions. There are three types of phreatophytic vegetative cover, significant to this study, defined within the riparian area: cottonwood-willow (*Populus fremontii* and *Salix gooddingii*), Mesquite bosque (*Prosopis velutina*), and a mixture of the two types. There are other types of vegetation suspected of using groundwater along the floodplain, namely tamarisk and saccaton grass, however they are not considered within this study as they were deemed insignificant on the regional scale.

Along the floodplain of the San Pedro River, the cottonwood-willow (*Populus-Salix*) are the dominant and sub-dominant overstory species. They form a narrow forest gallery along the floodplain, and are obligate phreatophytes, relying almost solely on groundwater for their water needs. The mesquite (*Prosopis*) are present generally as a subdominant tree or shrub within and near the cottonwood-willow forest gallery. Mesquite exist as an opportunistic phreatophyte, relying on groundwater when easily available and taking advantage of shallow water resources from recent precipitation events. Mesquite also exist as an upland species (where groundwater is out of reach) relying on water from precipitation alone (Snyder and Williams, 2000).

The water used by plants for evaporation and transpiration processes is referred to as evapotranspiration (ET). As this study is interested only in the interaction of plants with groundwater, all further references to ET assume only groundwater use. This assumption holds fairly well for cottonwood and willow trees, but tends to be an overestimate of mesquite groundwater consumption, as studies have not been able to conclusively differentiate between mesquite's groundwater and surface water sources. Mesquite, as mentioned before, is opportunistic in its water consumption. Water sources for mesquite plants can vary depending on site location (Goodrich et. al., 2000; Snyder and Williams, 2000).

Water use for ET can be addressed as a rate. Evapotranspiration rate estimates from the ADWR given per sub-watershed are, 2.455×10^{-3} m/day, 2.279×10^{-3} m/day, 2.029×10^{-3} m/day, for the Benson, Redington, and Sierra Vista sub-watersheds respectively (ADWR, 1991). Estimates from a more recent study show ET rates based on vegetation type, 2.074×10^{-3} m/day for cottonwood-willow and 1.027×10^{-3} m/day for mesquite (Scott, 1999). The larger ET estimates by the ADWR may be due in part to near stream pumping. Estimates from Scott (1999) have been utilized in this study.

As a side note, because of the beauty and essential wildlife habitat associated with the riparian area along the San Pedro River, the San Pedro River National Conservation Area (SPRNCA) was created in 1988. The SPRNCA has served to protect the riparian area, and has laid dormant many previously active agricultural areas now lying within its boundaries. The reduction of groundwater use caused by the creation of the SPRNCA will be addressed further in Chapter 5. Figure 4-5 shows the relationship of agricultural and riparian areas. The boundary of SPRNCA is also delineated in Figure 4-5.

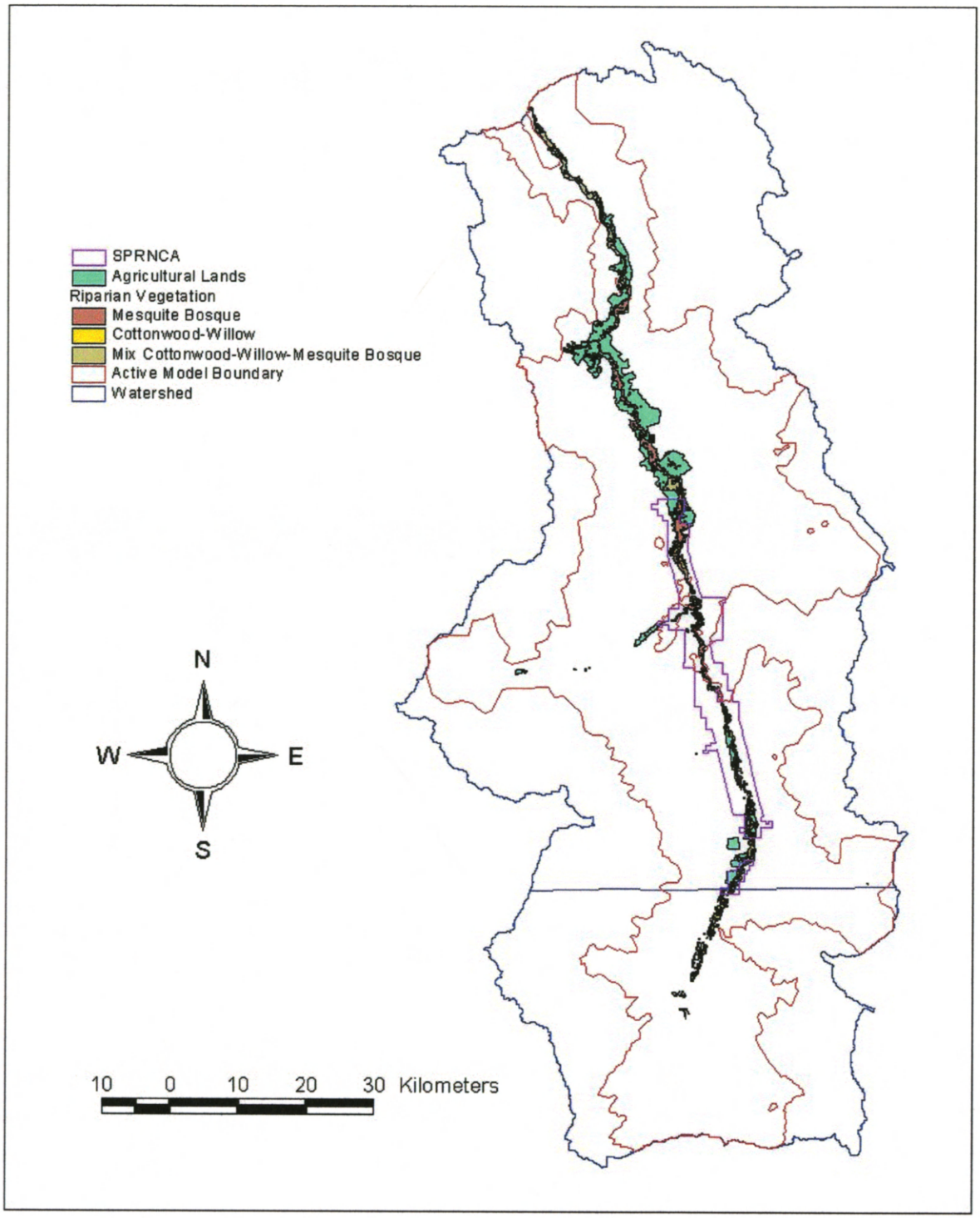

Figure 4-5 Riparian and agricultural areas

4.9 STREAMS AND DIVERSIONS

The streams included in the modeling area are the San Pedro and Babocomari Rivers, Ash Creek, Paige Creek, and Hot Springs Creek. There are two major diversions, namely the St. David Ditch and Pomerene Canal which both remove substantial amounts of stream flow from the San Pedro River.

The San Pedro River is the primary drainage for the San Pedro Basin. Flow in the San Pedro consists of two components, runoff and baseflow. Runoff is stream flow resulting from individual rainfall events on the watershed and occasional snow melt in the surrounding mountains. Baseflow is stream flow resulting from the discharge of groundwater to the stream and is characterized by sustained low flows showing relatively little daily variation. This model is treating only the baseflow component.

The San Pedro River is perennial in many areas. The perennial flow is due to factors involving the discharge of groundwater to the stream, which provides a steady and reliable source of water to the river. The areas of the river that gain water from groundwater, are thus referred to as gaining reaches. Causes for the gaining reaches include geologic restrictions, which force groundwater to the surface, resulting in stream flow in addition to stream flow caused by normal water table conditions.

The San Pedro River in other areas exhibits intermittent behavior, with seasonal appearance and disappearance of flow. Causes for intermittence include seasonal phreatophyte use of water, as well as groundwater pumping. The notable absence of water occurs primarily in the summers, when plants along the river have the greatest water demand, as well as water is being removed by near stream pumping which is then

applied to irrigable crops. Water returns to these areas when phreatophyte and irrigation demands for water are lowest, during the winter and early spring.

The Babocomari River is the largest tributary to the San Pedro River, with its confluence near Fairbanks. The Babocomari maintains perennial flow in two reaches at a distance of approximately 4 and 15 miles from the confluence with the San Pedro River however, flow in this tributary has been ungaged until recently (Putman et al, 1988).

The Ash, Paige, and Hot Springs Creeks flow into the San Pedro River north of Benson. Both Paige and Hot Springs Creeks flow into the San Pedro north of the Narrows. No published data were obtained on flow rates or total discharges for Ash or Paige Creeks. However, Ash Creek apparently did flow perennially prior to the development of the area (ADWR, 1991). Both Ash and Paige Creeks were given estimated baseflows of 978 m^3/day (289 acft/yr). Hot Springs Creek has an estimated baseflow of 6229 m^3/day (1846 acft/yr). The values for baseflows given above were calculated in the report by Jahnke (1994), and are maintained here for consistency with that report. For further information on the calculation of these baseflows, it is suggested that the reader refer to this report.

Diversions into the St. David Irrigation Ditch, located 7 miles south of St. David, began in the 1881. The ditch is 8 miles long and is estimated to have a maximum capacity of 61165 m^3/day (25 cfs) (Putman et al, 1988). Average diversions from 1967 to 1990 recorded by ADWR have taken place at an average rate of 14948 m^3/day (4425 acft/yr) (ADWR, 1991). The St. David Irrigation District supplements low surface water diversions with groundwater from two wells under its control. However, the St. David Irrigation District did not begin to significantly supplement the surface diversions with

pumped groundwater until 1947. The only diversion considered is that of surface water flow within the ditch.

Diversions into the Pomerene Canal began in 1912, when the ditch was known as the Benson Canal. The current dam and works were constructed about ¾ of a mile upstream from the original location in 1934 due to the repeated destruction of the previous works. The canal has been in use since that time, extending approximately 7 miles from its head (Putman et al, 1988). The average yearly flow in the canal calculated by the ADWR (1991) is 5283 m^3/day (1563 acft/yr). Thus, again, only the diversion of surface water is considered as part of the steady state representation of this irrigation canal.

The location of all included streams and diversions within this study of the Upper San Pedro Basin are displayed in Figure 4-6. The inclusion of Ash Creek, Paige Creek, Hot Springs Creek, Pomerene Canal and the St. David Ditch (and consequently their flow rates) is consistent with the modeling approach taken by Jahnke (1994) for the Middle San Pedro Basin.

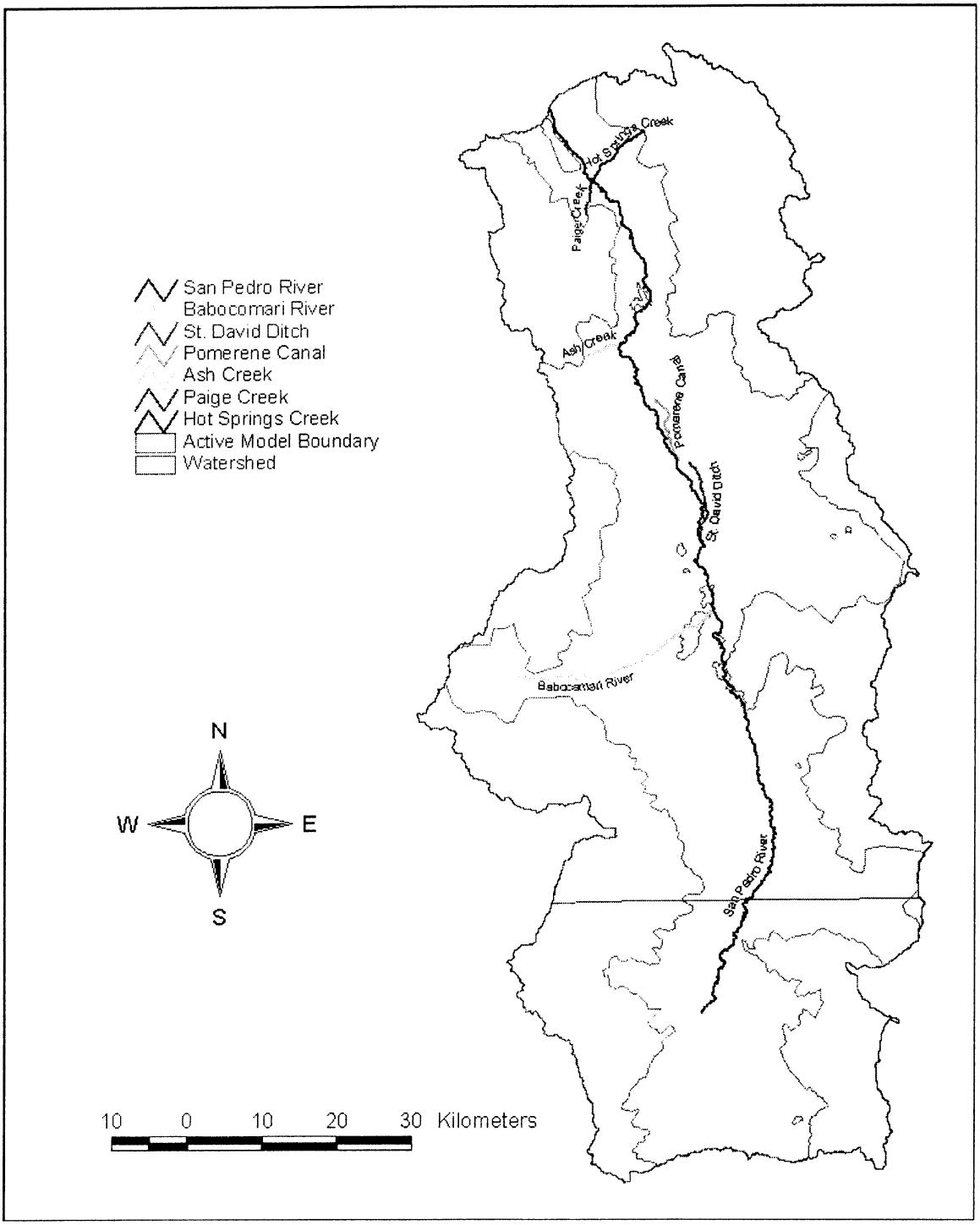

Figure 4-6 Streams and diversions

CHAPTER 5
WELL PUMPING

5.1 U.S. WELLS

The use of wells in the U.S. portion of the San Pedro Basin is recorded and maintained by the Arizona Department of Water Resources (ADWR). Annual well pumpage amounts are reported only for wells within groundwater basins that have been designated as Active Management Areas (AMA's) or Irrigation Non-expansion Areas (INA's) with a pump capacity greater than 35 gallons per minute. Historically, the state of Arizona has not kept close tabs on wells outside of AMA's and INA's however, the information maintained by the ADWR is contained in two areas: the Well Registry and the Groundwater Site Inventory (GWSI).

5.1.1 Well Registry

When the Groundwater Management Act went into effect in 1980, the legislation required all wells to be constructed in Arizona must be registered, and any well in existence before 1980 must also be registered. The Well Registry contains information concerning greater than 130,000 wells throughout the state. The information reported to ADWR by either the well owner or the well driller however, may not have been verified by the state. Information may be incomplete because well registration, while required, is voluntary. There are probably many unregistered wells in existence that are not included

in the Well Registry. Therefore, the State of Arizona and the ADWR do not guarantee the accuracy of this information. No warranty of any kind is expressed or even implied regarding its suitability or usefulness for any purpose.

The positional accuracy of the Well Registry is limited because the well locations are reported to ADWR by township, range, section and section subdivision down to the nearest ten acres (quarter-quarter-quarter section). In order to map these locations every section in the state has been subdivided into 64 ten-acre cells, 16 forty-acre cells and 4 one hundred sixty-acre cells with a label point assigned to the center of each cell. These center points are then used to represent the approximate locations of the wells. There can be more than one well on a location point because all wells within the same ten-acre cell are assigned to the same label point. This method for positioning well points limits the accuracy of any well point to plus or minus 150 meters.

5.1.2 Groundwater Site Inventory

Once maintained by the USGS and now maintained by ADWR, the GWSI differs from the Well Registry in both content and in purpose. The GWSI has more detailed information about the construction method, location, and more recently measured water levels of each well. Each of the GWSI wells has been verified by ADWR field measurements. Each well position is denoted by township-range, latitude-longitude, and UTM. Although there is significantly more information contained in the GWSI, there are fewer wells recorded, approximately 40,000.

5.1.3 Well Selection

The wells selected were within the active model boundary of the San Pedro Basin. All non-pumping wells were eliminated (i.e. observation wells). Because of the more precise and accurate information contained in the GWSI, all wells completed from 1940 to 1979 (as determined from the registration number) were used from this database. The number of wells within this time period totaled 1491. The active time period for these wells was determined by completion date of the well, as recorded in the GWSI. If the completion date for a well was unknown, the well was then determined to be active from the earliest recorded water level reading. If these criteria were not found, remarks recorded in the GWSI were used to determine the earliest time for which a particular well was known to be active. The remarks portion of the database was also used to determine the time for which many wells were destroyed or turned off.

Out of the 1,491 recorded wells, 545 wells had unknown completion dates. The groundwater flow model presented in the next chapter covers 58 years (1940-1997). The first 46 years (1940 to 1985) were subdivided into 11 unequal stress periods (see Table 5-1). The 545 wells were listed in a north-to-south ranking by site identification number (a number consisting of the well location by latitude and longitude combined), and were partitioned into 50 consecutive groups. The first 49 groups had 11 wells, and the last group had 5 wells. The first well from each of the first 49 groups was assigned to stress period 1, the second well was assigned to stress period 2, ... and the eleventh well was assigned to stress period 11. From the last group (50), well 1 was assigned to stress period 7, well 2 to stress period 8,... and well 5 to stress period 11. At the end of this

process, each of the 545 wells had been assigned a stress period; the beginning of each stress period marked the completion date for each well. This method also insured that the wells were uniformly distributed over the north-south direction.

Well information from 1980 to 1997 was taken from the Well Registry. This information was deemed to be as accurate for this time period, and certainly more comprehensive than the GWSI for the same dates. According to representatives from the ADWR, many wells in the registry were never drilled or used. In order to determine which of the registered wells were actively pumping, this report developed the following requirements: the wells must have an approval or installation date, a driller's log, and not have a non-pumping wells designation. Many of these non-pumping wells were classified as test, monitoring, drainage, or exploration. Some of the non-pumping wells had no classification.

Within both the Well Registry and the GWSI, for some wells, there are designations not only of well type but also of primary water use. If there was no primary use designated for a particular well, water use was determined by secondary or tertiary water uses, or by a method that will be described later. The water use types used in the basin are stated below.

- Public Supply Wells
- Irrigation Wells
- Domestic Wells
- Stock Wells
- Industrial Wells

- Commercial Wells
- Institutional Wells

If no water use type was distinguished (only in GWSI did this occur), water use was determined by the following:

- Wells within 1000m of the floodplain, having greater than or equal to 100 gallon per minute (gpm) test pumping rate were considered irrigation wells
- Wells with less that 100 gpm test pumping rate were considered domestic wells outside of the floodplain
- Wells within the floodplain with no associated test pumping rate were assigned as irrigation wells
- All other wells with no associated test pumping rate were considered domestic wells

Previous modeling exercises in the basin have used a technique attributing pumping rates to an area rather than a well point (Freethey, 1982; Putman et al, 1998; Vionnet and Maddock, 1992; and Corell et al, 1996). There are several reasons for the areal attributes. One of the most common is due to the application of the finite difference grids to the basin. If one grid is replaced by another grid of greater density, as was the Freethey (1982) model grid with the Corell et al(1996) model grid, the pumping associated with a single cell in the original grid may get smeared out into multiple cells in the higher density grid. For example, if a single grid cell in the original model contains a well pumping 120 acre-feet, and that cell is divided into four cells in the new grid, these four cells would be assigned wells pumping 30 acre-feet per year.

Another example of areal attributes would be assigning a pumping rate to an irrigated area. If one assumes that an irrigated field is 100 acres and a value of 3 acre-

feet of water is used to irrigate each acre of irrigated land per year, a well with a pumping rate of 300 acre-feet per year would be assigned to this plot of land. This practice is used primarily to determine the amount of water pumped in an area when the location of a well point and well pumpage are not known.

According to the ADWR in its recommendations for future studies, "model results could be improved by a more accurate location of agricultural pumpage in both time and space, as well as a better knowledge of the vertical distribution of pumpage in the aquifer" (Corell et al, 1996). Using the information in the Well Registry and the GWSI concerning well location and well construction within the San Pedro Basin, pumping rates were assigned to individual wells. Figure 5-1 shows the location, as well as the primary water use of the final wells selected for this modeling study within the Upper San Pedro Basin.

5.1.4 Distribution of Well Pumping

The use of individual wells is a unique modeling strategy in the San Pedro Basin to this point. In order to determine pumping rates for wells in the basin, estimates from previous studies were used. Estimates from previous studies however, had reduced irrigation pumpage by 30 percent to account for recharge. It was difficult to extract which wells were used for irrigation and which were not. Because of this 30 percent reduction, pumping rates remained conservatively low, unless actual pumping rates could be obtained. The remainder of this chapter will describe the process by which these pumping estimates were attributed to individual wells (see Figure 5-1).

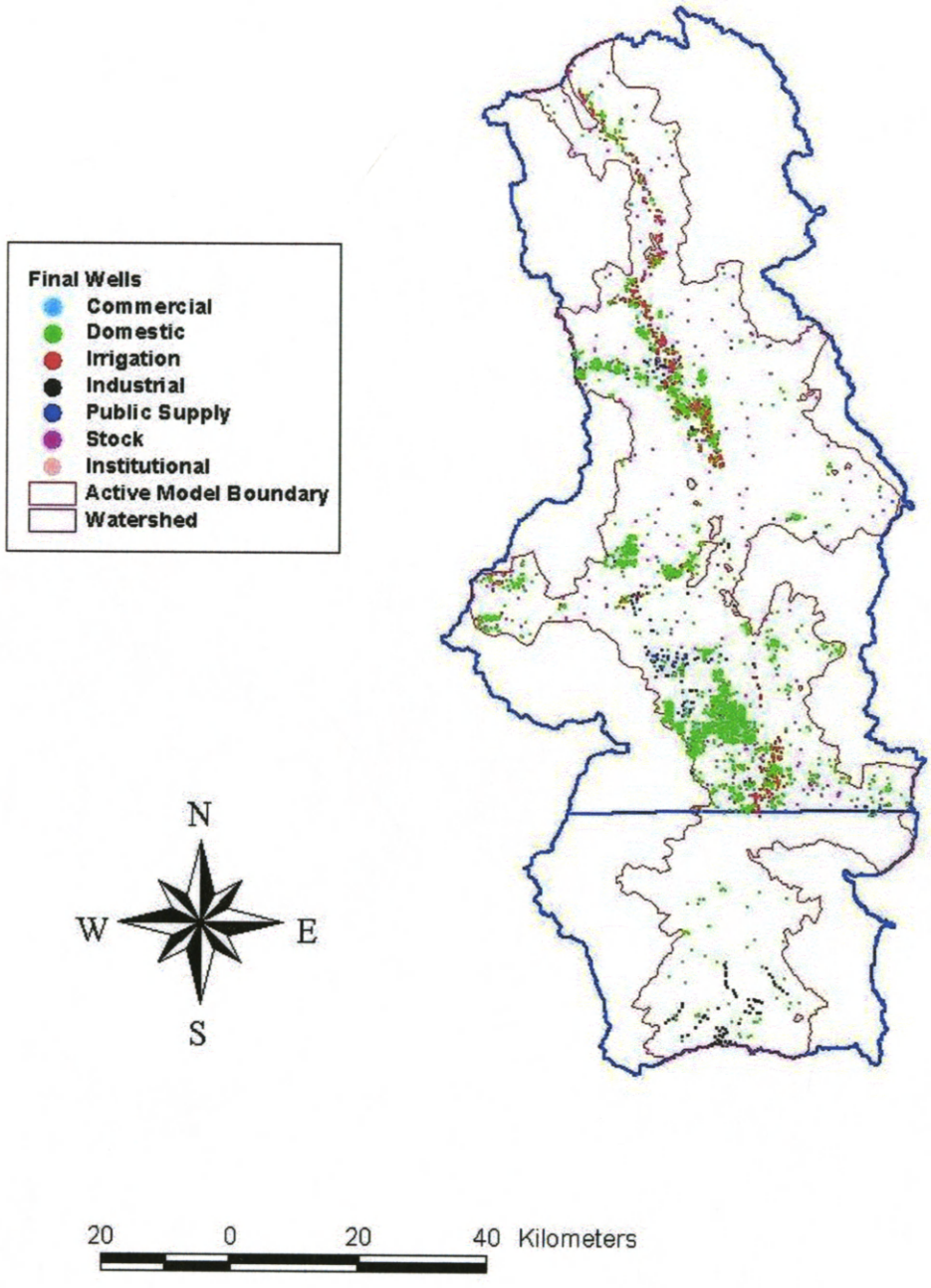

Figure 5-1 Final wells used for simulation

Initial estimates for individual well pumpage were taken from basin wide estimates of pumping. These initial basin wide pumping estimates were obtained from Corell et al. (1996) and Jahnke (1994). Estimated pumping was then distributed by the size and type of the well. For the seven years since 1990 (the last year of available information), estimates for pumping were extrapolated using information from 1990. The average pumping rate for an individual well, of a particular well type, was attributed to new wells of that type introduced after 1990. The pumping rates for the particular year were then summed, and redistributed to individual wells. Figures 5-2 and 5-3 show schematic representations of how pumping estimates for the entire U.S. portion of the basin were then attributed to individual wells.

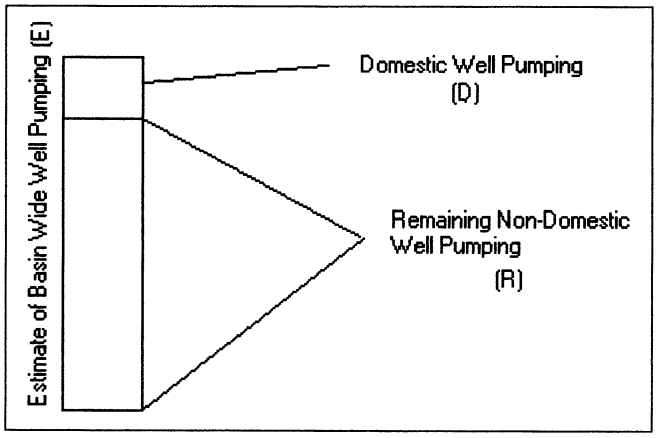

Figure 5-2 Schematic of well pumping distribution

All domestic wells were given a similar pumping rate (discussed further in the Domestic Wells section of this chapter). Each domestic well was assigned a pumping rate of 0.68 m^3/day (0.5 ac-ft/year). The sum of the rates of domestic well pumping (D) was removed from the initial estimate of basin wide well pumping (E), taken from

previous studies by the Corell et al (1996), and Jahnke (1994). The remaining portion of the estimated pumping was non-domestic (R) as seen in Figure 5-2. This process is described in Equation 2.

$$E - D = R \tag{2}$$

The remaining non-domestic well pumping (R) was distributed to individual wells based on the cross-sectional area of the casing for an individual well. It is assumed that there is a direct relationship between the area of a well casing and the amount of water pumped. The limitation on the volume of water pumped from an individual well is its capacity. The capacity is directly related to the area of the well casing. Another assumption is that the cost for creating a large diameter well limits the user to drilling a well only big enough for the wells primary use. A final assumption is that the user of a particular well intends to pump that well to its greatest capacity (minimal expense, maximum yield).

Based on the above assumptions, the distribution of this remaining pumping (R) to individual wells used the process displayed below in Figure 5-3 and Equation 3. Figure 5-3 and Equation 3 show that the area of an individual non-domestic well casing (I_i) was then divided by the total of non-domestic well casing areas (T). The diameters of well casings were obtained from the Well Registry database. If a well did not have a known well casing diameter, it was assigned a well casing diameter based on the average well casing size of that particular well type (i.e. public supply, irrigation, industrial.). The resulting number is the fraction of the total well casing area held by an individual well (P_i).

$$I_i / T = P_i \tag{3}$$

When multiplying the remaining non-domestic pumping rate (R) by the percent area held by an individual well (P_i), the result is the pumping rate of an individual well (Q_i) as seen in Equation (4).

$$R \cdot P_i = Q_i \tag{4}$$

The total number of years represented by the model is 58, from 1940 through 1997. The 58-year development period is divided into 23 stress periods, ranging in

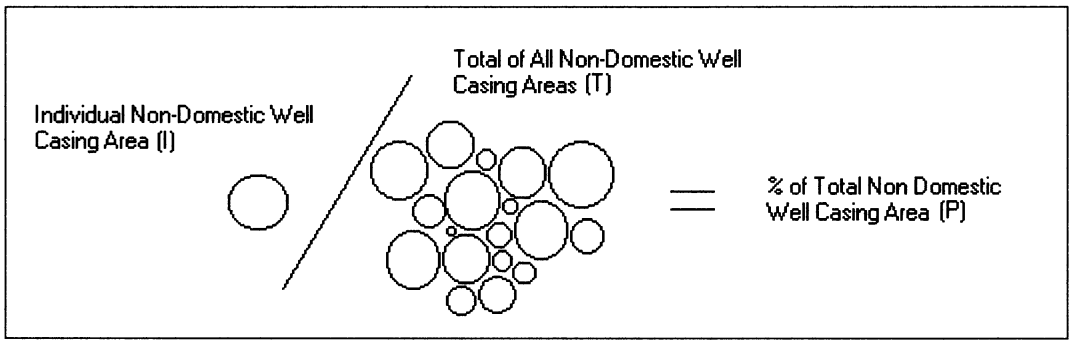

Figure 5-3 Schematic of well casing areas

length from 1 to 13 years. The pumping for each year within a stress period was summed and an average pumping rate was assigned to the stress period. Table 5-1 shows the modeled years and their representative stress periods.

5.1.5 Public Supply Wells

The pumping rates for many public supply wells were changed from the initial estimates mentioned above. The change took place on a company-by-company basis. Pumping information from water companies contained the total volume of water pumped for the entire company, and was not well specific. In order to distribute the total pumping to individual wells, the process of assigning pumping rates based on the cross sectional

area of well casings was used again. The casing cross-sectional areas for all the wells operated by a particular company were totaled. The cross-sectional area of an individual well casing was divided by the total of the cross-sectional well areas within the company. The fraction obtained was then multiplied by the companies' total pumping value in order to obtain a pumping rate associated with an individual well. The public supply wells not associated with a particular company retain the initial estimate assigned to them.

Table 5-1 Stress periods

Stress Period	Years
1	1940-41
2	1942-45
3	1946-50
4	1951-63
5	1964-66
6	1967
7	1968
8	1969-72
9	1973-76
10	1977
11	1978-85
12	1986
13	1987
14	1988
15	1989
16	1990
17	1991
18	1992
19	1993
20	1994
21	1995
22	1996
23	1997

The pumping values for public supply wells were obtained from the individual water companies, municipalities, the ADWR, and from the Arizona Corporation Commission (ACC). Most information coming from individual water companies and

from the ACC was for the year 1997, the last year of the transient model (stress period 23). The information obtained from the ADWR was contained in the Hydrographic Survey Report (HSR) of 1991.

The information gleaned from the HSR concerning water use by water companies within the San Pedro Basin was for the years 1980-1988. Water use estimates for the years between 1988 and 1997 were interpolated. When water use information was not available for 1997, an 11% increase from 1988 to 1997 was assumed. This increase is consistent with pumping figures from Bell Vista Water Company, one of the larger water providers in the basin. Values of pumping for years prior to 1980 assumed a linear increase from each company's inception date.

It was made clear in obtaining the water use information from private water companies in the basin, that the water use figures were metered or billed water sales. This figure in most cases is less than the total amount of water pumped by any company. In the case of Bella Vista Water Company in 1997, the billed water sales totaled 1,050,267,970 gallons. The actual amount of water pumped by company wells exceeded this number by approximately 50 million gallons (Gignac, 2000). This is nearly a 5% difference. In the case of a smaller Cloud Nine Water Company, according to the ACC, the metered water sales totaled 3,796,000 gallons in 1997. The un-metered water sales for that same year added up to 14,454,000 gallons, nearly 4 times the amount metered.

The values utilized in this study are the metered water volumes. The reasons for this are the availability of pumping information, the reliability of pumping information (unmetered water use is deemed unreliable due to the fact that it is "unmetered"), and any

error inherent in this research in regards to pumping errs towards the conservative low side (minimal impact to the hydrologic system). Table 5-2 displays individual water companies' pumping rates for each stress period. Figure 5-4 follows showing the total amount of public supply pumping by stress period.

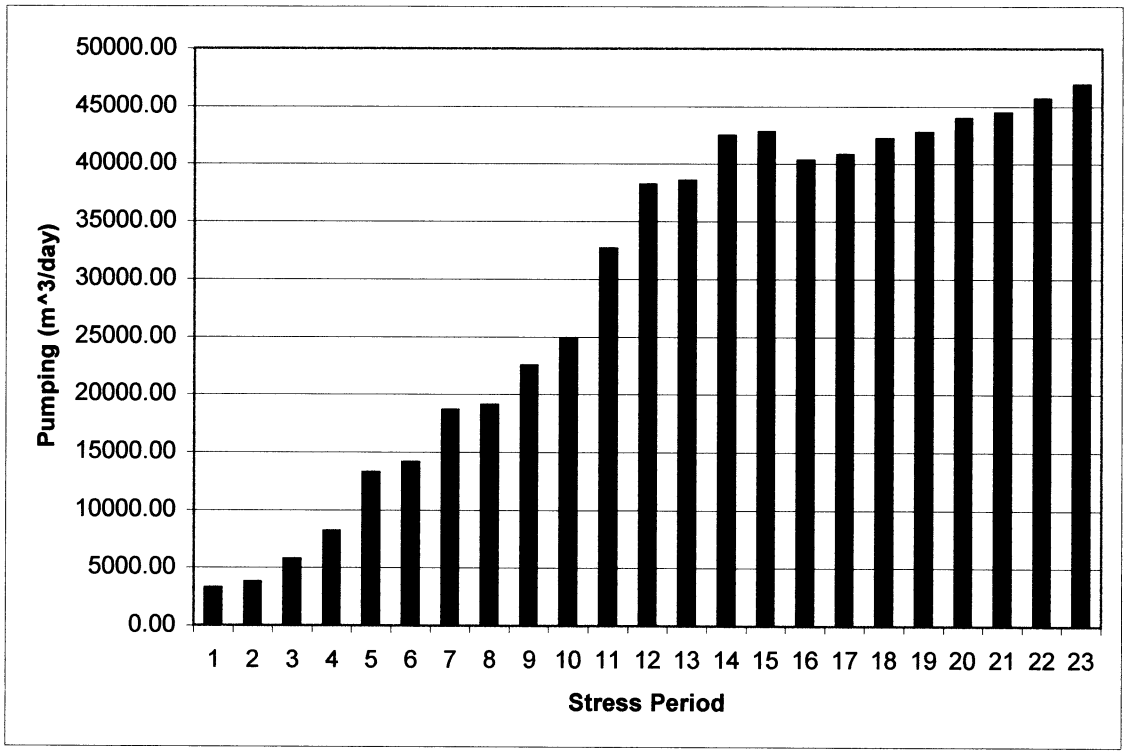

Figure 5-4 Total U.S. public supply pumping for each stress period

Public Supply Pumpage (m^3/day)																								
Stress Period	1	2	3	4	5	6	7	8	9	10	11	12	13	14	15	16	17	18	19	20	21	22	23
Years	1940-41	1942-45	1946-50	1951-63	1964-66	1967	1968	1969-72	1973-76	1977	1978-85	1986	1987	1988	1989	1990	1991	1992	1993	1994	1995	1996	1997
Water Company																								
Antelope Run	0	0	0	0	0	0	0	0	0	0	0	5	1	14	24	34	44	54	64	74	84	94	104	
AZ Water Co., Bisbee System	0	0	0	521	1657	1958	2109	2485	3088	3464	3616	3060	3186	3251	3291	3330	3370	3410	3450	3489	3529	3569	3609	
AZ Water Co. Fuller and Sulger Systems	0	0	0	92	718	958	1077	1377	1856	2155	2524	2896	2804	2913	2948	2984	3019	3055	3091	3126	3162	3197	3233	
Bella Vista Water Co.	0	0	0	469	1330	1551	1862	1939	2382	2859	5999	9514	9333	9823	10118	9613	9390	10073	10121	10682	10709	10980	10892	
Benson	500	572	681	1087	1350	1385	1402	1475	1693	1836	2036	2417	2098	2308	2237	2315	1987	2160	2158	2353	2311	2361	2276	
Cochise Water Co.	0	0	0	0	4	6	10	15	23	28	35	67	85	103	121	139	158	176	194	212	230	248	266	
Coronado Water Co.	0	0	0	4	32	43	48	61	82	96	100	100	105	109	114	119	124	129	134	139	143	148	153	
Crystal Water Co.	0	0	0	0	0	0	0	0	0	0	17	39	38	38	37	36	36	35	34	33	33	32	31	
East Slope Water Co.	0	0	0	0	59	117	146	220	337	410	491	489	603	593	611	629	646	664	682	700	717	735	753	
Holiday Ent. Water Co.	0	0	0	0	11	19	23	32	48	57	72	74	78	77	83	88	93	99	104	109	115	120	125	
Huachuca City	0	0	0	2	79	132	158	224	330	396	514	612	927	907	918	929	940	951	962	973	984	995	1006	
Indiada Water Co.	0	0	0	0	0	0	0	7	18	24	30	27	28	28	32	35	38	42	45	48	51	55	58	
Lucky Hills Water Co.	0	0	0	0	0	1	2	3	5	6	7	4	3	1	1	1	1	1	1	1	2	2	2	
Mescal Lakes Water Co.	0	0	0	0	0	0	0	0	3	6	16	53	79	84	97	109	122	134	147	159	172	184	197	
Miracle Valley Water Co.	0	0	0	2	39	58	68	92	130	154	166	122	97	134	124	114	104	93	83	73	63	53	42	
Mustang Water Co.	0	0	0	0	0	0	0	0	3	7	16	21	23	25	27	29	32	34	36	38	40	42	45	
Naco Water Co.	0	0	0	52	111	126	134	152	182	200	223	245	235	245	257	269	282	294	307	319	331	344	356	
Nicksville Water Co.	0	0	0	5	28	36	40	50	66	76	92	97	98	115	126	136	148	160	171	182	193	204	215	
Pomerene Domestic	0	0	16	136	245	272	286	320	375	409	431	438	436	429	462	494	527	559	592	624	657	689	722	
Pueblo Del Sol Water Co.	0	0	0	0	0	0	0	0	191	382	630	791	1064	1217	1475	1732	1990	2247	2505	2762	3020	3277	3535	
Sierra Vista	0	0	0	40	146	175	190	226	285	321	411	666	531	570	575	579	583	587	591	596	600	604	608	
Southland Utility	0	0	0	0	0	0	17	61	130	174	234	296	311	338	348	359	369	380	391	401	412	422	433	
St. David Water	0	0	0	0	0	0	0	73	190	264	337	384	423	424	456	488	520	552	584	616	648	680	712	
Sue Juan Water Co.	0	0	0	13	47	57	62	73	92	104	145	198	189	208	195	185	174	164	153	143	132	122	111	
Whetstone Water Co.	0	0	0	0	0	0	0	0	0	0	36	73	73	74	74	75	75	76	77	77	78	78	79	
Willow Lakes Water Co.	0	0	0	0	0	0	0	0	7	14	21	33	33	34	34	34	34	34	34	34	34	34	34	
Total Pumping (m^3/day)	500	572	698	2424	5857	6896	7433	8885	11516	13243	18207	22722	22875	24061	24785	24858	24808	26163	26706	27964	28448	29270	29597	
Total Pumping (ac-ft/yr)	148	169	206	717	1733	2041	2200	2629	3408	3919	5386	6724	6769	7120	7334	7356	7340	7742	7903	8275	8418	8661	8758	

Table 5-2 Pumping from individual U. S. water companies

5.1.6 Military Wells

Military wells were not defined as a type of water use by the ADWR, but are considered separately for convenience in this study. Military wells are defined as simply those wells located on the property of Fort Huachuca. Many of these wells had a previous designation of either domestic, public supply, or irrigation within the ADWR classification system. When information was obtained from Fort Huachuca concerning annual pumping by the base, this annual pumping rate was then distributed among those wells located on base property by well casing area. Pumping by stress period for Fort Huachuca can be seen in Figure 5-5. The first three stress periods exhibit the initial pumping rates that were not changed, as pumping volumes were not available from the Fort before 1963.

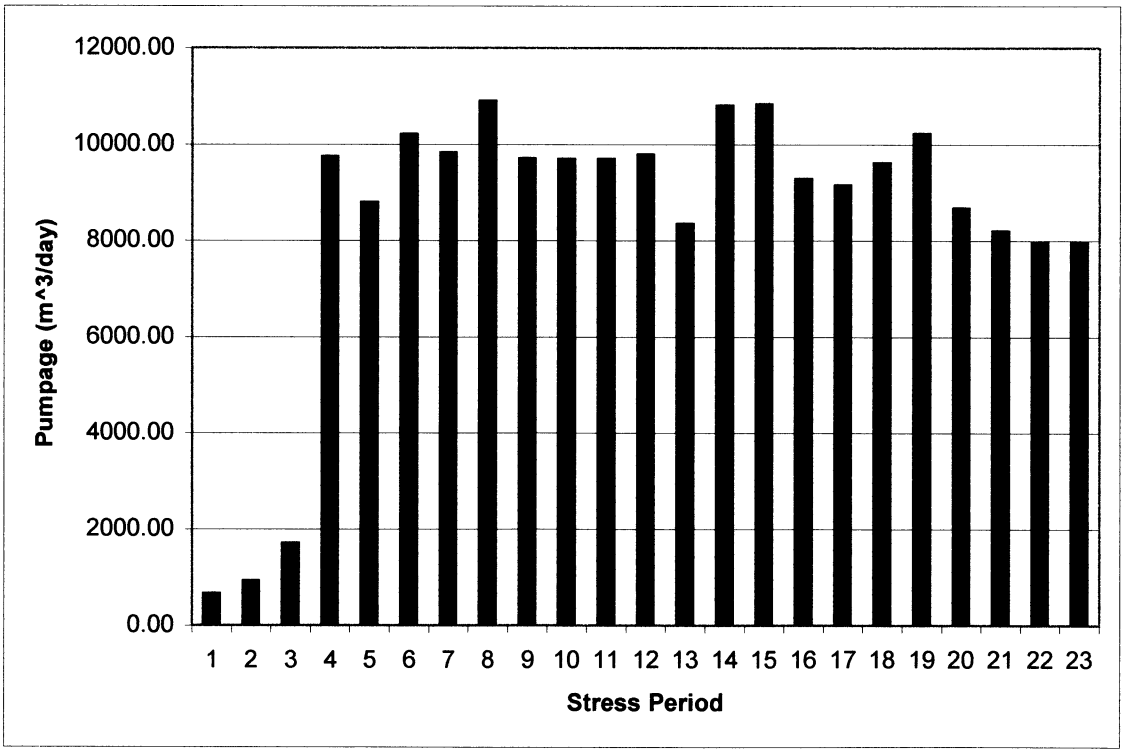

Figure 5-5 Total Fort Huachuca pumping for each stress period

5.1.7 Irrigation Wells

One of the largest uses of groundwater in the San Pedro Basin is for irrigation. Unfortunately, in spite of its great use, irrigation is the most difficult type of water use to assess. The difficulty lies in the fact that well locations were not recorded by the state until 1980, and like all other private water users in the San Pedro Basin, water pumping records are not required by the ADWR. Many irrigation wells that were in use for a long period of time before 1980 may have been destroyed, abandoned, or their primary use has changed. The GWSI provided information on many of these wells, however it should be noted that many wells might have existed that are not accounted for in this study.

Irrigation in the Hereford-Palominas area of the San Pedro Basin was substantially reduced due to the creation of the SPRNCA. All of the irrigation wells within its boundaries ceased to operate after its creation in 1988 (stress period 14). There are still some inholdings within the SPRNCA, such as a few domestic residences/subdivisions in Escopule Estates and a scout camp that operate wells (Whetstone, 2000). These few wells are classified as domestic pumping.

Although irrigation in the SPRNCA was eliminated, basin wide irrigation was only reduced slightly. Large-scale irrigation near the cities of St. David, Benson and northward has continued. Irrigation rates since the creation of SPRNCA have remained relatively constant as indicated in Figure 5-6.

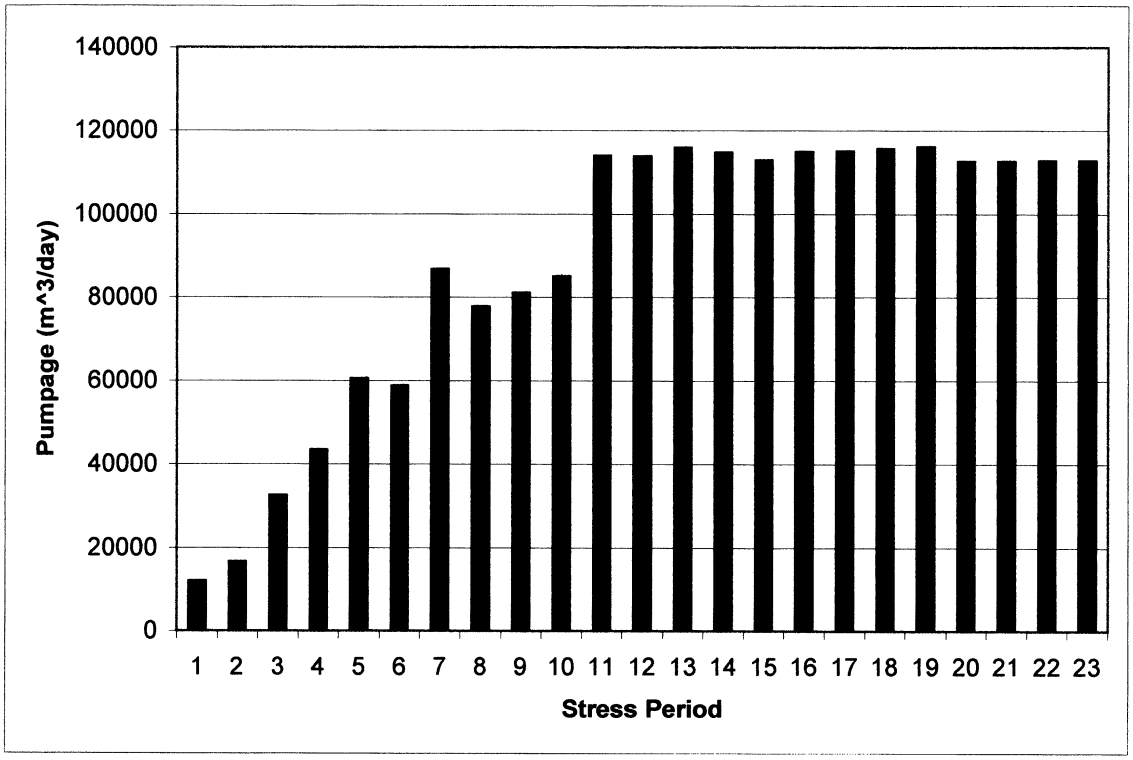

Figure 5-6 Total U.S. irrigation pumping for each stress period

5.1.8 Domestic Wells

Domestic wells are by definition those wells used for water in the home. The ADWR estimated that the average water used by a home was 1.68 m^3/day (0.5 acre-ft per year) (ADWR, 1991). Each well classified with the major water use type as domestic within the GWSI or the Well Registry, was given this pumping rate. When information about a particular well was received (such as an indication that this well is on the property of Fort Huachuca) the pumping rate was then altered accordingly.

Domestic wells differ from Public supply wells in that they are used on a smaller scale. They provide water to individual homes or subdivisions, remaining un-attached to a municipal water supply. Figure 5-7 shows the rates associated with domestic pumping within the Upper San Pedro Basin. The jump in pumping rates observed between stress

period 10 and 11 is due in part to an increase in reliable information from the ADWR concerning the location of more domestic wells after 1980, as well as the large time interval (8 years) covered in stress period 11. In actuality, the transition between years is much smoother.

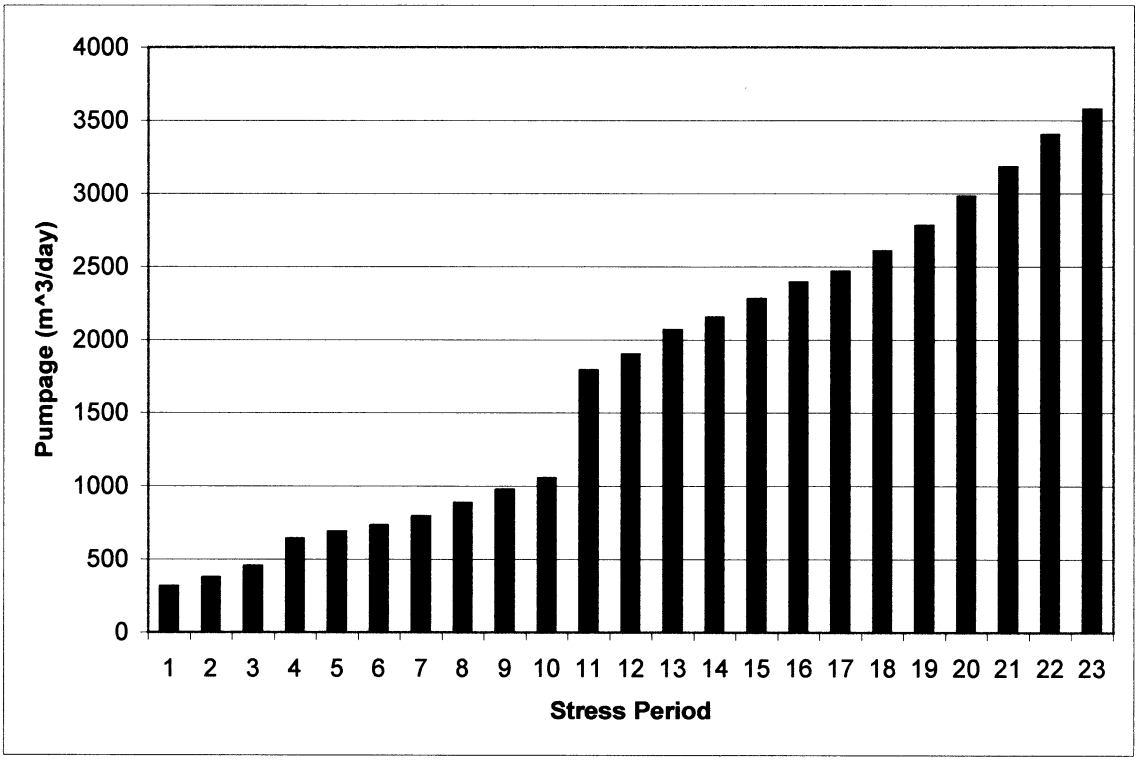

Figure 5-7 Total U.S. domestic well pumping for each stress period

5.1.9 Stock Wells

Stock ponds and reservoirs are located throughout the San Pedro Basin. The majority of the water used by stock ponds is accounted for in seepage and evaporation, with the actual amount used by livestock accounting for a negligible amount (ADWR, 1991). The wells considered as stock wells are those designated within the GWSI or the Well Registry as primary use by stock.

As with all other well types, the pumping for individual wells was determined by the casing area. It is assumed that the pumping rates account for evaporation only, having no associated recharge as the water pumped is effectively removed from the groundwater system. Figure 5-8 shows a general increase in stock well production until stress period 15, where after this time, the number of stock wells remained nearly constant.

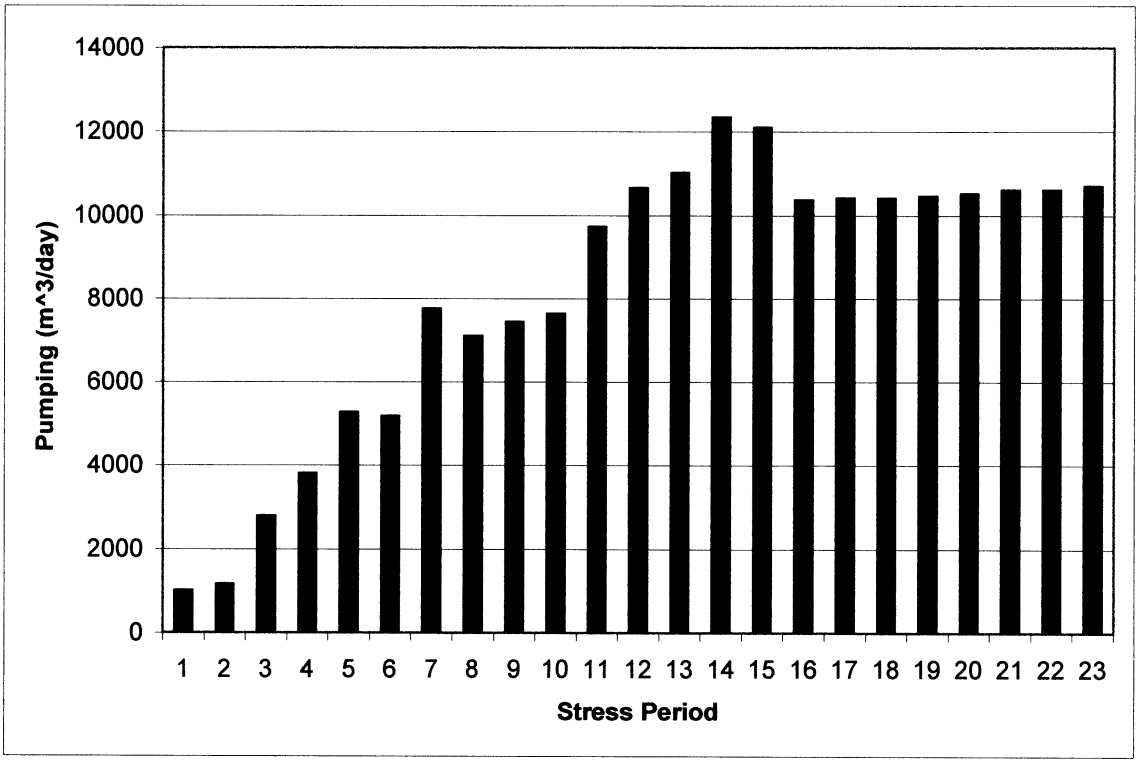

Figure 5-8 Total U.S. stock well pumping for each stress period

5.1.10 Industrial, Commercial, and Institutional Wells

The primary industrial wells within the U.S. portion of the basin are those operated by sand and gravel operations and Apache Nitrogen Products, Inc. No pumping

figures were obtained from Apache Nitrogen, therefore pumping was estimated by well casing area as mentioned above.

Commercial and institutional wells are owned by a commercial fish hatchery and the LDS church. The few wells designated as commercial or institutional were given pumping based on well casing area. Pumping rates by stress period are displayed below in Figure 5-9.

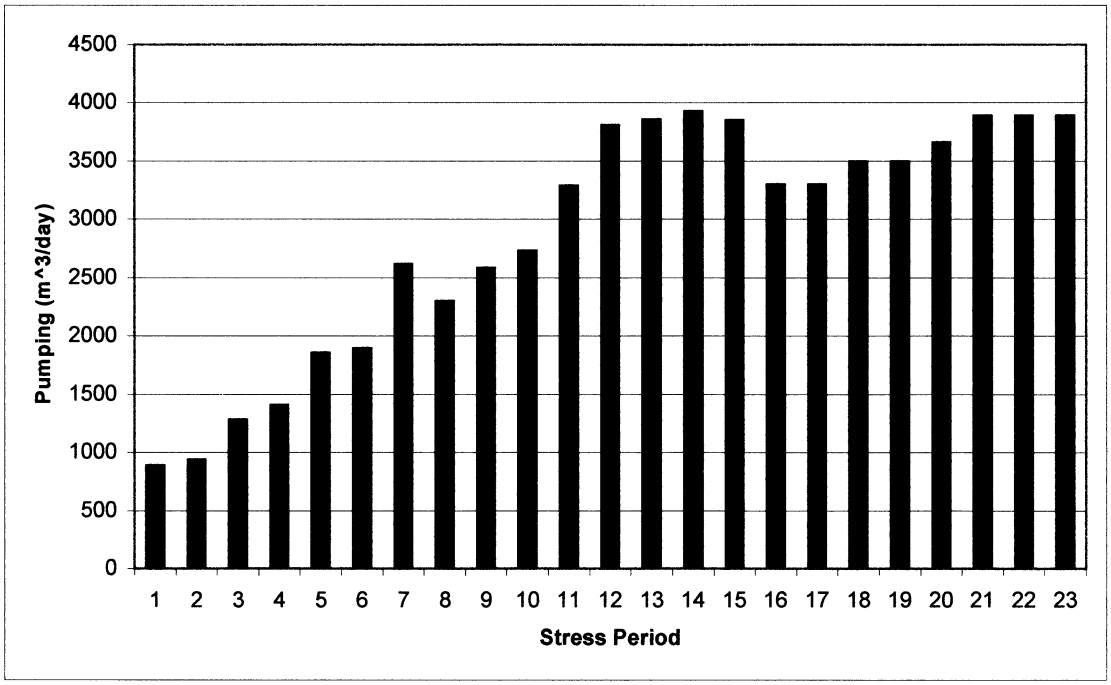

Figure 5-9 Total U.S. industrial, commercial, and institutional pumping each stress period

5.2 MEXICAN WELLS

The use of groundwater in Mexico is variable. According to ADWR, the majority of agriculture taking place within the Mexican portion of the San Pedro Basin utilizes primarily surface water resources (ADWR, 1991). The agriculture supplements groundwater to their water use rarely, and then only when the local economy is able to

support groundwater pumping. Essentially, groundwater use has typically been governed by local economic conditions such as drought and inflated production costs.

Very little information is available on Mexico's limited groundwater use. However, the information gathered allowed groundwater production to be divided into two categories, domestic and industrial. In order to determine when a well became active, the total number of wells (both domestic and industrial) was divided into the number of stress periods. This equaled about 5 wells per stress period. The 5 wells were selected by their location, in the hopes of giving an even spatial distribution.

5.2.1 Domestic Wells

Domestic wells are all the recorded wells not owned by the mining operations in Cananea . Some of these wells may be owned communally by ejidos, and may have some use in agriculture, however specific water demand for these areas is unknown. It was assumed that these wells have a pumping rate equal to domestic well pumping in the United States (0.5 Acft/yr). Allowing the assumption that Mexican use of water is less per individual, this pumping rate stands as a low estimate of domestic pumping by each well, especially considering one well's many possible uses. Domestic pumping rates for individual stress periods can be seen in Figure 5-10.

The water for the city of Cananea has been provided by the mining company operating at Cananea (see below) through 1997, the last year evaluated by this current study (López, 1999). It is unknown what percentage of mine pumpage has been put to domestic use within Cananea. It is also unknown if mine pumping provides water for outlying areas.

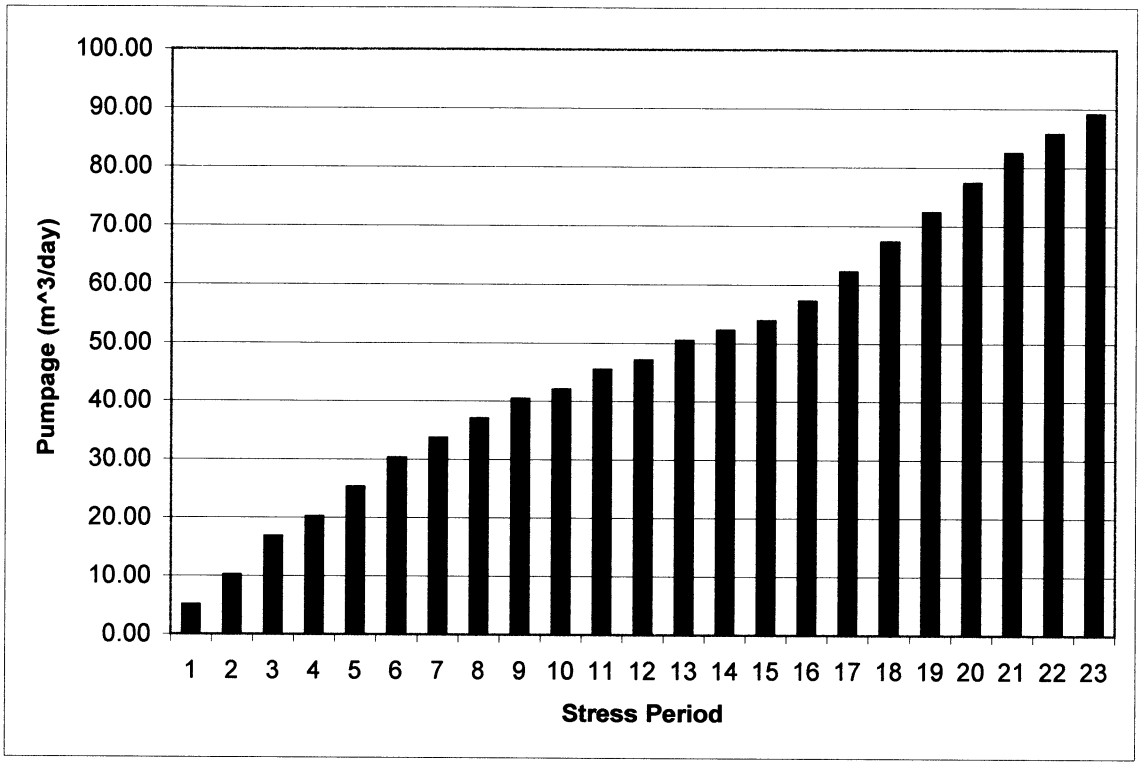

Figure 5-10 Total Mexican domestic pumping each stress period

5.2.2 Industrial Wells

Industrial wells are those wells owned and operated by the mine, Mexicana de Cananea. According to López (1999), the mine used approximately 19,000,000 m^3 of water in 1990 and 12,000,000 m^3 of water in 1999. It is assumed that the amount of water used in 1999 was similar to 1997, and therefore this pumping amount was applied to that year. A linear pumping distribution was given to those years prior to 1990, and between 1990 and 1997 where information is unavailable. This linear distribution of pumping can be seen in Figure 5-11.

The wells owned by the mine are operated on a rotation. One well will be operated for a period of time, and then another well will then be turned on and the former well shut off (López, 1999). This helps to reduce the cone of depression occurring at any

one location. The water pumped by the mine is not recharged into the San Pedro Basin, as it is effectively removed from the San Pedro Basin and utilized in mining processes on the south side of the water divide in the Rio de Sonora watershed.

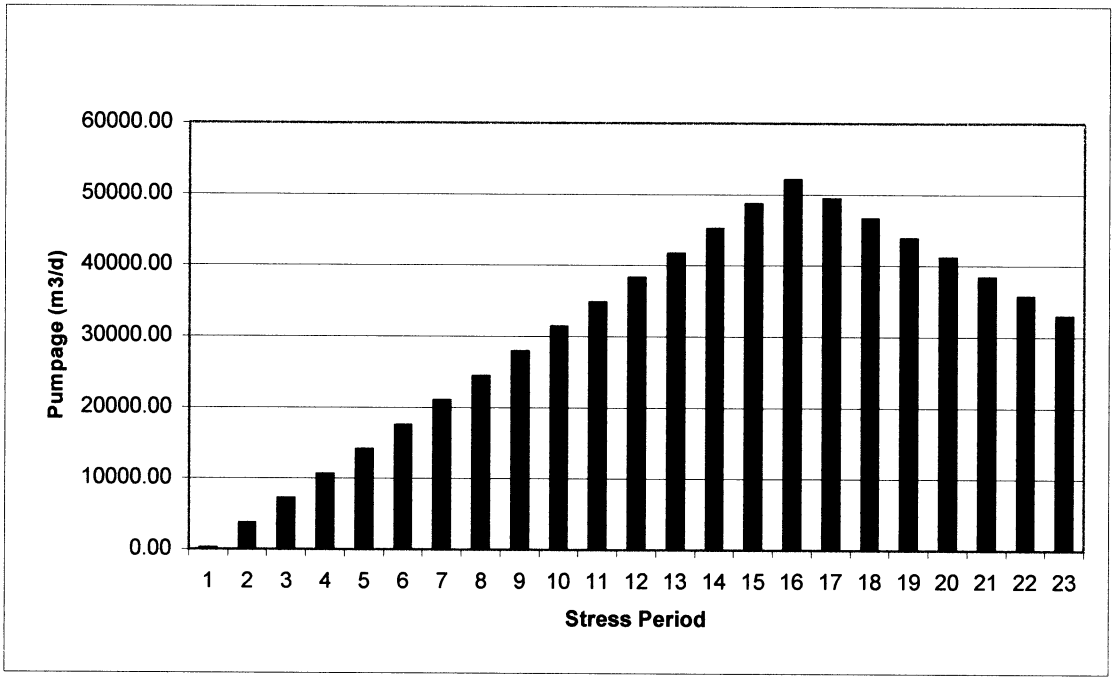

Figure 5-11 Total Mexican industrial pumping for each stress period

5.3 TOTAL PUMPING

Figure 5-12 shows the total pumping for the entire study area accumulated by water use type over the 23 stress periods. The occasional disjointed jumps in total pumping from stress period to stress period is because the stress periods may be composed of different number of years. In particular, stress period 11 is composed of 8 years, while stress periods 10 and 12 are composed of only 1 year.

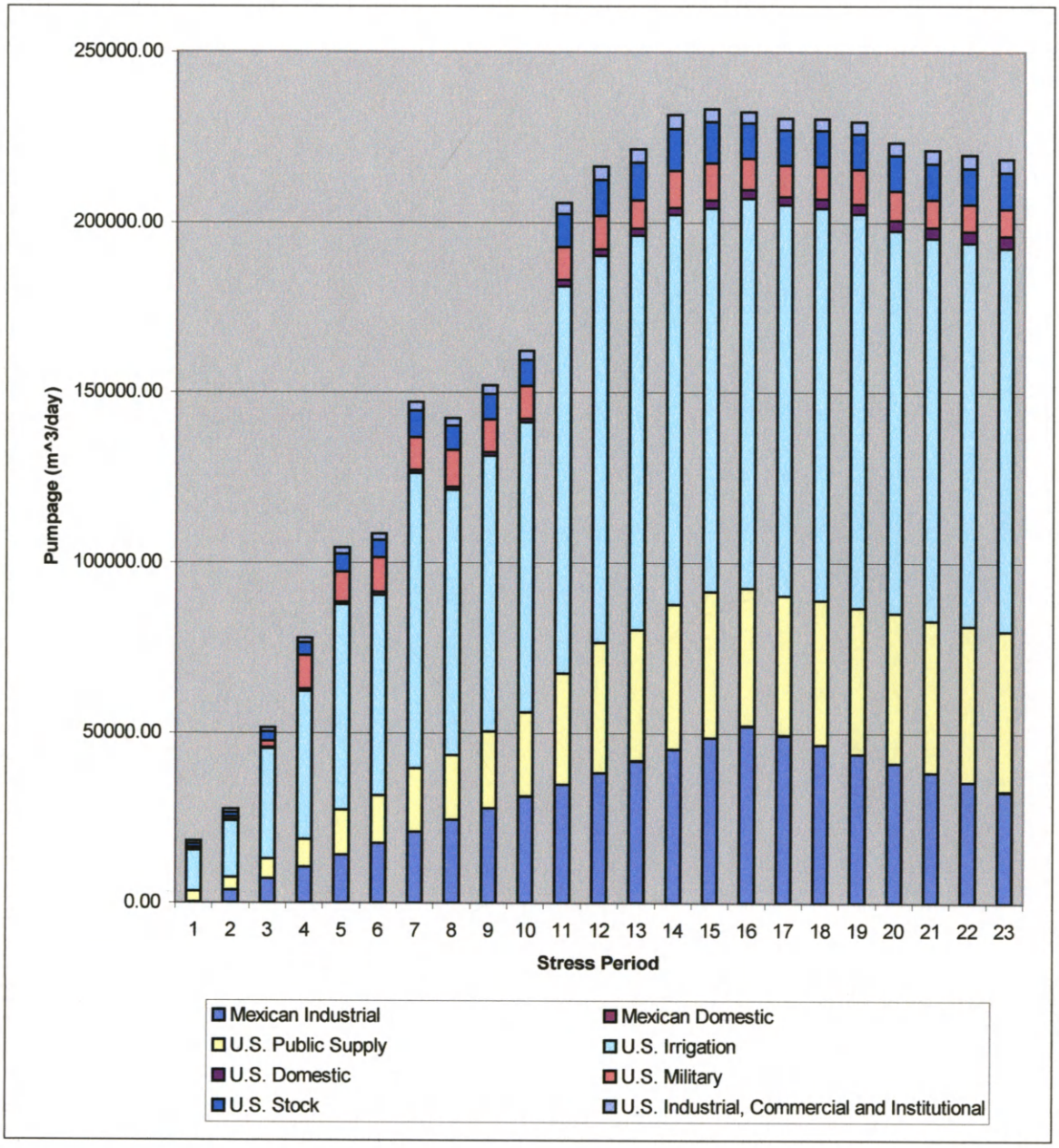

Figure 5-12 Distribution of all pumping in Upper San Pedro Basin by type for each stress period

CHAPTER 6
NUMERICAL MODEL

6.1 MODELING METHOD

The creation of the numerical model was served by the infusion of the conceptual model into a finite difference grid (addressed below) through the use of Department of Defense Groundwater Modeling System (GMS) software. GMS is an interface between GIS applications and hydrologic computer models including MODFLOW, MT3D, RT3D, MODPATH, SEEP2D, and FEMWATER. GMS assists in conceptual model creation, mesh and grid generation, geostatistics, and post-processing. The interface used in GMS contains 10 different modules (GMS, 1999). The map module is used extensively in developing the conceptual foundation of the current model, and a three dimensional grid module is used during interaction with MODFLOW packages. GMS is selected for this study because it automates grid construction, facilitates generation of head contours, and allows model representation in real-world coordinates consistent with the GIS applications mentioned in Chapter 4.

6.2 FLOW MODEL

This section briefly describes the flow model used by this study. The governing partial differential equation for three-dimensional ground-water flow of constant density through a saturated, heterogeneous, anisotropic porous media of spatial domain D is

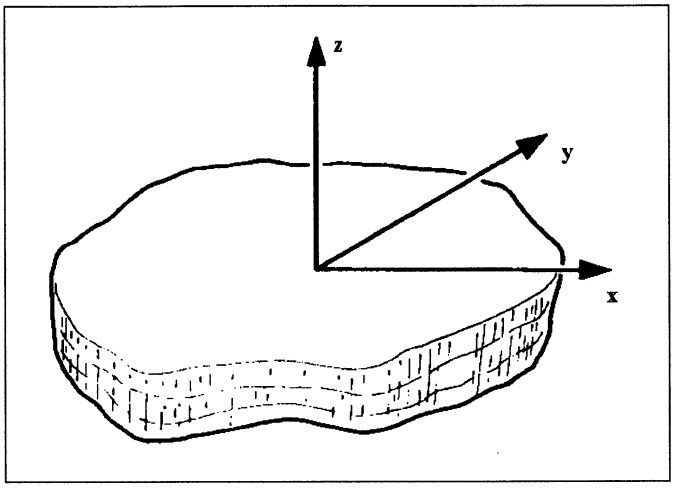

Figure 6-1 Domain D and surface Γ (The volume of the figure constitutes D and the surface areas – top, bottom and sides constitutes Γ)

$$\nabla \cdot [\mathbf{K}(\hat{x}) \cdot \nabla h(\hat{x},t)] = S_s(\hat{x}) \frac{\partial h(\hat{x},t)}{\partial t} + W(h,\hat{x},t) \tag{5}$$

and is subject to the initial conditions,

$$h(\hat{x},0) = H_0(\hat{x}) \tag{6}$$

within the domain *D,* and boundary conditions,

$$\left[\mathbf{K} \cdot \nabla h \cdot \hat{n} - c_b(H_b - h) - Q_b\right]_\Gamma = 0 \tag{7}$$

along the boundary Γ of the domain *D*, and where:

h is the hydraulic head [L],

$\hat{x}$ is (x,y,z), the three-dimensional coordinate directions and are assumed parallel to the principal coordinate directions of hydraulic conuctivity [L],

t is the time [T],

K is the hydraulic conductivity tensor [L/T],

S_s is the specific storage of the aquifer material [L^{-1}],

W is the volumetric flux per unit volume and represents sources and sinks [T^{-1}],

$\hat{n}$ is the normal vector pointing outward from the boundary Γ [L],

c_b is a coefficient that controls the quantity of stress-induced flow across the boundary Γ, [T^{-1}],

1. if $c_b = 0$, there is no stress-induced flow from the boundary, the boundary is a prescribed boundary, and the nature recharge and discharge through the boundary are unaffected by pumpage,

2. if $c_b = \infty$, there is a prescribed head condition on Γ, and

3. if c_b is otherwise, the boundary is a head-dependent boundary;

H_b is a prescribed head [L], and Q_b is a prescribed flow per unit surface area of the boundary Γ [LT^{-1}].

Because of the complexities associated with the previous equations, specifically those pertaining to heterogeneities, the distribution of stresses and irregularly shaped boundaries, analytical solutions are rarely possible except under the simplest of situations. Mathematical models simulating groundwater conditions thus require numerical methods to approximate their solutions. Numerical solutions can be obtained by applying finite-difference methods to a system which replaces the continuous spatial and time domains with a set of discrete points in time and in space, and solves for the head values at these points.

The Modular three-dimensional Finite-Difference Groundwater Flow Model (MODFLOW), developed by Mc Donald and Harbaugh (1988), applies a finite-difference scheme to Equations (5) - (7) and replaces the continuous formulation with a finite set of discrete points in time and space (see Figure 6-2). The aquifer system is divided in blocks called cells, and is described in terms of rows, columns, and layers. For every cell, there is a point at its center called a "node" where the head is to be calculated.

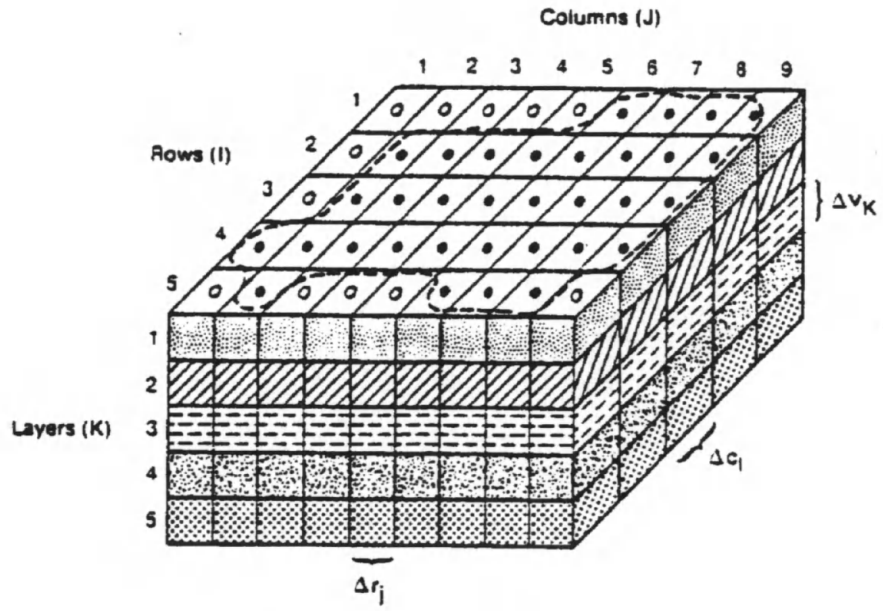

Figure 6-2 A discretized hypothetical aquifer system (from McDonald and Harbaugh 1984)

The period of simulation is divided into a series of stress periods, and within a stress period, all parameters are constant. Each stress period is divided into a series of time steps. For this study, there are 23 stress periods divided into 58 one-year time steps. MODFLOW computes the head and a mass balance at each node for each time step. The program has a modular structure allowing the user to incorporate a series of packages or modules to simulate different processes associated with groundwater: evapotranspiration, recharge, drains, well pumping, and stream-aquifer interaction.

6.3 FINITE DIFFERENCE GRID

The finite difference grid applied to the modeled region is oriented in a southeastern-northwestern direction, paralleling the predominant flow direction of the San Pedro River. The system is discretized into 171 rows and 90 columns and separated into 4 layers, with finer grid resolution near the San Pedro River and near high-density

well occurrence (Figures 6-3, 4, 5, 6). Cell sizes range from 2.26×10^5 m^2 to 2.09×10^6 m^2 in areal extent. Refer back to Chapter 4 for discussion of layer properties, and Chapter 5 for a discussion of the San Pedro Basin's wells.

Figure 6-3 Layer 1 grid

Figure 6-4 Layer 2 grid

Figure 6-5 Layer 3 grid

Figure 6-6 Layer 4 grid

A prescribed head condition was given to the cells along the northern boundary of layer 3, below the floodplain, for the initial steady state simulation. These constant head cells were then changed to a constant flux boundary (simulated by wells) for the steady state and subsequent transient models, with a combined flux out of the system of 10593 m^3/day (3134 ac-ft/yr).

6.4 MOUNTAIN FRONT RECHARGE

The volume of mountain front recharge associated with the conceptual model was distributed to the uppermost active cells along the outside edge of the model boundary. The recharge rate associated with an individual cell was dependent upon the average precipitation of that cell's contributing basin. The process in equation form is as follows:

$$P_i / \Sigma (P_i) = R_i \qquad (8)$$

Where:

P_i = the average precipitation for the i^{th} individual basin (mm/year)

R_i = the fraction of the total mountain front recharge for the i^{th} individual basin

When R_i is multiplied by the volumetric flux of mountain front recharge (m^3/day) calculated in conceptual model (see Mountain Front Recharge section of Chapter 4), the result is the rate of mountain front recharge in the i^{th} basin. This recharge flux for a basin is then divided by the area of the cell where the basin discharges (m^2). The result of this calculation is the recharge rate of a particular cell (m/day). Figure 6-7 displays mountain front recharge cells' rates and their contributing basins' precipitation.

6.5 AGRICULTURAL RECHARGE

The agricultural recharge rates assigned to agricultural polygons were assigned to model cells based on the percentage of that polygon type contained within a model cell. The percentage contained in the cell was then multiplied by the recharge rate, giving the agricultural recharge rate for that particular cell. This process was completed for all cells containing any portion of agricultural polygons. All agricultural recharge cells were located in layer 2 of the model. The recharge rates assigned to an agricultural polygon were discussed previously in Chapter 4. Figure 6-8 shows the irrigation wells, agricultural polygons, and agricultural recharge cells and their respective locations within the Upper San Pedro Basin.

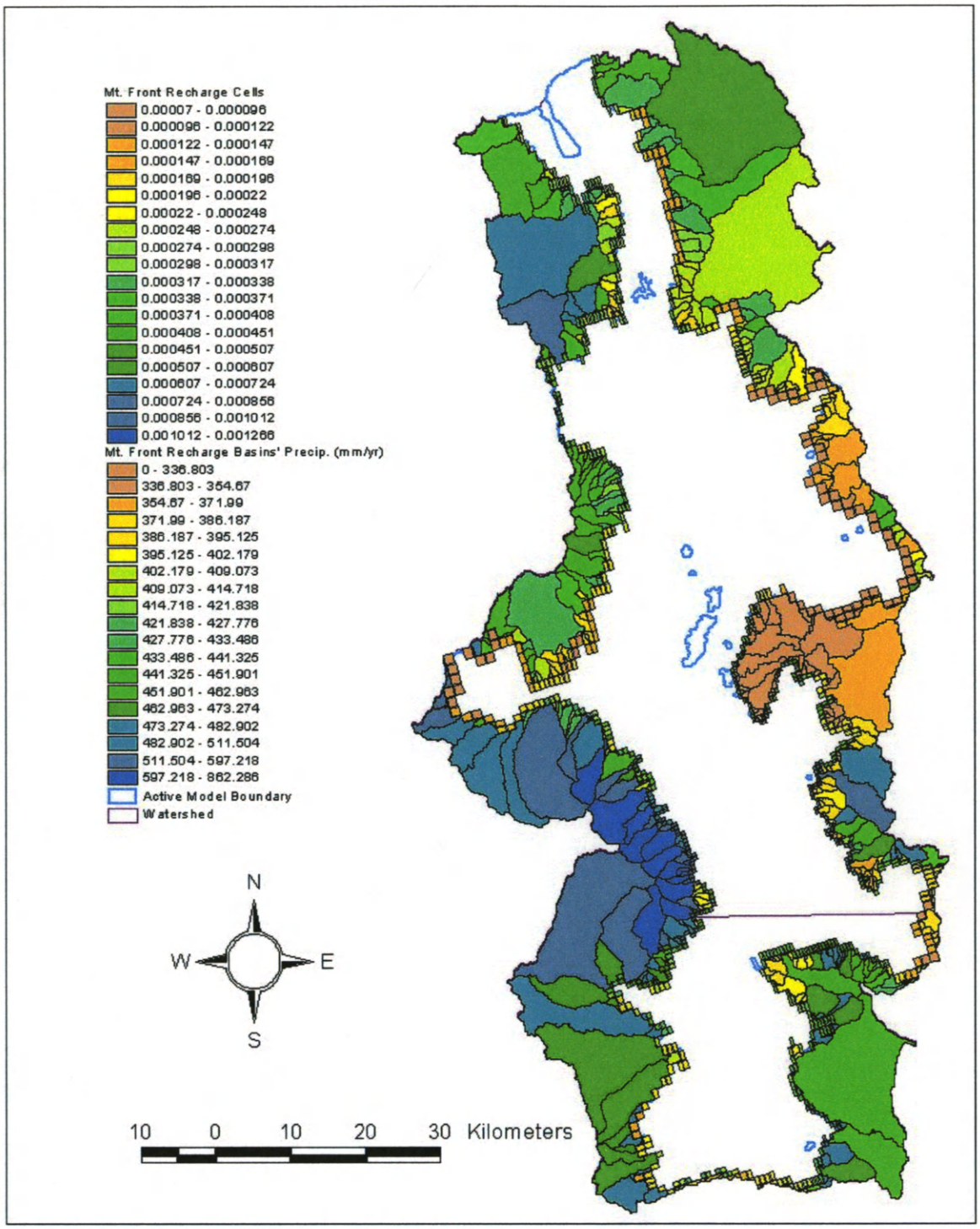

Figure 6-7 Mountain front recharge cells and contributing basins

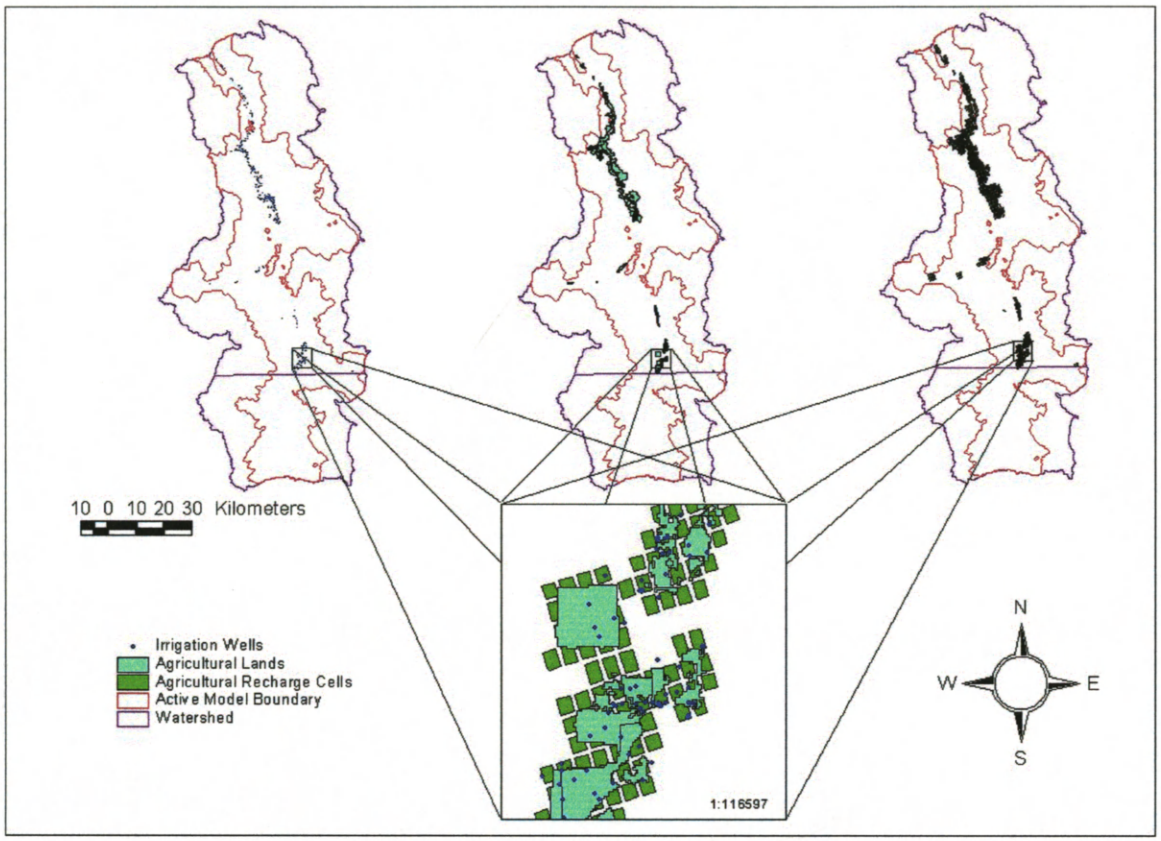

Figure 6-8 Agricultural recharge cells with associated pumping wells and recharge polygons

6.6 EVAPOTRANSPIRATION

The evapotranspiration rates for each vegetative type were assigned to their respective polygons. Evapotranspiration rates were assigned to model cells based on the percentage of that polygon type contained within the model cell. The percentage was then multiplied by the evapotranspiration rate, giving the evapotranspiration rate for that particular cell. This process was completed for all cells containing any portion of riparian vegetation polygons. Figure 6-9 shows the model cells overlain by riparian vegetation polygons.

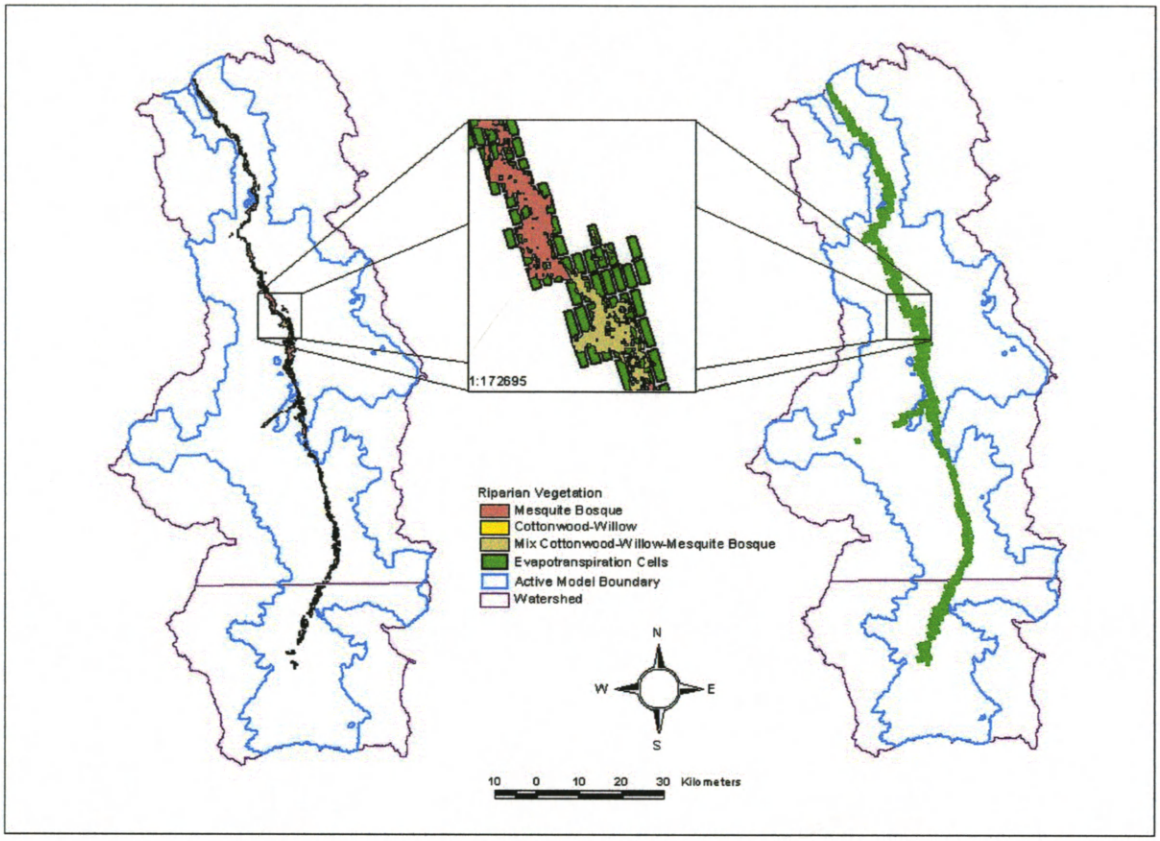

Figure 6-9 Evapotranspiration cells and associated riparian vegetation polygons

The average rate for riparian evapotranspiration presented in Chapter 4 was assigned as the maximum evapotranspiration rate in the numerical model. The actual extinction depth of the root zone in the riparian area is 5 meters, however, to compensate for the large cell size, an additional 5 meters was added to compensate for the averaging of vertical elevation variances within each cell. An extinction depth of 10 meters was assigned for the riparian areas. Figure 6-10 gives a schematic representation of this procedure.

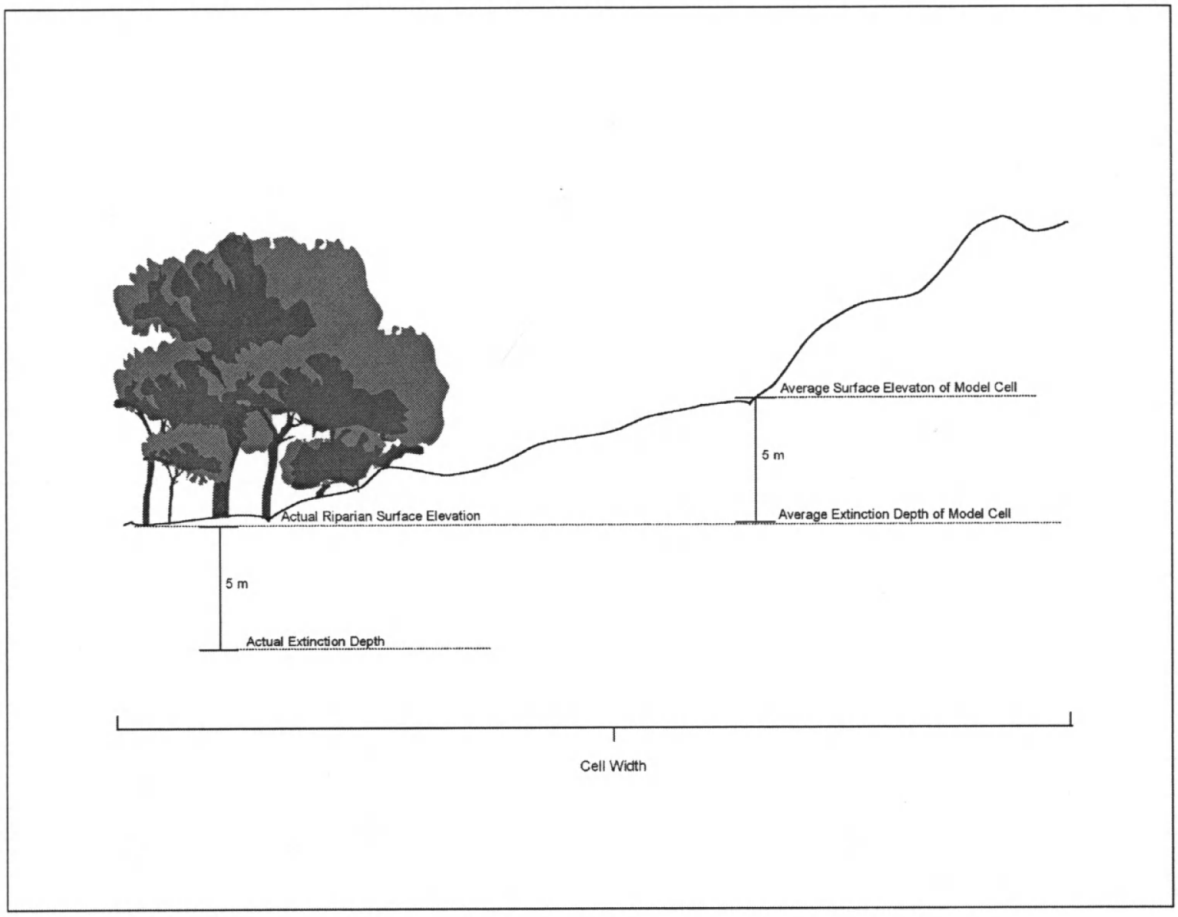

Figure 6-10 Adjustment of extinction depth for evapotranspiration cells

This procedure increases the availability for water in the riparian area, but the assigned maximum rate (the average riparian evapotranspiration rate) is never exceeded. This is believed to provide a more realistic volume of groundwater consumed by riparian evapotranspiration, without a reduction in cell size along the riparian corridor. The use of this tactic also allows for the modeling of some recovery by plant species in response to gradual watertable decline as suggested by Jahnke (1994).

6.7 STREAM-AQUIFER INTERACTION

Stream-aquifer interactions were simulated using the USGS Streamflow-Routing (STR) package (Prudic, 1989). The package was written for use in MODFLOW

(McDonald and Harbaugh, 1988) to calculate the streamflow stage and to simulate the ground and surface-water interactions. It is an accounting routine that tracks flow in one or more streams that interact with the groundwater, and limits the aquifer recharge to stream flow availability. With this package, portions of the streams are permitted to go dry, flow again, to be diverted, and to be merged with other streams or tributaries. Darcy's Law computes leakage to or from a stream reach as follows,

$$Q = \frac{KWL}{M}(H_s - H_a) \tag{9}$$

where (see Figure 6-11),

Q is the leakage to or from the aquifer through streambed [L^3T^{-1}],

K is the streambed vertical hydraulic conductivity [LT^{-1}],

W is the width of the stream [L],

L is the length of the stream reach [L],

M is the thickness of the streambed [L],

H_s is the stage elevation of the stream [L], and

H_a is the hydraulic head in the aquifer beneath the streambed.

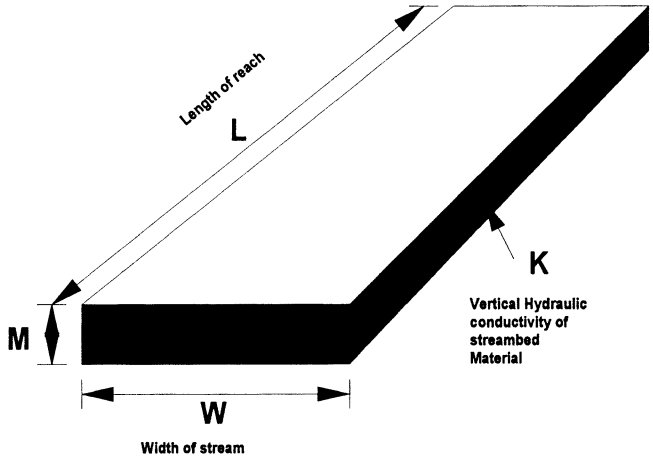

Figure 6-11 Streambed conductance = KLW/M (After [McDonald, 1988 #10]

It is customary to group the hydraulic conductivity terms with the geometric parameters to define the conductance of the streambed, and Equation (9) is rewritten as,

$$Q = C_R (H_s - H_a) \tag{10}$$

where the streambed conductance, C_R, is defined,

$$C_R = \frac{KWL}{M} \tag{11}$$

The streamflow routing package assumes constant streambed conductance for each stress period.

The package calculates stage in the stream by means of Manning's equation, assuming incompressible steady streamflow at constant depth and a rectangular channel,

$$Q_s = \frac{C_f}{n} AR^{2/3} S^{1/2} \tag{12}$$

where,

Q_s is the stream discharge [L^3T^{-1}],

C_f is the conversion factor (1.0 for S.I. units),

n is the Manning roughness coefficient [$L^{1/6}$],

S is the slope of the stream channel [0],

W is the width of the stream [L],

d is the depth of the stream [L],

A is the cross-sectional area of the stream, $A = Wd$ [L^2], and

R is the hydraulic radius, $R = \frac{Wd}{W + 2d}$ [L].

It is assumed that he stream depth is much less than the stream width, giving,

$$d = \left[\frac{Q_s n}{C_f W S^{\frac{1}{2}}} \right]^{\frac{3}{5}} \tag{13}$$

Segments represent streams in the model, and each segment is divided into reaches. The San Pedro River is divided into 358 reaches of varying length depending on the length of the stream associated with a particular cell. Each of the tributary streams and diversions to the San Pedro River are also divided into reaches in the same manner. The reaches are numbered from upstream to downstream for a particular segment. The segments of San Pedro River assume a width of 9.144 m (30 ft), a Manning roughness coefficient of 0.022, an average streambed thickness of 1.5m, and an average streambed vertical conductance of approximately 0.05 m/day. The Babocomari assumes a 5 m width, a roughness of 0.025, a streambed 1 m thick, and average vertical conductance of .375 m/day. All other tributaries to the San Pedro River assume a 3.6576 m (12 ft) width, a roughness of 0.03, a thickness of 0.6 m, and a conductance of 0.625 m/day. The diversions to the San Pedro River assume a 1.8288 m (6ft) width, a roughness of 0.03, a thickness of 0.3 m, and a conductance of 0.1 m/day. These values are consistent with the modeling approach taken by Jahnke (1994).

CHAPTER 7
CALIBRATION AND SENSITIVITY

7.1 CALIBRATION

The hydrologic model was calibrated for both steady state and transient conditions. Computed water levels were calibrated against measured water levels for individual well, and simulated baseflow was calibrated against baseflow determined in previous studies (Corell et al, 1996 and Jahnke, 1994). For both water level and baseflow calibrations, the values of the hydraulic parameters and boundary conditions were adjusted manually (trial-and-error) to provide better comparisons.

7.2 STEADY STATE

Under steady-state conditions, the natural recharge into a basin is equal to the natural discharge out of the basin and there is no loss of groundwater storage. Predevelopment or small-scale development conditions in a basin are usually modeled using steady state.

7.2.1 Water Level Measurements

The calibration of the hydrologic model, using water table conditions, was performed by correlating measured water levels, recorded by the ADWR in the Well Registry, to modeled water level conditions. Water level measurements at individual well locations taken before 1960, from around the San Pedro Basin, were used in this analysis. Although measurements from before 1940 would be ideal for calibration of

steady state conditions, there are relatively few of them, and the majority of them are within the floodplain. The year 1960 was selected as a cut off date because large scale development did not occur until after this time, as well as this date allowed for a better distribution of well measurements throughout the basin. Figure 7-1 shows the location of the wells selected for the steady state calibration process.

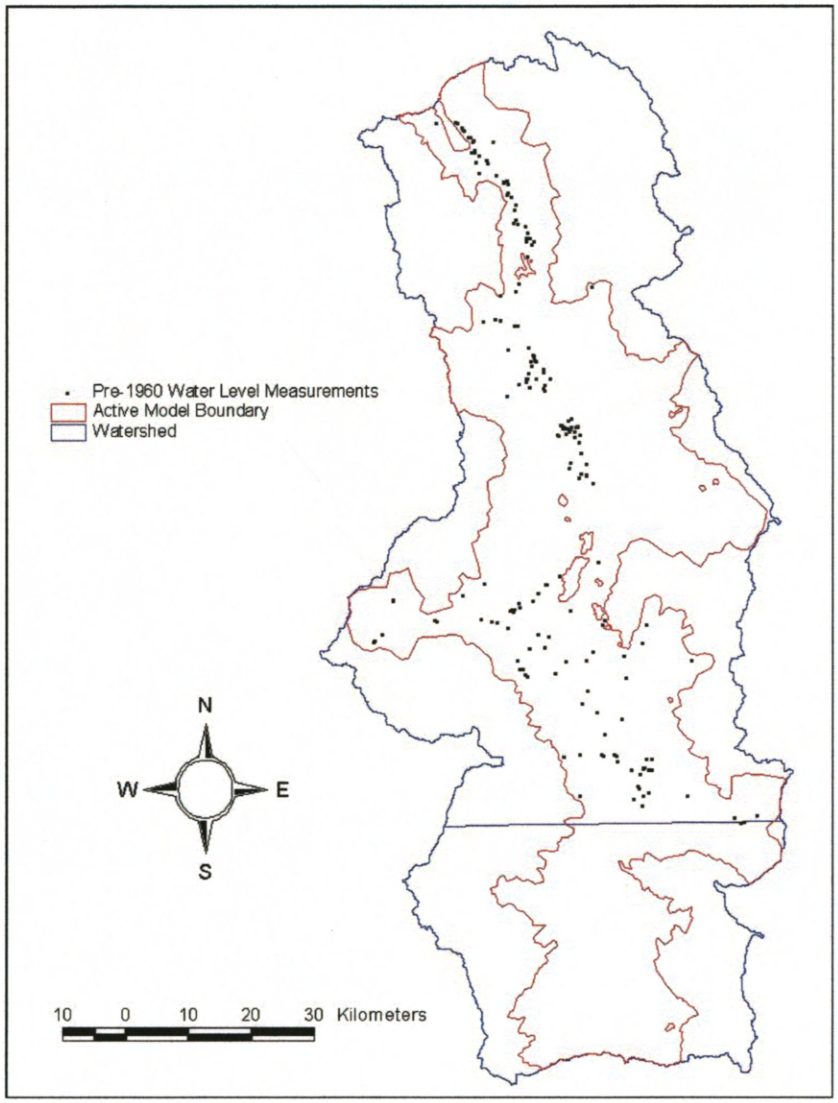

Figure 7-1 Location of pre-1960 water level measurements

A total of 209 wells were used for the steady-state evaluation, from which 8 wells were removed from the calibration process along the mountain front, near Nicksville, south of Sierra Vista. These wells were removed as they were thought to be associated with perched aquifer conditions caused by shallow bedrock along the pediment. The water levels of these wells were shallow, within 1-2 meters of the land surface. They are believed not to represent the regional aquifer system.

Water levels for the 201 observation wells were assigned to layers based on the depth of each of the wells. Because depth does not necessarily indicate screened interval, observed water levels might be a composite of heads from more than one layer. MODFLOW does not have the ability to calculate a composite head in a well that is screened through more than one layer. Fortunately, the majority of the 201 wells are screened within a depth represented by model layer 2. This layer includes both the floodplain and the upper portion of the regional aquifer system.

Figures 7-2 and 7-3 graph the final calibrated computed heads versus observed and computed heads versus residual. Error in the computed heads versus observed heads were deemed acceptable if residuals were less than 10 meters. The criteria of 10 meters residual is based on 1.0 percent of the total elevation change for the model domain, consistent with USGS standards.

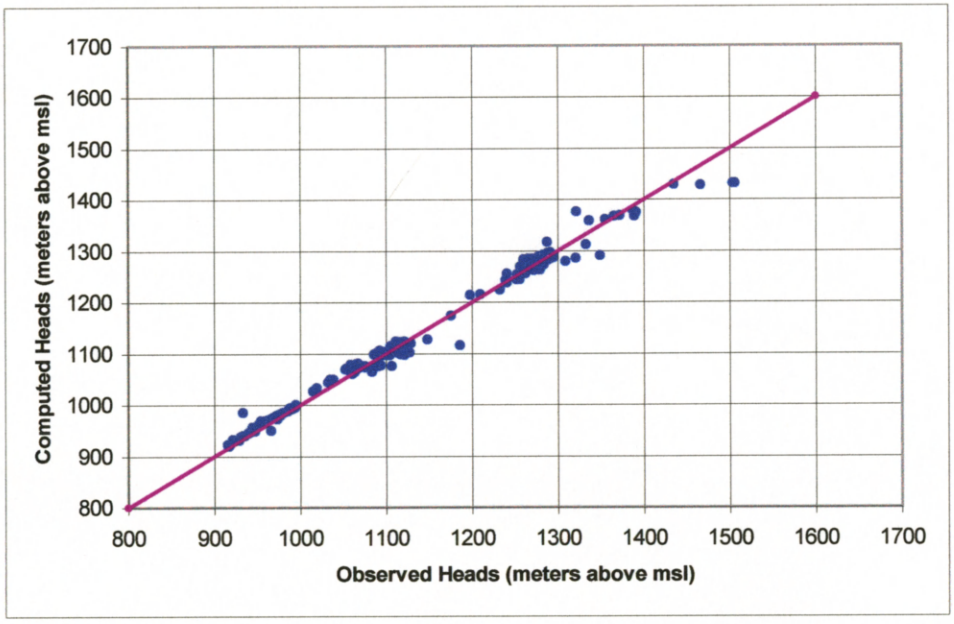

Figure 7-2 Computed versus observed heads for steady state simulation

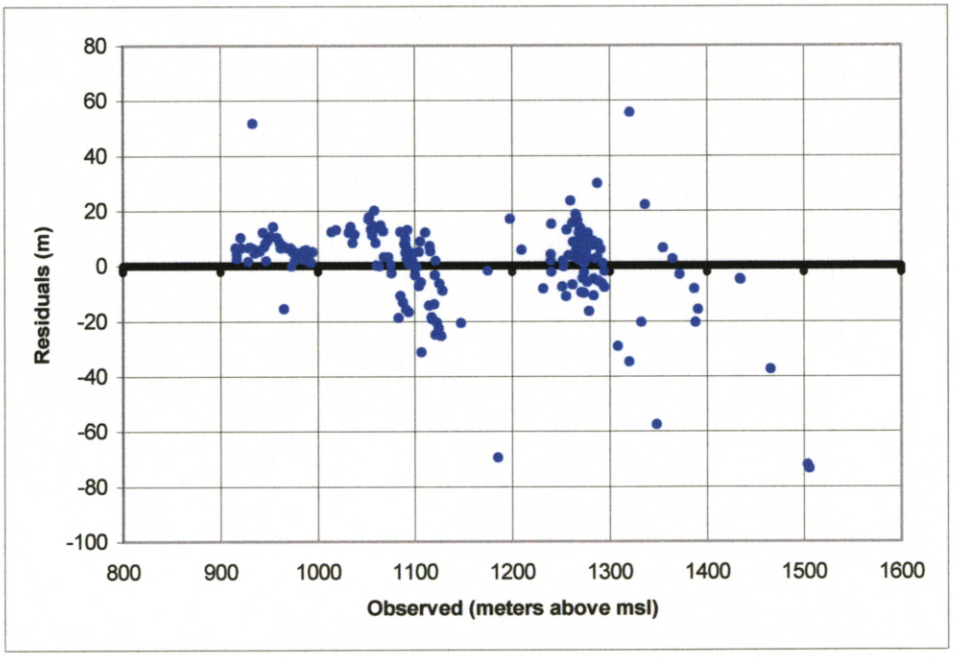

Figure 7-3 Residual versus observed heads for steady state simulation

The limitations of the spatial information for individual wells should be considered in evaluating the above graphs. As discussed in section 5 (Well Pumping) of this study, the locations of all wells within the registry are assigned to 10-acre blocks. This means that the location of any one well could be off by up to 150 meters horizontally. The reference elevation for most wells within the registry is taken from maps, meaning that elevations could be off anywhere from 3 to 25 meters (10 to 80 feet) depending on contour intervals. Water level information from these wells is compared to the simulated water levels of the nearest four model cells using a bilinear interpolation technique in GMS (1999). Model cells along many of the edges of the active model domain exceed one square kilometer in size.

Taking the above limitations into account, it is therefore conceivable that a water level from a well that is off by 150 meters horizontally and 25 meters vertically is compared to a simulated water level, interpolated over an area greater than 4 km^2. With this in mind, note that the outlying points which can be observed in Figures 7-2, 7-3 (and later in Figures 7-5, 7-6) are found along the higher elevations along the edges of the basin, where model cells are larger. Additionally, the regions along the edges of the basin are more variable in the subsurface as well, which may also account for the large discrepancies between observed and simulated.

The limitations mentioned above are presented not to discourage the use of these data points, simply that the model is only as good as the information that is input. As more precise well information is gathered within the basin, model precision can be

refined. For this study, it seems more beneficial that comparisons of simulated results to observed values be evaluated for general trends.

There are several statistical methods of evaluating observed versus computed water levels allowed by GMS. These analyses of the general trends are mean error (ME), mean absolute error (MAE), and root mean square error (RMS). According to the GMS v3.0 Reference Manual (1999) the mean error is computed as:

$$ME = \frac{1}{n}\sum_{i=1}^{n}(h_m - h_s)_i \tag{14}$$

where:

n = the number of simulations

h_m = measured head

h_s = simulated head

The mean error calculation provides a comparison of measured and computed head by taking the difference between them. A limitation to this method is caused by sign cancellation. An example of sign cancellation would be when the difference between the simulated value at is positive 10 meters. Compare this with another well where the difference between the simulated value at the well and the observed value of the well is negative 10 meters. The average difference between these two wells is zero, which can be misleading.

The mean absolute error eliminates the problem of misrepresentation of total error by sign cancellation, by taking the absolute value of the differences. Mean absolute error is calculated as (GMS, 1999):

$$MAE = \frac{1}{n}\sum_{i=1}^{n}\left|(h_m - h_s)_i\right| \tag{15}$$

The root mean square, or standard deviation error, may be calculated by (GMS, 1999):

$$RMS = \sqrt{\frac{1}{n}\sum_{i=1}^{n}(h_m - h_s)_i^2} \quad (16)$$

The root mean square error tends to heavily weight outlying points in the calculation. This occurs because of the squaring of the differences. When the majority of differences are small, with a few large ones, the error gives more significance to the few rather than the many.

Table 7-1 below shows all three different error calculations for the steady state simulation. Because of the limitations in calculating the mean error and root mean square error, the greatest priority as a calibration target value was given to the mean absolute error.

Table 7-1 Head error calculations for steady state simulation

The Mean Error	0.50
Mean Absolute Error	9.92
Root Mean Square Error	15.43

7.2.2 Streamflow/Gauging Measurements

Base flows of the San Pedro River at 2 locations, Palominas and Charleston, were used to calibrate the Steady State model. These baseflow measurements were taken from

Vionnet (1992). These measurements are displayed, along with baseflow measurements from two other gauging locations used in the transient calibration taken from Jahnke (1994), in Table 7-2. Values from 1990 are taken from Corell et al (1996).

Table 7-2 Baseflow discharge from previous studies

Baseflows Estimated by Previous Studies (cfs) (Vionnet, 1992; Jahnke, 1994; and Corell et al, 1996)							
Name of Gaging Station	1940	1950	1960	1970	1980	1990	1997
Palominas	4.27	*	*	*	*	2.70	*
Charleston	14.47	*	*	*	*	8.70	*
The Narrows	*	*	*	4.40	*	*	*
Redington	*	*	*	5.50	*	*	*

7.3 TRANSIENT STATES

For the purposes of this model, the transient states respond to the stresses of groundwater withdrawals and surface water diversions.

7.3.1 Water Level Measurements

Calibration of the transient model took place in much the same way as the steady state. Water-level information from the transient simulation was compared to observed water levels in several wells. The 225 wells selected had water level measurements in 1990. The simulated year 1990 was then used to make the evaluation.

Water level information from 9 wells located along the mountain front, near Nicksville, south of Sierra Vista, were then removed from the transient calibration, as they are likely to be, as mentioned above in the steady state section, representative of

perched conditions due to shallow bedrock and not the regional aquifer system. There were 216 wells remaining, shown in Figure 7-4, for evaluation of the transient simulation.

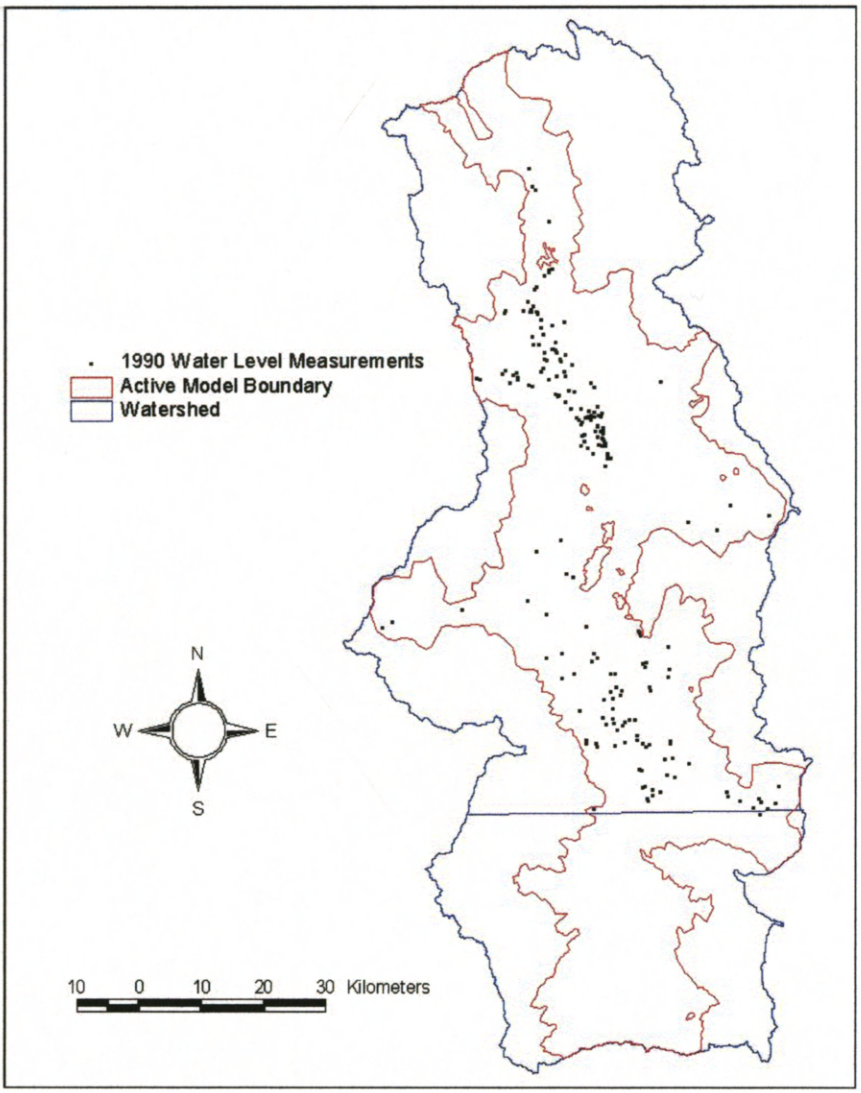

Figure 7-4 Location of 1990 water level measurements

Below in Figures 7-5 and 7-6 computed heads from 1990 are plotted against observed heads from that same year, and against their residuals.

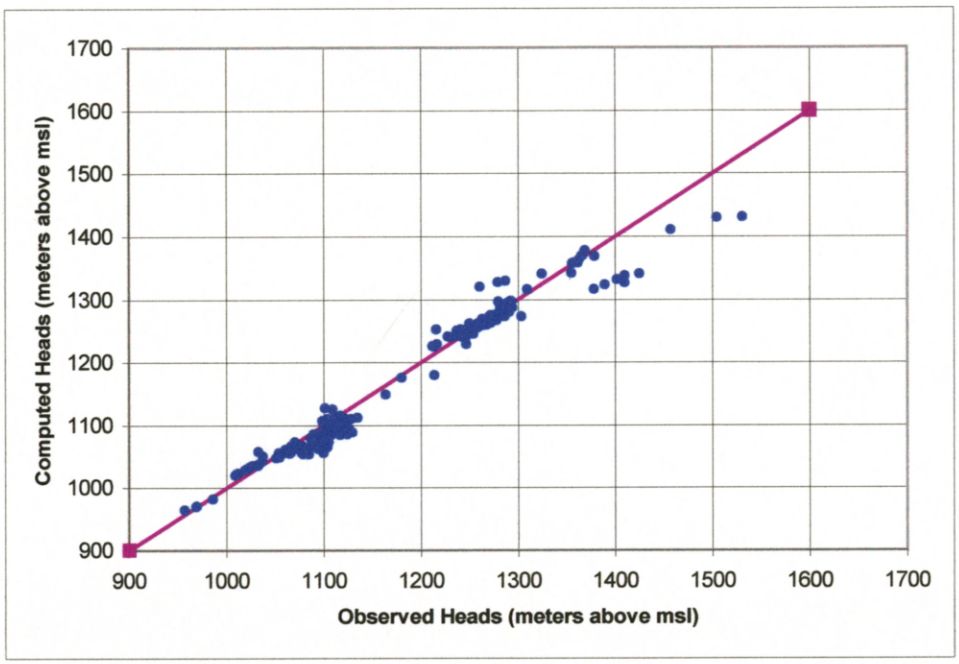

Figure 7-5 Computed versus observed heads for transient simulation

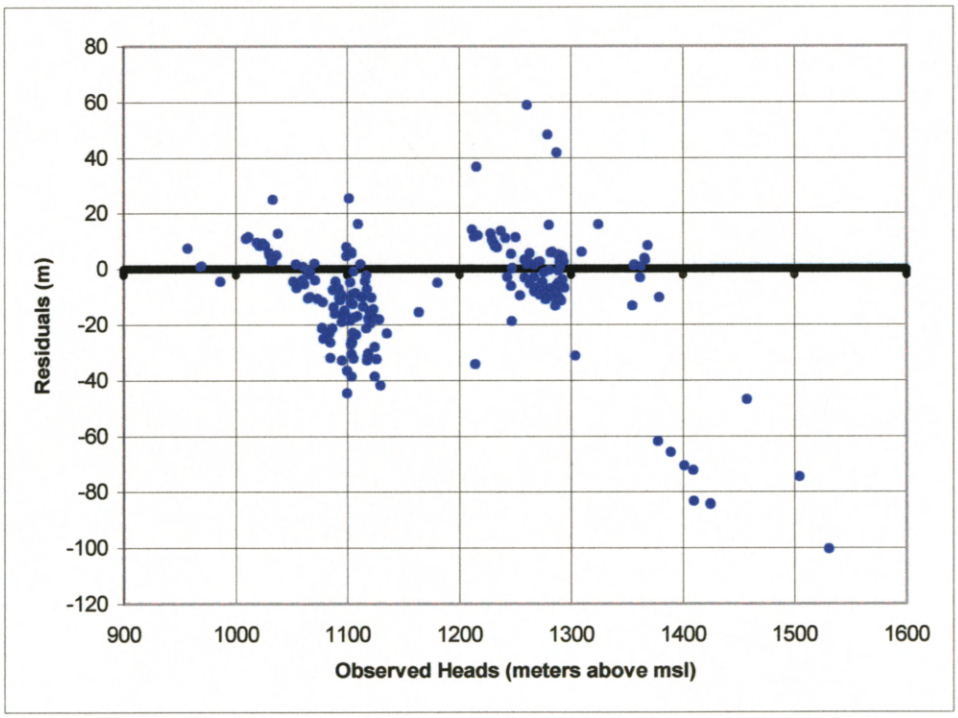

Figure 7-6 Residual versus observed heads for transient simulation

Table 7-3 below shows the error calculations for the transient simulation. The negative sign of the mean error indicates a slight bias of the model over predicting head levels. These over-predictions again occur at modeled regions at higher elevations.

Table 7-3 Head error calculations for the transient simulation

The Mean Error	-8.49
Mean Absolute Error	15.14
Root Mean Square Error	22.76

7.3.2 Streamflow/Gauging Measurements

Baseflow of the San Pedro River at two additional locations, "The Narrows" and Redington stream gages, along with the Palominas and Charleston guages, were used to calibrate the Transient model. The values of 1970 baseflow taken from Jahnke (1994) were used for comparison. The year 1970 was chosen for to reasons. The first is that there is no continuous information at these two sites prior to 1940, in order to make a comparison with the steady state (Jahnke, 1994). The second is that only after 1970 are the streamflow record lengths at these two sites sufficient to calculate baseflows. Table 7-3 displays the simulated flows at each of the used gages in ten-year increments. Compare these values to the baseflows shown in Table 7-1.

Table 7-4 Computed baseflows from steady state and transient simulations

Model Computed Baseflows (cfs)							
Name of Gaging Station	1940	1950	1960	1970	1980	1990	1997
Palominas	4.00	3.64	3.33	2.91	2.35	2.09	2.01
Charleston	13.24	12.22	11.49	10.34	9.03	8.83	8.87
The Narrows	13.61	11.19	9.03	6.17	2.98	1.38	0.88
Redington	14.67	11.85	9.40	6.17	2.59	0.82	0.62

7.4 SENSITIVITY

A limited sensitivity analysis consisted of testing two different parameters, streambed conductance (SC), and vertical conductance (VC) of the floodplain, because it was believed that these two parameter were critical to groundwater/surface water interactions. Steambed conductance was varied only along the San Pedro and Babocomari Rivers. These areas are located in the floodplain. The parameters were varied over a range of five orders of magnitude. This was accomplished by multiplying the calibrated values of SC and VC by 0.01, 0.1, 10, and 100. The results of this variation were compared using the observed water levels and stream flows at the four different stream gage locations, all taken from the steady state.

7.4.1 Streambed Conductance

Figure 7-7 and Figure 7-8 show that both stream flow and heads are extremely sensitive to changes in streambed conductance. Streamflow is significantly reduced when streambed conductance is decreased, and is just as significantly increased when streambed conductance is increased. This is reflects the gaining nature of most of the reaches along the San Pedro River.

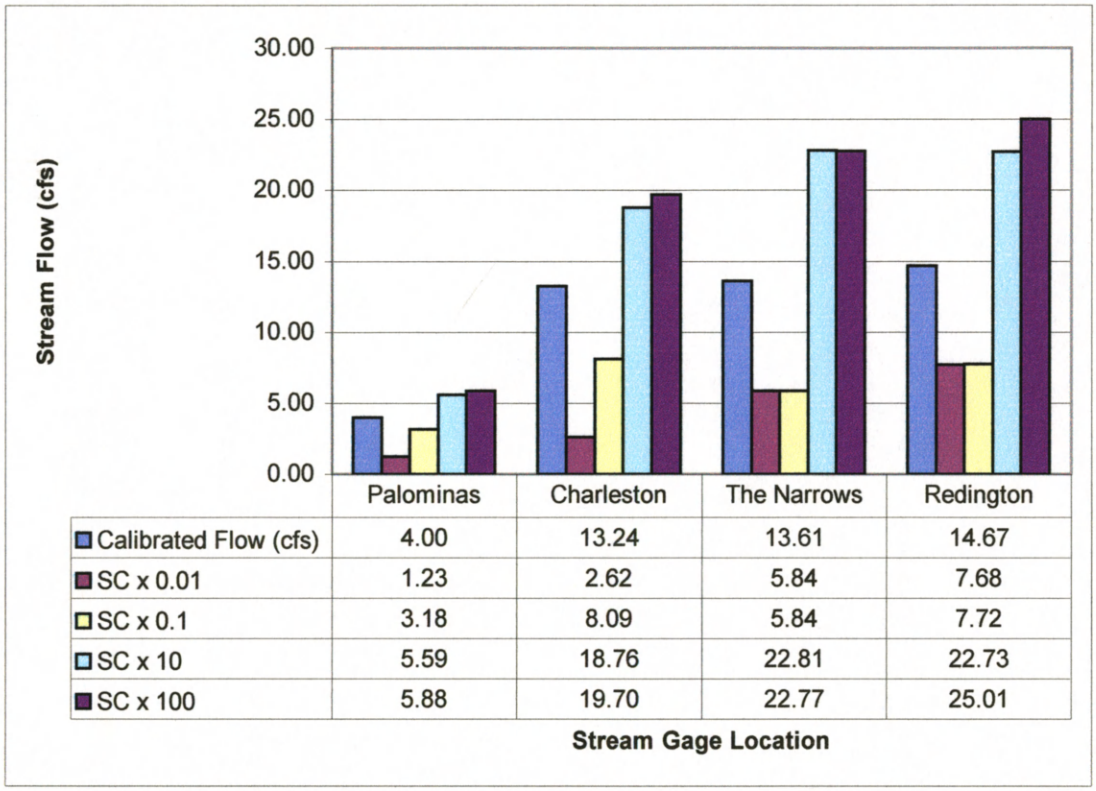

	Palominas	Charleston	The Narrows	Redington
Calibrated Flow (cfs)	4.00	13.24	13.61	14.67
SC x 0.01	1.23	2.62	5.84	7.68
SC x 0.1	3.18	8.09	5.84	7.72
SC x 10	5.59	18.76	22.81	22.73
SC x 100	5.88	19.70	22.77	25.01

Figure 7-7 Sensitivity of streamflow to changes in stream bed conductance

The average water level in the wells nears the rivers are significantly increased when streambed conductance was reduced. However, although water levels did decrease to some extent when streambed conductance was increased, the effect was not nearly as dramatic. It should also be noted that most of the changes in water level occurred in the Sierra Vista sub-watershed, while little change is observed in the Benson sub-watershed. Water levels increased in the Sierra Vista sub-watershed when streambed conductance was reduced, but water levels remained relatively unchanged in the Benson sub-watershed. This behavior is indicative of the fact that a large portion of the groundwater leaving the Sierra Vista sub-watershed leaves through the gaining reaches of the San

Pedro River. When this groundwater is restricted from discharging to the river, water levels in the surrounding area rise.

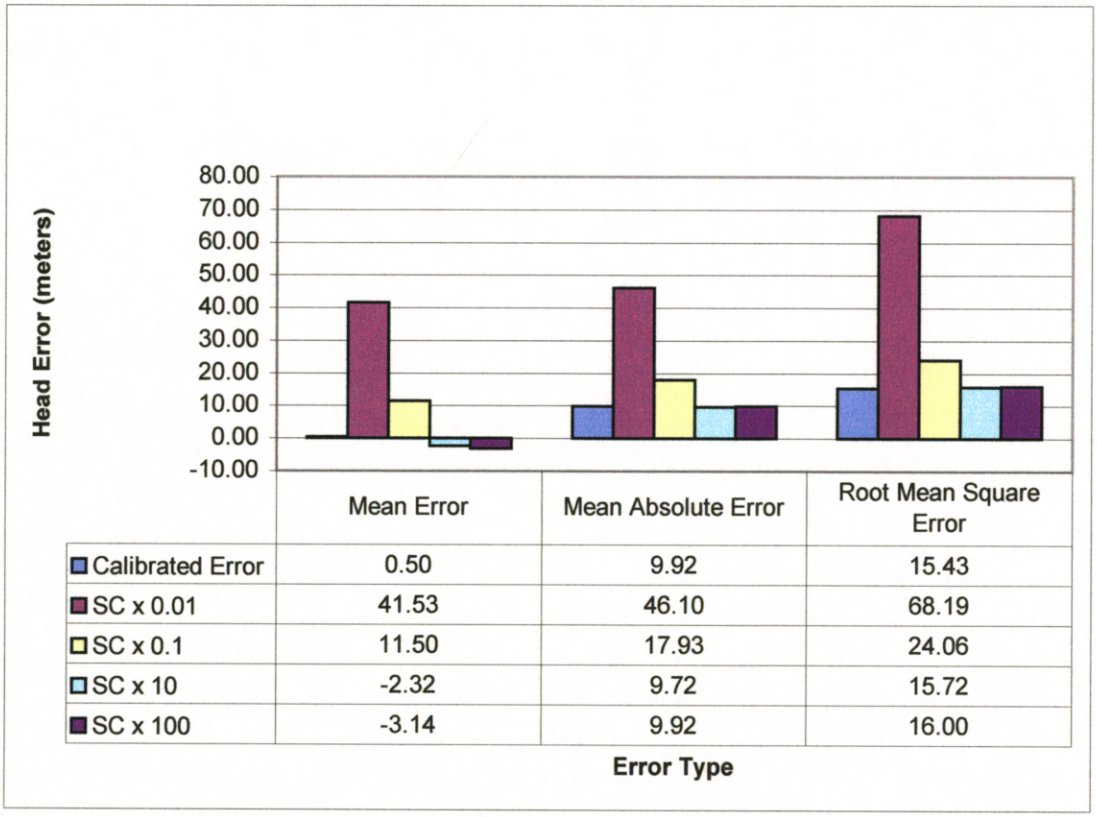

	Mean Error	Mean Absolute Error	Root Mean Square Error
Calibrated Error	0.50	9.92	15.43
SC x 0.01	41.53	46.10	68.19
SC x 0.1	11.50	17.93	24.06
SC x 10	-2.32	9.72	15.72
SC x 100	-3.14	9.92	16.00

Figure 7-8 Sensitivity of hydraulic head to changes in stream bed conductance

7.4.2 Floodplain Vertical Conductance

Variations in vertical conductance of the floodplain show little changes in either the water level or streamflow. Streamflow is seen to decrease only slightly at each of the stream gages when floodplain vertical conductance is reduced. When floodplain vertical conductance is increased, only the Palominas and Charleston stream gages show any changes, as seen in Figure 7-9.

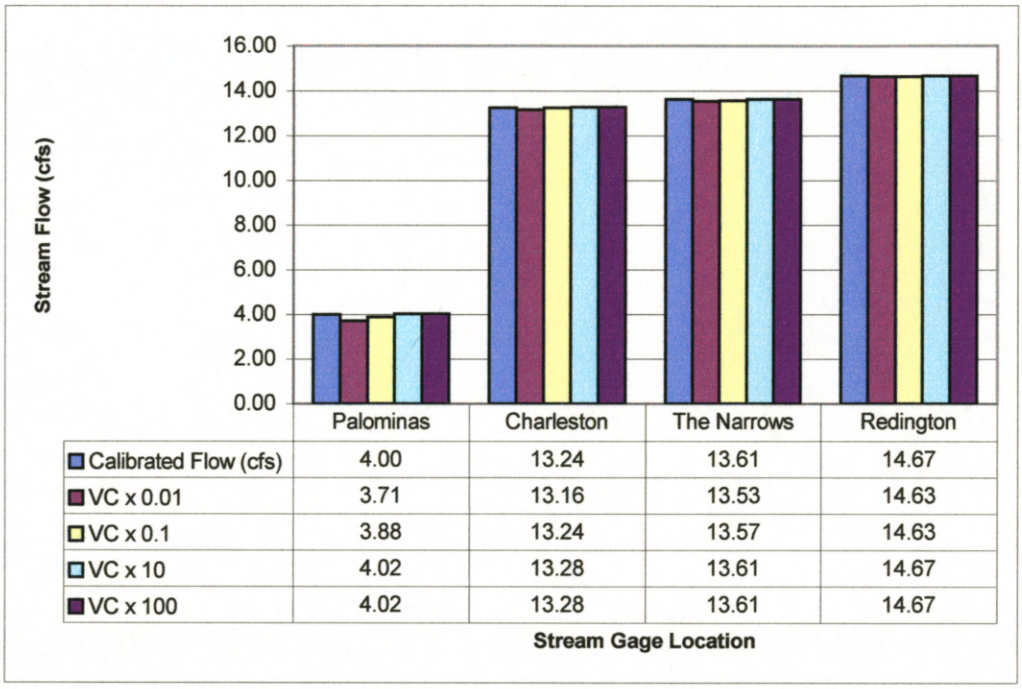

	Palominas	Charleston	The Narrows	Redington
Calibrated Flow (cfs)	4.00	13.24	13.61	14.67
VC x 0.01	3.71	13.16	13.53	14.63
VC x 0.1	3.88	13.24	13.57	14.63
VC x 10	4.02	13.28	13.61	14.67
VC x 100	4.02	13.28	13.61	14.67

Figure 7-9 Sensitivity of streamflow to changes in floodplain vertical conductance

A minimal effect is seen in water level changes due to the variation of floodplain vertical conductance. Water levels increase only slightly when the vertical conductance is reduced, and decrease only slightly when vertical conductance is increased, as seen in Figure 7-10.

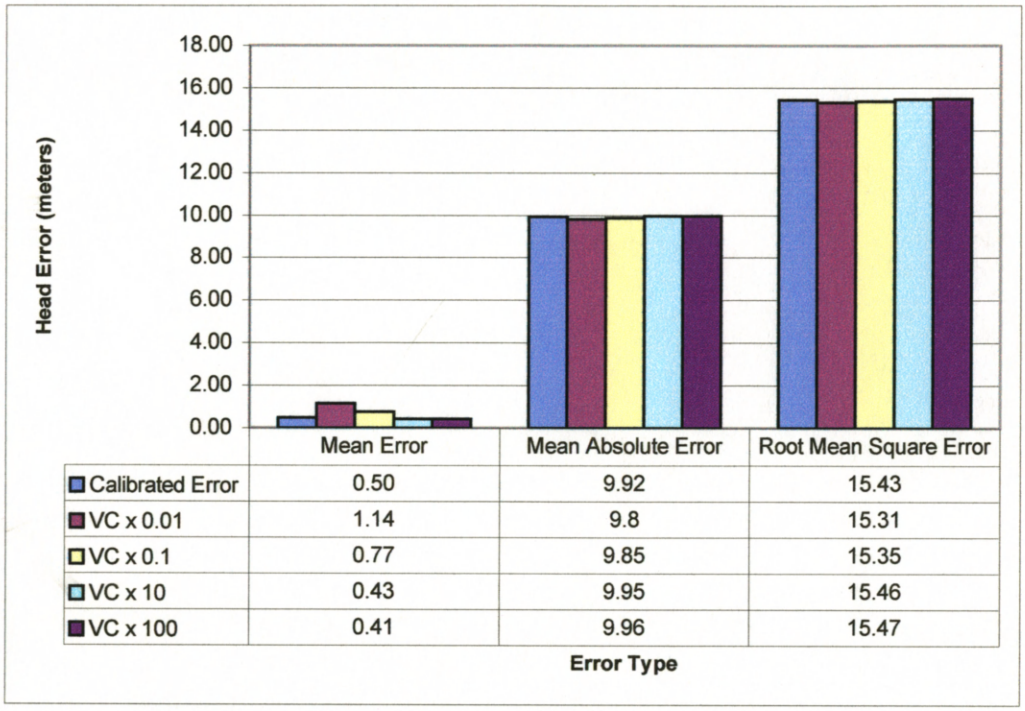

Figure 7-10 Sensitivity of hydraulic head to changes in floodplain vertical conductance

CHAPTER 8
RESULTS AND ANALYSIS

8.1 STREAM CAPTURE AND STORAGE LOSS

The effects of groundwater pumping in the Upper San Pedro Basin are examined by two ways: capture and water level decline. Capture is the way in which groundwater pumping affects the surface water and evapotranspiration systems. Whenever groundwater is pumped three things may happen (Theis, 1941). The recharge to the system may increase, the discharge from the system may decrease, and water may be removed from aquifer storage. In equation form, this is represented as:

$$(R + \Delta R) - (D - \Delta D) - Q = \Delta S/\Delta t \qquad (17)$$

Where,

R = natural recharge;

ΔR = change in recharge due to groundwater pumping;

D = natural discharge;

ΔD = change in discharge due to groundwater pumping;

Q = pumping rate;

$\Delta S/\Delta t$ = change in storage per unit of time.

Prior to development, the natural recharge is assumed to equal the natural discharge, which is represented by the equation

$$R = D \qquad (18)$$

Taking this into account, equation 17 simplifies to,

$$(\Delta R + \Delta D) - Q = \Delta S/\Delta t \qquad (19)$$

The term $(\Delta R + \Delta D)$ is called the capture.

The sources of capture in the Upper San Pedro Basin are evapotranspiration and stream discharge. Plates 1, 2, and 3 in the back cover display the capture rates for individual reaches along the San Pedro River for the years 1960, 1980, and 1997. The cumulative effects of capture from the stream can be seen in Plate 4, as streamflow decreases over time. In Figure 8-1 below, the change to key components of hydrologic system can be seen for each decade. As pumping increases, the rate of loss to both groundwater storage and stream capture also increase. As expected, an increase in pumping has an inverse effect on evapotranspiration processes. Evapotranspiration decreases as pumping increases. Agricultural recharge is included in order to complete the mass balance, in that, a portion of the pumping returns to the system as recharge.

By 1997, after taking into account agricultural recharge, 15.23% of pumping was taken from evapotranspiration, 65.66% taken from storage, and 19.11% was taken from streamflow.

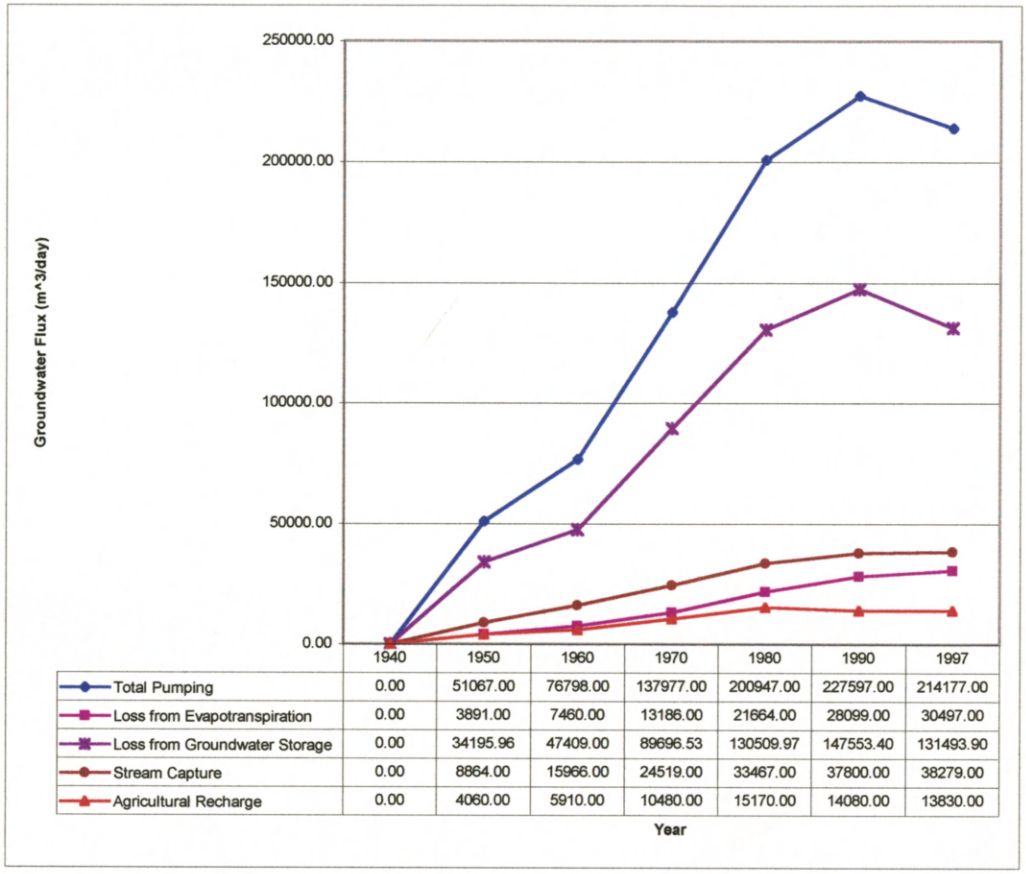

	1940	1950	1960	1970	1980	1990	1997
Total Pumping	0.00	51067.00	76798.00	137977.00	200947.00	227597.00	214177.00
Loss from Evapotranspiration	0.00	3891.00	7460.00	13186.00	21664.00	28099.00	30497.00
Loss from Groundwater Storage	0.00	34195.96	47409.00	89696.53	130509.97	147553.40	131493.90
Stream Capture	0.00	8864.00	15966.00	24519.00	33467.00	37800.00	38279.00
Agricultural Recharge	0.00	4060.00	5910.00	10480.00	15170.00	14080.00	13830.00

Figure 8-1 Mass balance flux components for the transient simulation

8.2 WATER TABLE DECLINE

Whenever there is storage loss to a groundwater system, there is a decline in water levels in the system. In the Upper San Pedro there are significant water table declines. Figure 8-2 shows 1940 simulated water levels taken from layer 2 of the model. Layer 2 was selected as it best represents the water table conditions in the Upper San Pedro Basin. Subsequent Figures 8-3, 8-4, and 8-5 show water level declines for the years 1960, 1980, and 1997. As seen from the previous figures, the areas with significant drawdown are near mining operations in Cananea, Sonora; and near the cities of Sierra Vista, Huachuca City, Benson, St David and Naco, Arizona. Other areas showing water table decline are near Pomerene-Hereford, and between "The Narrows" and Redington.

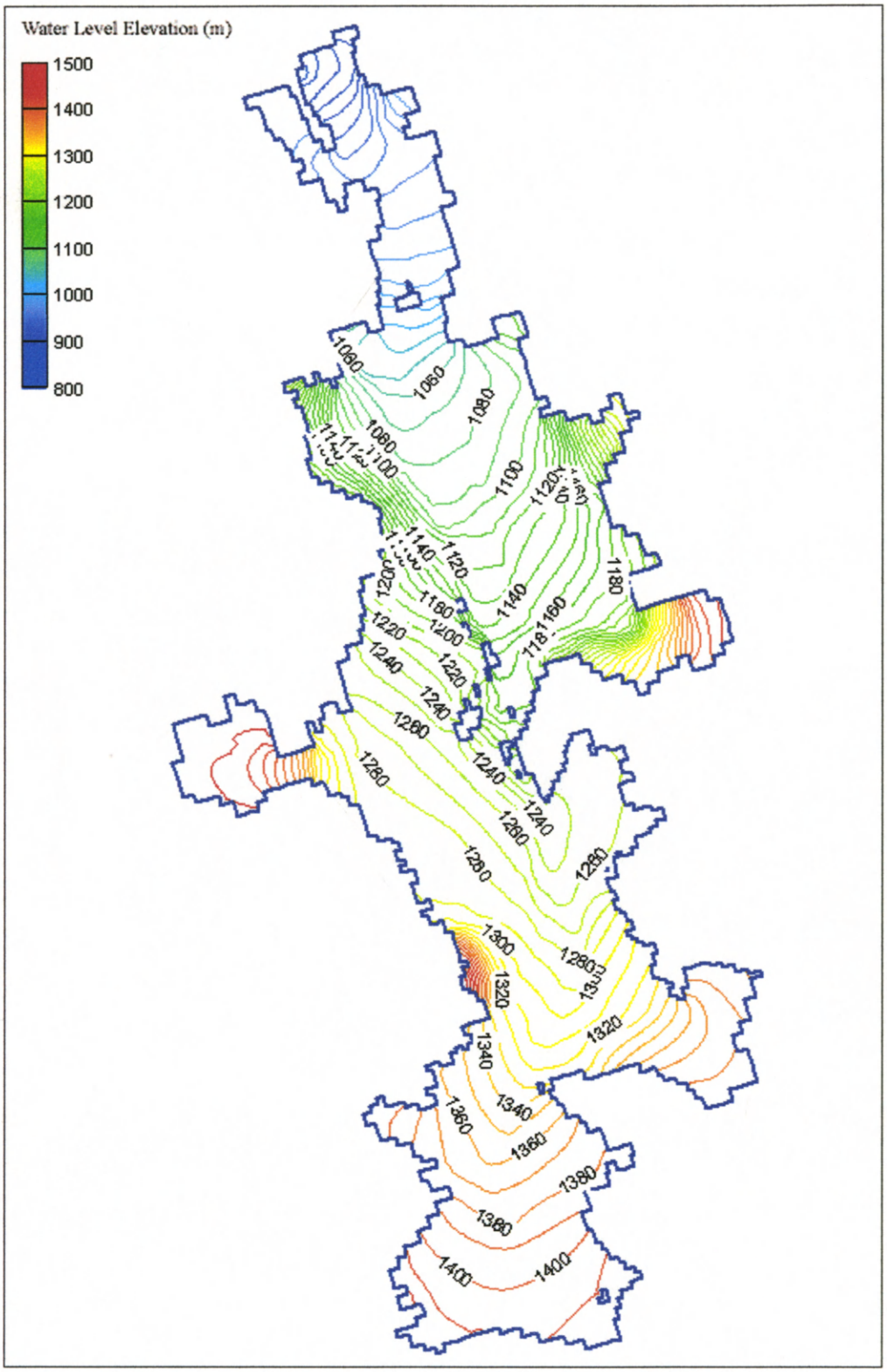

Figure 8-2 Simulated water levels for steady state (1940). Contour interval = 10 meters

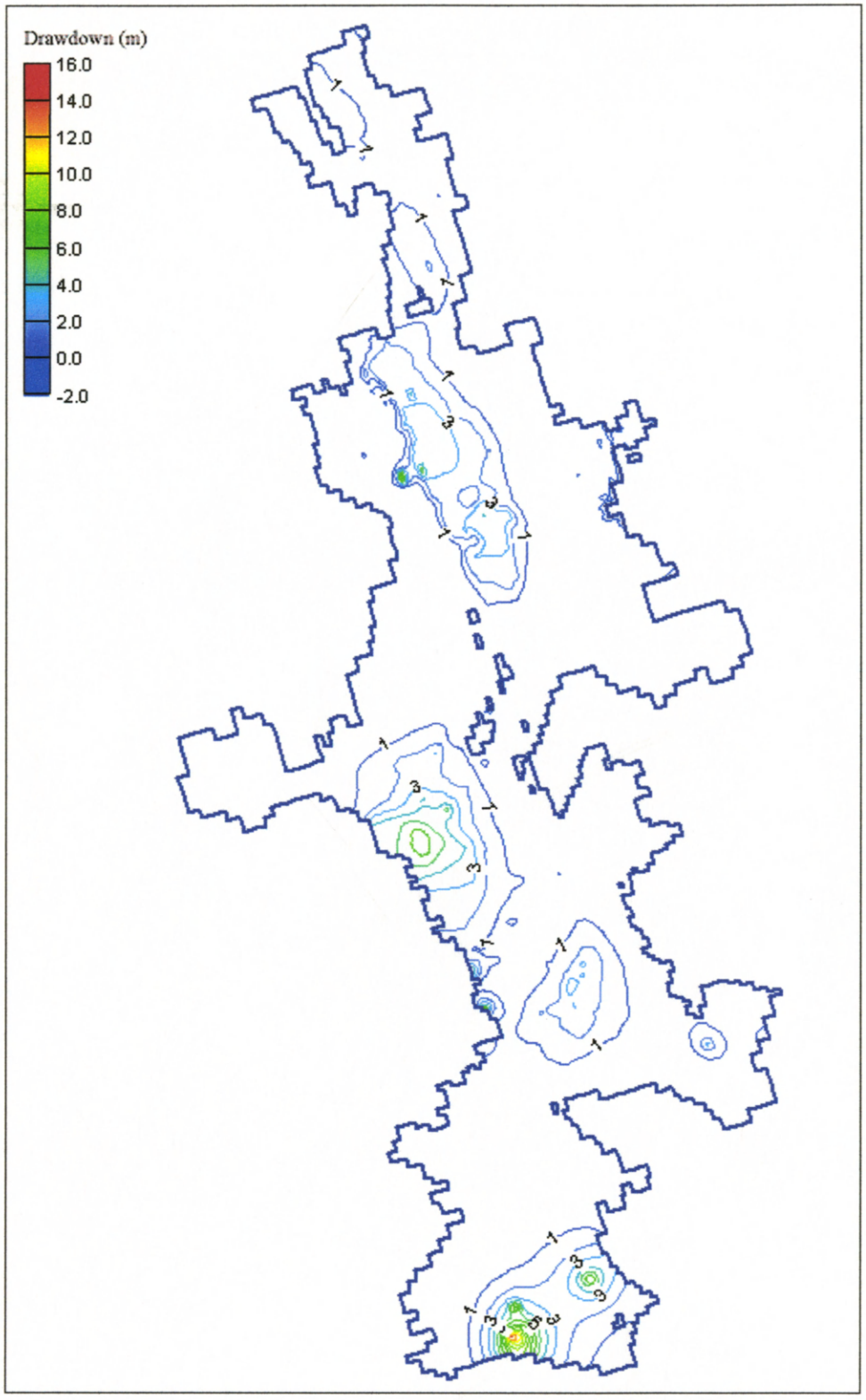

Figure 8-3 Simulated water level drawdown from 1940-1960. Contour interval = 1 meter

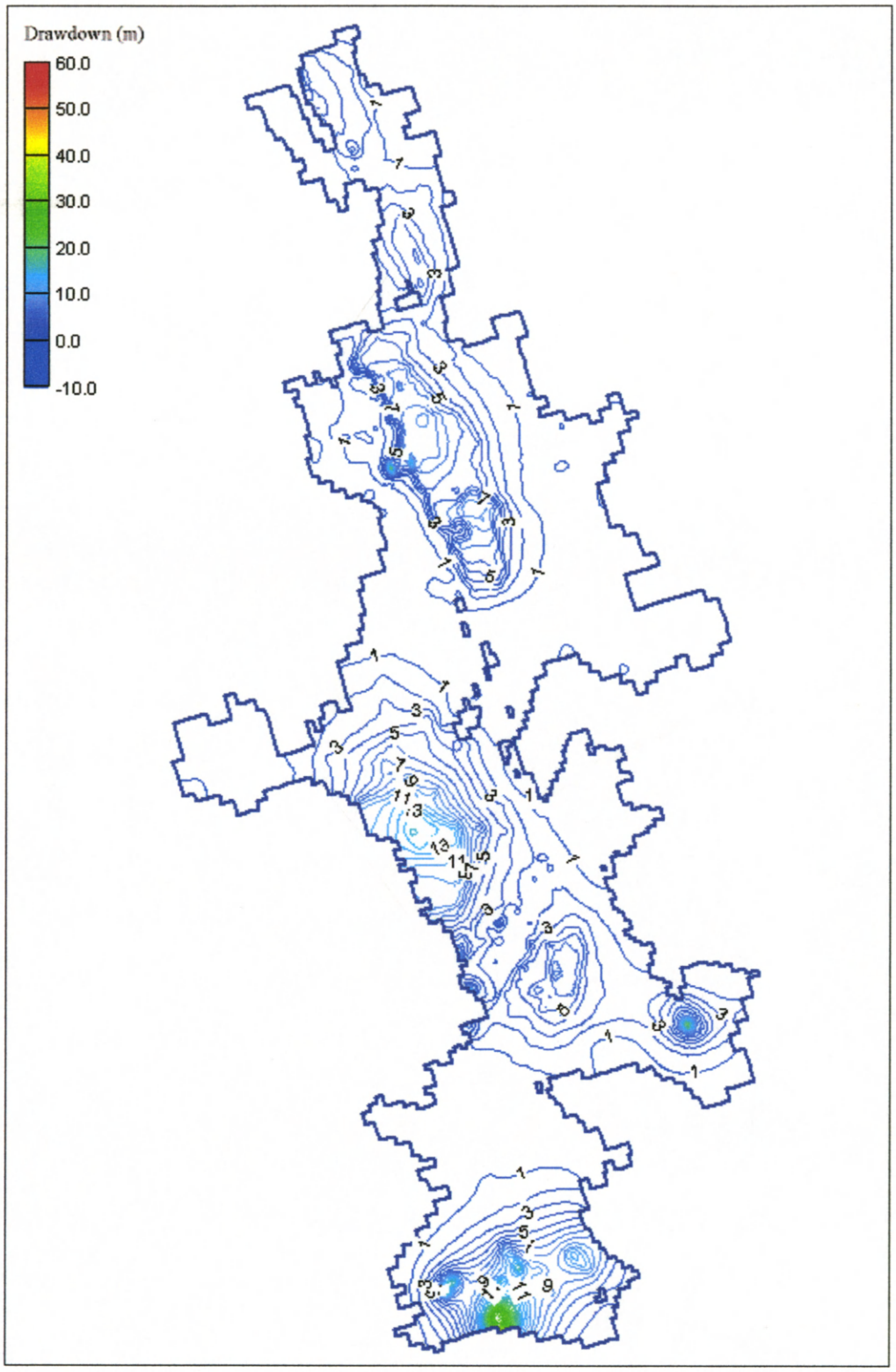

Figure 8-4 Simulated water level drawdown from 1940-1980. Contour interval = 1 meter

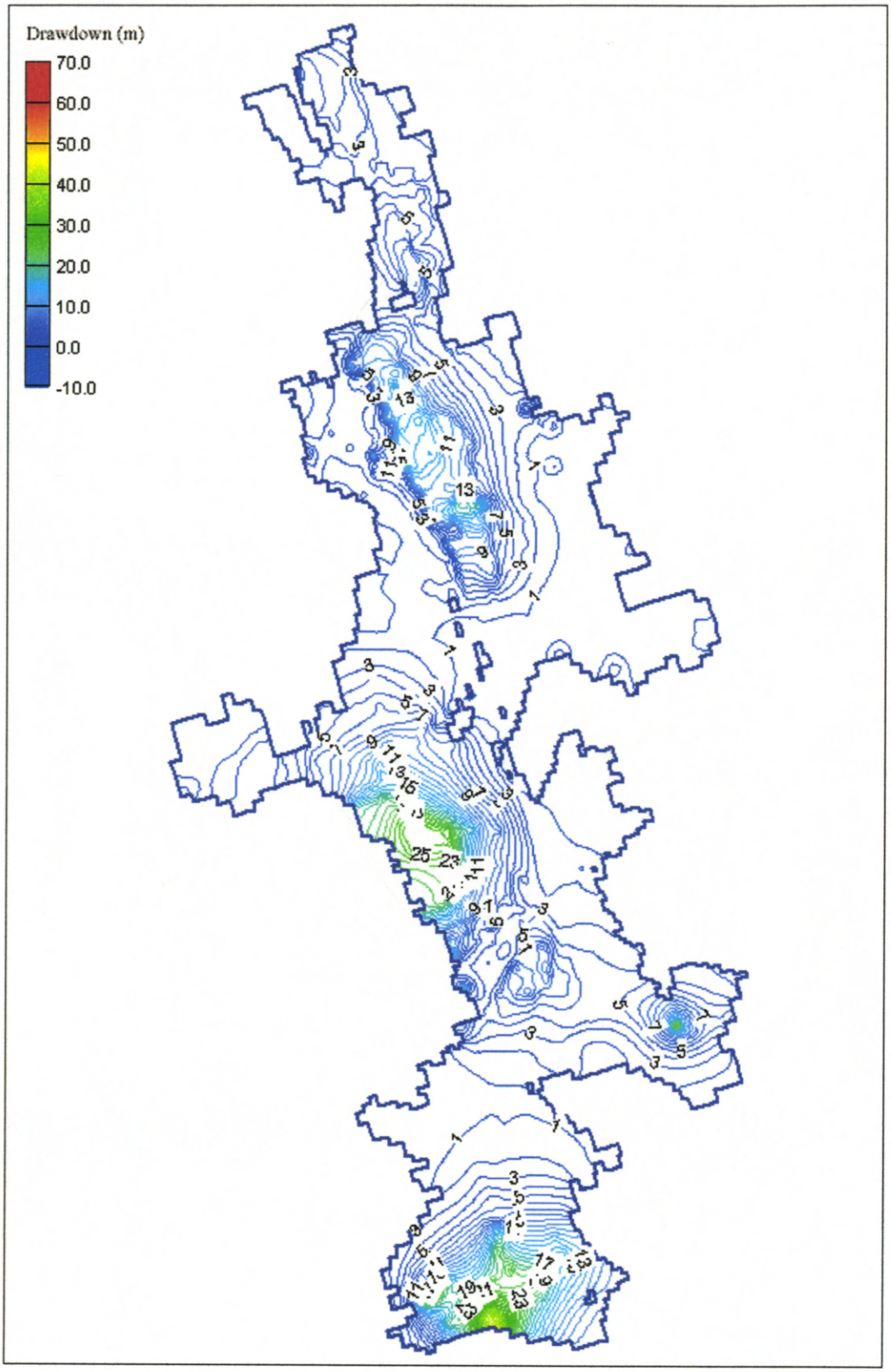

Figure 8-5 Simulated water level drawdown from 1940-1997. Contour interval = 1 meter

8.3 ALTERNATIVE FUTURE SCENARIOS

As mentioned in the Overview section, the current study is a component of the Alternative Futures study conducted by the Department of Defense, Desert Research Institute, and the Harvard Graduate School of Design. The Alternative Futures scenarios explore how urban growth and change in the rapidly developing Upper San Pedro Basin might influence the hydrology and biodiversity of the area. The study evaluates individual scenarios from the present time (1997-2000) to 20 years in the future (2020).

Presented below are 2 of the 10 scenarios evaluated by the Alternative Futures study. Presented first is the Open 2 scenario, followed by the Constrained 2 scenario. It is hoped that these two scenarios provide the reader with what are arguably two extremes (in relation to hydrological impact) of the possible futures in the basin.

8.3.1 Open 2 Scenario

The Open 2 scenario, from the Alternative Futures study, contains several pro-development measures that provide impacts upon ground and surface water systems. Open 2 assumes higher than accepted forecasted population growth in Arizona with major reductions of developmental control. Sonora also undergoes significant growth. The following is a list of some of the options considered by this scenario:

- Population increase in Arizona should be one half greater than that forecasted -- 2020 population is 111,500,
- 60% of new population lives in Rural, 15% in Suburban, 15% in Urban and 10% in Ex-Urban homes,
- A rural residential lot should be at least 1 acres within the basin and at least 1 acre within 1 mile of SPRNCA,
- Fort Huachuca remains open and doubles its current resident population,

- Kartchner Caverns should attract 200,000 people per year in 2020,
- Domestic water consumption public/company sources should remain at 1995 levels (60 gallons per day) and consumption from individually owned sources should also remain at 1995 levels (125 gallons per day),
- An INA should be established within the Upper San Pedro Basin; all existing irrigated agriculture remains, but proposed irrigated agriculture within 1 mile of the San Pedro River is prohibited,
- Cottonwood, willow and upland mesquite trees should not be removed,
- Ranching in the Upper San Pedro Basin should continue at its present intensity and locations,
- The leasing of state-owned land in the Upper San Pedro Basin for conservation purposes should not be allowed,
- Areas along the San Pedro River to the south that are not protected as par of the SPRNCA should be purchased for conservation purposes,
- The population of Cananea, Sonora doubles,
- Mining activity in Cananea, Sonora doubles,
- Sonora's conservation areas remain unchanged.

8.3.2 Constrained 2 Scenario

The Constrained 2 scenario, from the Alternative Futures study, provides a framework of conservation minded measures that in turn impact the ground and surface water systems. The Constrained 2 scenario assumes a reduced population growth in Arizona. Development occurs in the existing developed areas. The scenario gains potential conservation benefits from very large lot residential development. The following is a list of some of the options considered by this scenario:

- Population increase in Arizona should be one half less than that forecasted -- 2020 population is 78,500,

- 90% of new population lives in Urban and 10% in Ex-Urban homes,
- A rural residential lot should be at least 4 acres within the basin and at least 40 acres within 1 mile of SPRNCA,
- Fort Huachuca closes and its built facilities should be used for economic growth in the civilian sector with all the Training Area managed for conservation,
- Kartchner Caverns should attract 1,000,000 people per year in 2020,
- Domestic water consumption public/company sources is decreased by 20% from 1995 levels (48 gallons per day) and consumption from individually owned sources should also be reduced 20% from 1995 levels (100 gallons per day),
- All irrigated agriculture in the Upper San Pedro Basin is removed,
- Approximately half of the Cottonwood, willow and upland mesquite trees should be removed by the clearing of selected areas and that land managed to maintain a grassland ecosystem,
- Ranching in the Upper San Pedro Basin on state owned lands should be removed,
- The leasing of state-owned land in the Upper San Pedro Basin for conservation, purposes should be allowed by competitive bidding
- Areas along the San Pedro River that are not protected as part of the SPRNCA between Cascabel and the Mexican border should be purchased for conservation purposes (SPRNCA will span from Cascabel to the Mexican border),
- Mexico should establish an extension of the SPRNCA in Sonora; conserved habitat should extend to the town of Jose Maria Morelos, Mexico (near the headwaters of the San Pedro River).

The groundwater model is use to simulate the pumping effects of the two scenarios. Comparing the transient model results, one sees the positive and negative impacts to the hydrologic system. The Open 2 scenario provides a continued increase in pumping from present values and consequently an increase in the rate of storage loss. Capture from both the stream and the evapotranspiration also increase, as streamflows are diminished and evapotranspiration is reduced. Constrained 2 scenario exhibits some

increase of evapotranspiration from 1997-2000 conditions as well as reduced stream capture. All of these effects are due to the reduction in groundwater pumping (see Table 8-1). However, it should be noted that although the rate of loss from groundwater storage is reduced, it is in no way indicative of storage replenishment. Water is still being lost from storage, only at a slower rate.

Capture from individual stream reaches are displayed in a series of plates found in a packet on the back cover of this report. Plate 5 (from Open 2 scenario) shows the capture from the stream, as well as the number of reaches having no baseflow. Plate 6 shows the cumulative effect of the capture of water from streamflow, as many reaches have no baseflow (more than 1997). Plate 7 shows the capture for individual reaches associated with Constrained 2 scenario. Capture, in many areas, is positive due to the reduction of evapotranspiration caused by the removal of cottonwood, willow and mesquite trees. The cumulative effect can be seen in Plate 8, as streamflow increases over much of the San Pedro River when compared with 1997 and the Open 2 scenario conditions.

Table 8-1 Mass balance flux components for steady state, transient and Alternative Futures simulations (m^3/day)

	1940	1997-2000	Open 2 2020	Constrained 2 2020
Total Pumping	~0.00	214177.00	260856.00	94316.00
Riparian Evapotranspiration	71273.00	40776.00	37408.00	45871.00
Loss from Groundwater Storage	0.00	131493.90	179707.00	47515.00
Stream Capture	0.00	38279.00	38267.00	21050.00
Agricultural Recharge	0.00	13830.00	9000.00	370.00

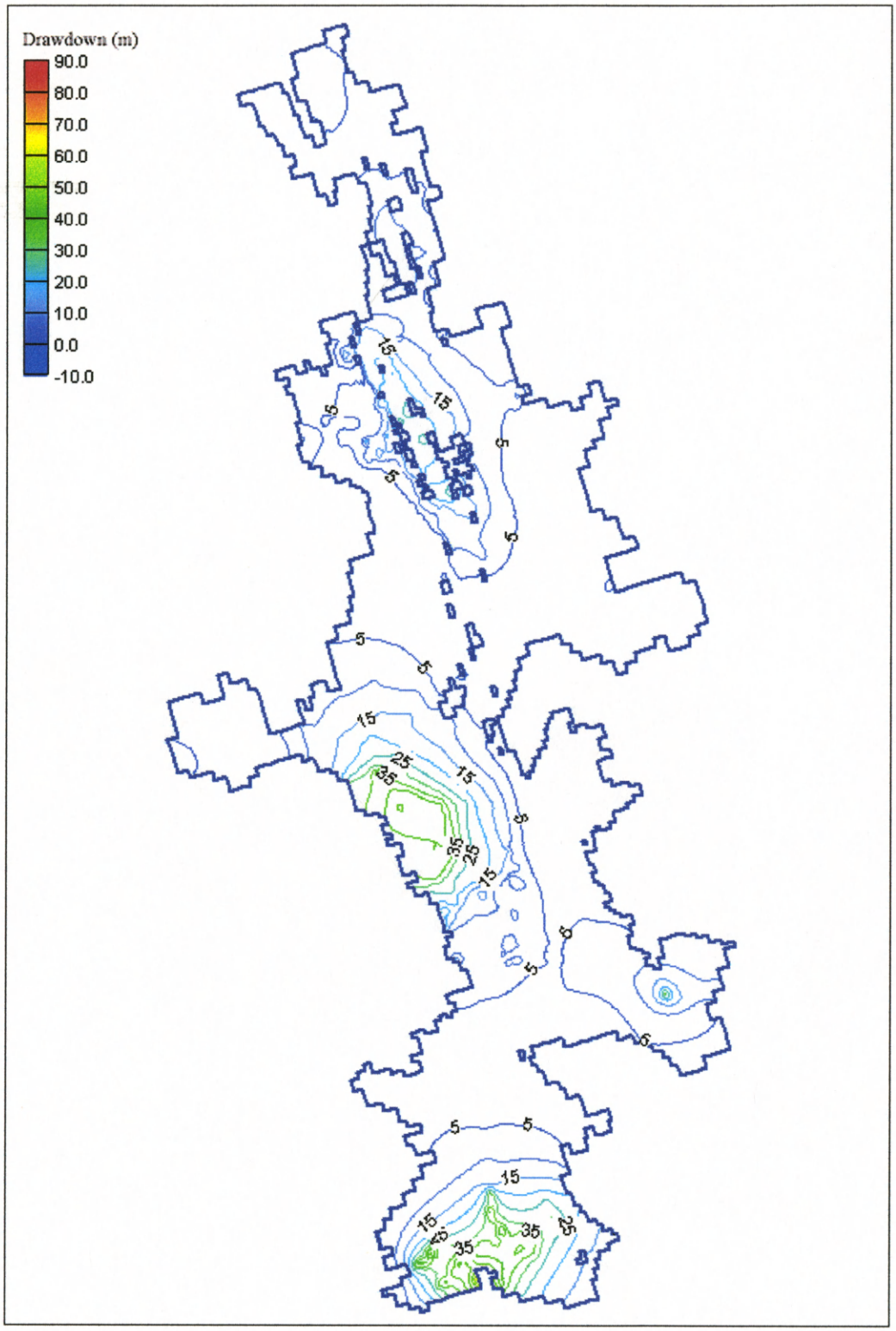

Figure 8-6 Simulated water level drawdown from 1940-2020 under the Alternative Futures Open 2 scenario. Contour interval = 5 meters

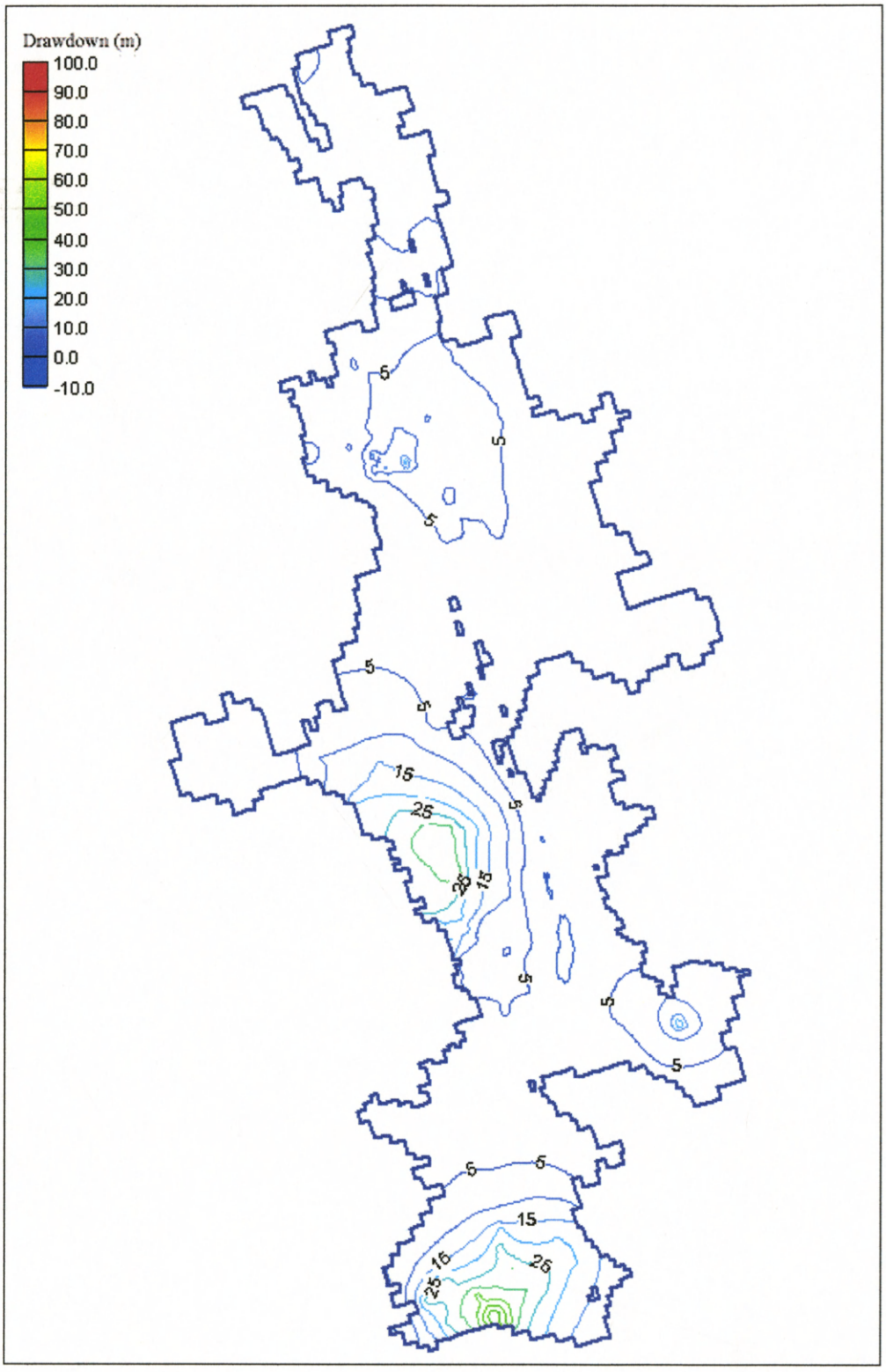

Figure 8-7 Simulated water level drawdown from 1940-2020 under the Alternative Futures' Constrained 2 scenario. Contour interval = 5 meters

Figure 8-6 shows a lowering of water levels throughout the basin from the Open 2 scenario pumping. The continued use of large-scale irrigation in the U. S. continues to reduce water levels near the San Pedro River, and increasing population creates a demand that lowers water levels dramatically around the cities. Figure 8-7 shows the results of simulating the Constrained 2 scenario pumping. It shows a continued lowering of water levels near the cities (although less substantial in comparison to Figure 8-6), however there is an increase of water levels near the San Pedro River

CHAPTER 9
CONCLUSIONS AND RECOMMENDATIONS

9.1 CONCLUSIONS

The hydrologic system of the Upper San Pedro Basin is highly complex, and because of the mathematical approximations and the geographical scale for this model, many of these complexities have been simplified. Although some accuracy is lost in the simplification, many larger trends associated with the impacts of groundwater pumping can still be determined. The larger trends from 1940 to 1997 indicated by the model are:

- Reduction of streamflow in the San Pedro River,
- Reduction of evapotranspiration by riparian vegetation along the floodplain of the San Pedro River,
- The formation of significant cones of depression near many communities and associated large losses of groundwater storage.

The depletion of streamflows in the San Pedro River by groundwater pumping can be readily seen in the some of the reaches near the Benson area. By 1997, these reaches have no baseflow. This is because by 1997, nearly 20 percent of the water pumped in the Upper San Pedro Basin was taken from the San Pedro River. Although baseflow still exists in the Charleston area in 1997, the model indicates that the flow has been reduced by more than 30% since 1940.

Since the creation of the SPRNCA, water levels along the protected portion of the floodplain have seen some recovery. However, water is still being taken from the riparian area outside SPRNCA. This pumping has lead to over 15 % of the water

pumped by 1997 to be taken from evapotranspiration, and thus to be taken from the riparian vegetation.

Cones of depression can be observed in excess of 25 meters beneath Sierra Vista, Arizona and greater than 40 m near Cananea, Sonora in 1997. Lesser water table declines can be seen along the floodplain near the communities of St. David and Benson,and near the city of Naco. The water level declines are indicative of losses from groundwater storage. By 1997, over 65% of the water pumped was taken from storage.

The results of this study are not unlike the results of previous studies in the San Pedro Basin. Previous studies have all indicated cones of depression, reduction of streamflows, and loss from groundwater storage and evapotranspiration (Vionnet, 1992; Jahnke, 1994; Corell et al, 1996). This study serves to further substantiate the evidence presented previously, as well as provide a framework for analysis of Alternative Futures within the basin. This framework provides decision makers within the basin an avenue for testing the impacts of possible policy changes. The framework also provides to future investigators of the basin an improved model for advancement of hydrologic study in the area.

9.2 RECOMMENDATIONS

Although pumping rates in this study were associated with individual wells, these rates were still estimates. As information becomes available, these estimates should be replaced with actual pumping rates. In addition to revising pumping rates, information on well locations could be more precise, in keeping with the field checked sites of the GWSI. As the GWSI is expanded to including more wells in the area, the depths and screened intervals of individual wells should be input into the model for a better

simulation of vertical distribution of pumping, and in turn a better simulation of hydraulic heads in different layers. Essentially, with greater precision of well information comes greater precision of results from any future modeling effort.

Recharge processes in the basin should be studied further in order to better distribute mountain front recharge throughout the basin. Although recharge distribution based on average precipitation of contributing basins was generally successful, recharge in some areas was still reduced during calibration. There should be some consideration of the changes in infiltration capacity for these areas. Specific research of the processes of recharge in ephemeral streambeds, primarily along the mountain front where infiltration occurs, would be very beneficial.

Agricultural recharge should be further refined to include factors of individual field sizes, crop type, method of irrigation, and actual water applied (having components of both surface and pumped groundwater). Additionally, artificial recharge, or use of effluent as a recharge component, should be considered in future models. The use of recharge basins was not considered in the current modeling attempt.

The inclusion of measured streambed conductances would be beneficial in further understanding the communication of groundwater and surface water. The model is very sensitive to changes in streambed conductance, thus real measurements would be very beneficial in the calibration process.

Information of more well locations, measured water levels, and pumping rates in Mexico should be included in future studies. Measured hydraulic parameters, and depth to crystalline bedrock in Mexico would also be very beneficial, since factors such as hydraulic conductivity and basin shape were assumed in the current model.

CHAPTER 10
REFERENCES

Agüero, Arturo Rodríguez, "History of Cananea, Mexico," Divided Waters, Common Ground: Cooperative Research and Management of Binational Resources in the Upper San Pedro River Basin of Sonora and Arizona, San Pedro Conference Proceedings, November 1999.

Anderson, T. W., Geoffrey W. Freethey, and Patrick Tucci, Geohydrology and Water Resources of Alluvial Basins in South Central Arizona and Parts of Adjacent States, U.S. Geological Survey Professional Paper 1406-B, United States Government Printing Office, Washington, 1992.

Arias, Hector, Instituto del Medio Ambiente y el Desarrollo Sustentable del Estado de Sonora (IMADES), Hermosillo, Sonora, Mexico, 1999.

Arizona Department of Water Resources, Arizona Well Registry Distribution Database CD-ROM, 1st Ed, 1999.

Arizona Department of Water Resources, Groundwater Site Inventory, November 1999.

Arizona Department of Water Resources, General Assessment. Volume 1, Hydrographic Survey Report for the San Pedro River watershed. Arizona Department of Water Resources, Phoenix, Arizona, 1991.

Bahre, Conrad Joseph, A Legacy of Change: Historic Human Impact on Vegetation in the Arizona Borderlands, University of Arizona Press, Tucson, Arizona, 1991.

Chehbouni A., D. C. Goodrich, M.S. Moran , C. J. Watts, Y.H. Kerr, G. Dedieu, W. G. Kepner, W.J. Shuttleworth and S. Sorooshian, "A Preliminary Synthesis of Major Scientific Results During the SALSA Program," Special SALSA Edition of Journal of Agricultural and Forest Meteorology (JAFM), (in press) June, 2000.

Church of Jesus Christ of Latter Day Saints, Church History in the Fullness of Times, Salt Lake City, Utah, 1989.

Corell, S.W., Corkhill, Frank, Lovvik, Daryl, Putman, Frank, A Groundwater Flow Model of the Sierra Vista Subwatershed of the The Upper San Pedro Basin, Southeastern Arizona. Arizona Department of Water Resources Modeling Report No. 10, 1996.

Daly, Chris and George Taylor, Arizona Average Monthly or Annual Precipitation 1961-90, Water and Climate Center of the Natural Resources Conservation Service, Portland, Oregon, 1998.

"Digital Geologic Map Database of Southeast Arizona, version 1.3", unpublished working document, U.S. Geological Survey SW. Field Office, Tucson, AZ. (No authorship).

Digital Raster Graphics http://mcmcweb.er.usgs.gov/drg/drg_overview.html

Final Report Regional Recharge Research for Southwest Alluvial Basins, U. S. Geological Survey SWAB/RASA Project, 1980.

Freethey, Geoffrey W., Hydrologic analysis of the Upper San Pedro Basin from the Mexico U.S. Boundary to Fairbank, Arizona. U.S. Geological Survey Water-Supply Paper 1819-D, 1982.

Gettings, Mark E. and Brenda B. Houser, Depth to bedrock in the Upper San Pedro Valley, Cochise County, southeastern Arizona, Open-File Report 00-138, 2000.

Gignac, Judy, Owner of Bella Vista Water Company, Personal communication, June 12, 2000.

GMS v3.0 Reference Manual, Brigham Young University, Environmental Modeling Research Laboratory, 1999.

Gray, R. S., Late Cenozoic sediments in the San Pedro Valley near St. David, Arizona. Ph.D. Dissertation, Department of Geoscience, The University of Arizona, Tucson, 1965.

Goodrich, D.C., R. Scott , J. Qi, B. Goff, C. L. Unkrich, M.S. Moran, D. Williams, S. Schaeffer, K. Snyder, R. MacNish, T. Maddock, D. Pool, A. Chehbouni, D. I. Cooper, W. E. Eichinger, W.J. Shuttleworth, Y. Kerr, R. Marsett, W. Ni, "Seasonal Estimates of Riparian Evapotranspiration Using Remote and *In-Situ* Measurements," Special SALSA Edition of Journal of Agricultural and Forest Meteorology (JAFM), (in press) June 2000

Hadley, Diana, "Historical Land Use Context for the Upper San Pedro River Basin, Sonora, Mexico," Divided Waters, Common Ground: Cooperative Research and Management of Binational Resources in the Upper San Pedro River Basin of Sonora and Arizona. San Pedro Conference Proceedings, November 1999.

Halvorson, P. F., An Exploration Gravity Survey in the San Pedro Valley, Southeastern Arizona. M.S. Thesis, Department of Geosciences, The University of Arizona, Tucson, 1984

Huckleberry, Gary, Historical Channel Changes on the San Pedro River, Southeastern Arizona. Arizona Geological Survey, Open File Report 96-15, June 1996 (revised October 1996).

Jahnke, Philip, Modeling of Groundwater Flow and Surface/Groundwater Interaction for the San Pedro River Basin from Fairbank to Redington, Arizona. M.S. Thesis, Department of Hydrology and Water Resources, The University of Arizona, May 1994

Kepner, William G., C. J. Watts, C. M. Edmonds, D. T. Heggem, and T. G. Wade, A Landscape Approach for Detecting and Evaluating Change in a Semi-arid Environment. U.S. Environmental Protection Agency (EPA/600/C-00/002), Office of Research and Development, Las Vegas, Nevada

Lombard, James P, Draft Modeling Report for San Pedro River Stream Flow Simulations During the Time Period From 1998-2028 Using the University of Arizona Middle San Pedro Modflow Model. The Nature Conservancy, Arizona Chapter, 1998.

López, Isaac, "Water Issues Related to Mining in the San Pedro River Basin," Divided Waters, Common Ground: Cooperative Research and Management of Binational Resources in the Upper San Pedro River Basin of Sonora and Arizona. San Pedro Conference Proceedings, November 1999.

MacNish, R.D., C.L. Unkrich, Evelyn Smythe, D.C. Goodrich, and Thomas Maddock, III "Comparison of Riparian Evapotranspiration Estimates based on a Water Balance Approach and Sap Flow Measurements," Special SALSA Edition of Journal of Agricultural and Forest Meteorology (JAFM), (in press) June, 2000

Maidment, David R., Handbook of Hydrology, Mcgraw-Hill, Inc., San Francisco, 1993.

Madrid, Carmen, Arizona Corporation Commission, Utilities Division, 1997 Annual Reports for Individual Water Companies within Cochise County, June 15, 2000.

McDonald, Michael G., and Arlen W. Harbaugh, A Modular Three-Dimensional Finite-Difference Ground-Water Flow Model. U. S. Geological Survey TWI 6-A1, 1988.

Moran, John, City of Benson, Arizona, Personal communication, June 23, 2000.

Pool, D.R. and Alissa L. Coes, Hydrogeologic Investigations of the Sierra Vista Subwatershed of the Upper San Pedro Basin, Cochise County, Southeast Arizona. USGS Water Resources Investigations Report 99-4197, Tucson, Arizona, 1999.

Putman, F., K. Mitchell and G. Bushner, Water Resources of the Upper San Pedro Basin, Arizona. Arizona Department of Water Resources, Hydrology Division, 1988.

Scott, Russell L., Riparian and Rangeland Soil-Vegetation-Atmosphere Interactions in Southeastern Arizona. PhD Dissertation, Department of Hydrology and Water Resources, The University of Arizona, 1999.

Slack, Don, Department Head, Department of Agricultural and Biosystems Engineering, The University of Arizona, Personal communication, April 28, 2000.

Snyder, Keirith A. and David G. Williams, "Water Sources Used by Riparian Trees Varies Among Types on the San Pedro River, Arizona," SALSA Special Issue, Journal of Agriculture and Forestry Meteorology. (in press), June 2000.

Theis, Charles. V., The Effects of A Well on the Low of a Nearby Stream, Transactions, American Geophysical Union, 1941, Pp 734-738

US Digital Elevation Model-http://edc.usgs.gov/glis/hyper/guide/usgs_dem

Vionnet, Leticia Beatriz, and Thomas Maddock III, Modeling of Ground-Water Flow and Surface/Ground-Water Interaction for the San Pedro Basin-Part 1-Mexican Border to Fairbank, Arizona. Department of Hydrology and Water Resources, HWR No. 92-010, 1992.

Whetstone, Jack, Bureau of Land Management, Personal Communication, March 28, 2000.

Wickizer, John D., Pumpage Figures for U. S. Army Garrison Fort Huachuca, Arizona 1963-1999, February 2000.

APPENDIX A
CONVERSION TABLES

Table A-1 Length conversion factors

To convert from these units	To these units, multiply by the tabulated factor	
	ft	**mile**
meter (m)	3.2808	$6.2137 * 10^{-4}$
kilometer (km)	3280.8	0.62137

Table A-2 Area Conversion Factors

To convert from these units	To these units, multiply by the tabulated factor	
	ft^2	**acre**
square meter (m^2)	10.764	$2.4711 * 10^{-4}$
hectare (ha)	107,639	2.4711

Table A-3 Volume Conversion Factors

To convert from these units	To these units, multiply by the tabulated factor		
	ft^3	**gal**	**acre-ft**
cubic meter (m^3)	35.315	264.17	$8.1071 * 10^{-4}$

Table A-4 Velocity or Rate Conversion Factors

To convert from these units	To these units, multiply by the tabulated factor		
	cm/s	**ft/s**	**gal/day-ft^2**
meter/day (m/d)	0.0011574	$3.7973 * 10^{-5}$	24.542

Table A-5 Discharge Conversion Factors

To convert from these units	To these units, multiply by the tabulated factor			
	ft^3/s	**gal/min**	**MGD**	**acre-ft/year**
cubic meter/day (m^3/d)	$4.0873 * 10^{-4}$	0.18345	$2.6417 * 10^{-4}$	0.29591